Biochemical Pharmacology 248 (2026) 117620

Contents lists available at ScienceDirect

Biochemical Pharmacology

journal homepage: www.elsevier.com/locate/biochempharm

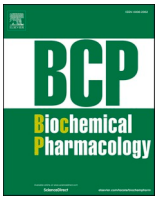

Review

Pharmacological targeting of nuclear factor (erythroid-derived 2)-like 2 (NRF2): a potential strategy to improve the efficacy of oncological photodynamic therapy

Daniel J. de Klerk [a,b,c,1], Mark J. de Keijzer [d,e,1], Leonardo P. Franchi [f,1], Jiahao Tian [a,b,g], Maxim A. Gureev [h], Yingnan Ge [a,b], Bárbara Mesquita [d], Gideon E. Saelman [i], Isis Van herteryck [j], Lionel M. Dias [a,b], Lianne R. de Haan [i], Mingjuan Li [a,b,d], Lenka N.C. Boyd [i,k,l], Tessa Y.S. Le Large [i,k,l], Elisa Giovannetti [k,m], Geert Kazemier [i,l], Perry D. Moerland [n], Yunlei Li [g], Andrew P. Stubbs [g], Mathias Devreese [j], Yuri B. Porozov [h,o], Joanne Verheij [l,p], Twan Lammers [q], Yazan S. Khaled [r], Byron Baron [s], Lingfeng Wu [t,*], Michal Heger [a,b,d,e,**], on behalf of the Photodynamic Therapy Study Group

[a] *Applive Research Laboratories, College of Medicine, Jiaxing University, Jiaxing, Zhejiang, PR China*
[b] *Jiaxing Key Laboratory for Photonanomedicine and Experimental Therapeutics, Department of Pharmaceutics, College of Medicine, Jiaxing University, Jiaxing, Zhejiang, PR China*
[c] *Precision Medicine in Oncology (PrMiO), Department of Pathology, Erasmus MC Cancer Institute, Erasmus Medical Center, Rotterdam, the Netherlands*
[d] *Department of Pharmaceutics, Utrecht Institute for Pharmaceutical Sciences, Utrecht University, Utrecht, the Netherlands*
[e] *Molecular Biophysics and Biochemistry, Department of Chemistry, Faculty of Science, Utrecht University, Utrecht, the Netherlands*
[f] *Department of Biochemistry and Molecular Biology, Institute of Biological Sciences (ICB 2), Federal University of Goiás (UFG), Goiânia, Goiás, Brazil*
[g] *Department of Pathology and Clinical Bioinformatics, Erasmus Medical Center, Rotterdam, the Netherlands*
[h] *School of Computer Science, Physics and Technology, HSE University, Saint Petersburg, Russian Federation*
[i] *Department of Surgery, Amsterdam University Medical Center, Vrije Universiteit, Amsterdam, the Netherlands*
[j] *Department of Pathobiology, Pharmacology and Zoological Medicine, Faculty of Veterinary Medicine, Ghent University, Merelbeke, Belgium*
[k] *Laboratory of Medical Oncology, Department of Medical Oncology, Amsterdam University Medical Center, Vrije Universiteit, Amsterdam, the Netherlands*
[l] *Imaging and Biomarkers, Cancer Center Amsterdam, Amsterdam, the Netherlands*
[m] *Cancer Pharmacology Laboratory, Associazione Italiana Per la Ricerca Sul Cancro (Italian Association for Cancer Research) Start-Up Unit, Fondazione Pisana Per la Scienza, Pisa, Italy*
[n] *Department of Epidemiology and Data Science, Amsterdam University Medical Center, University of Amsterdam, Amsterdam, the Netherlands*

Abbreviations: $^1O_2$, Singlet oxygen; 5-ALA, 5-Aminolevulinic acid (photodynamically inactive); β-TrCP, β-transducing repeat-containing protein; λ_{max}, The wavelength at which there is an absorption maximum; μCT-FLT, Micro-computed tomography-fluorescence tomography; ABC, ATP-binding cassette transporter; Akt, RAC(Rho family)-alpha serine/threonine-protein kinase; AMPK, AMP-activated protein kinase; AP-1, Activator protein-1; ARE, Antioxidant responsive element; ATP, Adenosine triphosphate; BAX, BCL-2-associated X; Bcl-2, B-cell lymphoma 2; bZIP, Basic leucine zipper; CUL3, Cullin 3; CYP3A5, Cytochrome P450 3A5; DNA-PKcs, DNA-dependent protein kinase catalytic subunit; ECH, Erythroid cell-derived protein with Cap'n'collar homology; Em, Emission; EMT, Epithelial-mesenchymal transition; ER, Endoplasmic reticulum; ERK, Extracellular signal-regulated kinase; Ex, Excitation; GCL(C/M), Glutamate-cysteine ligase (catalytic or modifier subunit); GSH, Glutathione (reduced form); GSK-3β, Glycogen synthase kinase 3β; HIF-1, Hypoxia-inducible factor 1; *HMOX1*, Heme oxygenase 1 (gene); HO-1, Heme oxygenase 1 (protein); HSP, Heat shock protein; HUVEC, Human umbilical vein endothelial cells; JNK, C-Jun N-terminal kinase; IC_{50}, Half-maximum inhibitory concentration; ip, Intraperitoneal; iv, Intravenous; KEAP1, Kelch-like ECH-associated protein 1; KRAS, Kirsten rat sarcoma viral oncogene homologue; LC_{50}, Half-maximum lethal concentration (*in vitro*); LD_{50}, Half-maximum lethal dose (*in vivo*); LogP, Octanol:water partition coefficient; MAF, Musculoaponeurotic fibrosarcoma; MAPK, Mitogen-activated protein kinase; miR, MicroRNA; MMP, Matrix metalloproteinase; MRP, Multidrug resistance-associated protein; mTOR, Mechanistic target of rapamycin; NA, Information not available; Neh, NRF2-ECH homology; NFE2L2, NFE2 like BZIP transcription factor 2; NF-κB, Nuclear factor kappa-light-chain-enhancer of activated B cells; NO, Nitric oxide; NQO1/2, NAD(P)H quinone dehydrogenase 1/2; NRF2, Nuclear factor (erythroid-derived 2)-like 2; $O_2^{\bullet -}$, Superoxide anion; NSCLC, Non-small cell lung cancer; PCNA, Proliferator cell nuclear antigen; PD-L1, Programmed death ligand 1; PDT, Photodynamic therapy; PI3K, Phosphoinositide 3-kinase; PMF, 3′,4′,5′,5,7-Pentamethoxyflavone; PPARγ, Peroxisome proliferator-activated receptor gamma; PpIX, Protoporphyrin IX (photodynamically active); PRMT, Protein arginine methyltransferase; PS, Photosensitizer; ROS, Reactive oxygen species; PTEN, Phosphatase and tensin homolog; sc, Subcutaneous; SOD, Superoxide dismutase; STAT, Signal transducer and activator of transcription; $t_{1/2}$, Circulation half-life; TGF, Transforming growth factor; TMPyP4, 5,10,15,20-Tetrakis-(N-methyl-4-pyridyl)porphine; TNFα, Tumor necrosis factor alpha; VEGF, Vascular endothelial growth factor; WT, Wild-type.

* Corresponding author at: Department of Urology, The Affiliated Hospital of Jiaxing University, Jiaxing, Zhejiang, PR China.
** Corresponding author at: Jiaxing Key Laboratory for Photonanomedicine and Experimental Therapeutics, Department of Pharmaceutics, College of Medicine, Jiaxing University, Jiaxing, Zhejiang, PR China.
E-mail addresses: sandy4813@163.com (L. Wu), michal.heger@photonanomedicine.com, m.heger@uu.nl (M. Heger).

https://doi.org/10.1016/j.bcp.2025.117620
Received 13 September 2025; Received in revised form 2 December 2025; Accepted 5 December 2025
Available online 31 December 2025

[o] Advitam Laboratory, Belgrade, Serbia
[p] Department of Pathology, Amsterdam University Medical Center, University of Amsterdam, Amsterdam, the Netherlands
[q] Department of Nanomedicine and Theranostics, Institute for Experimental Molecular Imaging, Center for Biohybrid Medical Systems, University Hospital RWTH Aachen, Aachen, Germany
[r] Leeds Institute of Medical Research, St. James's University Hospital, Leeds, United Kingdom
[s] Centre for Molecular Medicine and Biobanking, University of Malta, Msida, Malta
[t] Department of Urology, The Affiliated Hospital of Jiaxing University, Jiaxing, Zhejiang, PR China

ARTICLE INFO

Keywords:
Redox homeostasis
Oxidants
KEAP1
Antioxidant responsive elements
Transcription factor
Photochemotherapy
Pharmacological inhibition
Tumor survival signaling

ABSTRACT

The recalcitrance of tumors to photodynamic therapy (PDT) has been linked to PDT-induced activation of survival pathways in sublethally afflicted cancer cells that modulate cellular responses to oxidative stress and damage. Survival signaling manifests in regions of the tumor where the tumor cells are insufficiently photosensitized or subjected to inadequate fluence rates. The survival signaling in these tumor regions is believed to account for tumor recurrence. Accordingly, PDT efficacy can be improved by intervening in these pathways using molecular inhibitors of key modulators of survival signaling, thereby increasing the number of lethally afflicted cancer cells and with it therapeutic efficacy. A promising target for pharmacological intervention is the nuclear factor (erythroid-derived 2)-like 2 (NRF2) pathway, which induces the antioxidant and xenobiotic stress response that helps cells cope with prolonged periods of hyperoxidative stress after PDT. This review outlines our current understanding of this pathway, how it is activated, and how it confers cytoprotective effects and ensures cell survival. Additional distinguishing features of the review are that (1) studies are addressed in which PDT activation of the NRF2 pathway has been demonstrated; (2) a non-exhaustive overview of NRF2 pathway inhibitors is presented that could serve as potential adjuvants in PDT regimens to augment therapeutic efficacy in treatment-resistant tumors and cancers that recur after PDT; (3) molecular docking analyses are included that show potential interactions between the NRF2 inhibitors and the redox sensor KEAP1; and (4) an elaborate account is provided of the potential bottlenecks and caveats that can be encountered when using NRF2 inhibitors in the development of fourth-generation photosensitizers for oncological PDT.

1. Introduction

1.1. Photodynamic therapy

Photodynamic therapy (PDT) is a clinically approved, minimally invasive two-stage therapeutic procedure that combines light energy with a light-sensitive drug called a photosensitizer (PS) to destroy tumor parenchymal cells and tumor-associated stromal cells after light activation. Following systemic or topical administration (stage 1), PS molecules hyperaccumulate in the tumor tissue compared to healthy tissue as a result of the enhanced permeability and retention effect or receptor-mediated uptake (e.g., binding of PS-lipoprotein complexes to cognate lipoprotein receptors overexpressed on cancer cells). When illuminated at a resonant wavelength (stage 2), usually within the therapeutic window (650–800 nm), photon absorption by PS electrons will lead to a vibronic transition from the ground state to a singlet state and subsequently to a lower-energy triplet state. The triplet state has a longer lifetime compared to the singlet state, which enables the excited PS to react with molecular oxygen (O_2) to form singlet oxygen ($^1O_2$) via a type II photochemical reaction (energy transfer) [1]. The triplet state PS can also react directly with (bio)molecules or O_2 to produce molecular radicals or superoxide anion ($O_2^{\bullet-}$) and other types of reactive oxygen species (ROS) and radical transients, respectively (type I photochemical reaction that entails intermolecular electron transfer) [1]. Extensive photoproduction of ROS and other radical transients induces hyperoxidative stress, which causes various forms of cell death through mainly 3 different mechanisms [2–5].

First, the induction of cancer cell death emanates from the direct cytotoxicity of photochemically produced ROS. The ROS oxidize biomolecules such as proteins [6], (phospho)lipids [7], and nucleic acids [1,5] and with it perturb the functionality of vital pathways [8] and critical structures. As many clinically approved PS are lipophilic, PDT-induced oxidative damage primarily affects the plasma membrane and the membranes of organelles such as mitochondria, endoplasmic reticulum (ER), and lysosomes, culminating in a mix of chiefly necrotic, apoptotic, and necroptotic cell death [3,4,7,9] and to a lesser extent autophagy-associated cell death, paraptosis-like cell death, and ferroptosis [2,8,10–12].

Second, besides direct oxidative damage to cells, hypoxia rapidly manifests in the illuminated tissue as the available O_2 is converted to ROS [6,12]. Additionally, since some PS are also taken up by endothelial cells that line the intratumoral vasculature, PDT induces vascular damage, thrombosis, and hemostasis [8]. The photochemical destruction of tumor microvasculature leads to hypoxia or anoxia as well as metabolic starvation of cancer cells [7,8,13]. Severe oxidative stress and hypoxia trigger aforementioned forms of cell death that collectively account for cancer removal.

Third, execution of the different modes of cell death facilitates the release of damage-associated molecular patterns, tumor-associated antigens, and oxidized biomolecules that are recognized and acted upon by different (sub)sets of immune cells [14,15]. The mobilization of the innate and adaptive immune system leverages into sterile inflammation and an anti-tumor immune response [14,16]. The immune response not only targets the PDT-treated primary tumor but also non-illuminated metastatic lesions and circulating cancer cells, also known as the abscopal effect [17], both occurring as a result of a process referred to as immunogenic cell death [16].

1.2. Suboptimal responses to photodynamic therapy

Despite the PDT-mediated triggering of multiple effective routes to cancer cell demise, there are instances where surviving cancer cells evade the primed immune system, as a result of which the tumor subsequently regrows – an observation that has been documented in mice [18–21] and humans [22–24]. In the clinical setting this *de facto* means that PDT becomes life-extending rather than curative, which should not be the end goal from the onset. Therefore practical solutions to optimize cure rates are needed.

In addition to post-treatment immune escape, post-PDT tumor regrowth has been in part attributed to incomplete photochemical destruction of target tissue [25,26]. This particular damage profile

[1] Equal contributors.

manifests mainly in tumor regions that were insufficiently illuminated and/or photosensitized during PDT [27,28], such as optically distal segments of bulkier tumors [29,30] or hypoperfused and stroma-dense regions in the tumor. In case of optically distant tumor regions, sublethal fluence rates (defined as the amount of photons traversing an infinitesimal voxel of tissue) are generated owing to Beer-Lambert law-related laser-tissue interactions, which lead to insufficient ROS production and hence a level of damage that is recoverable by tumor cells (Fig. 1A). The distance of photons from the site of incidence is proportional to fluence rate in that light attenuates with depth due to scattering and absorption (Beer-Lambert law). A lower photon density in deeper situated tissue (i.e., lower fluence rate relative to the light at incidence) corresponds to a lower rate of photon absorption by the PS and therefore a lower rate of molecular oxygen conversion to ROS. A

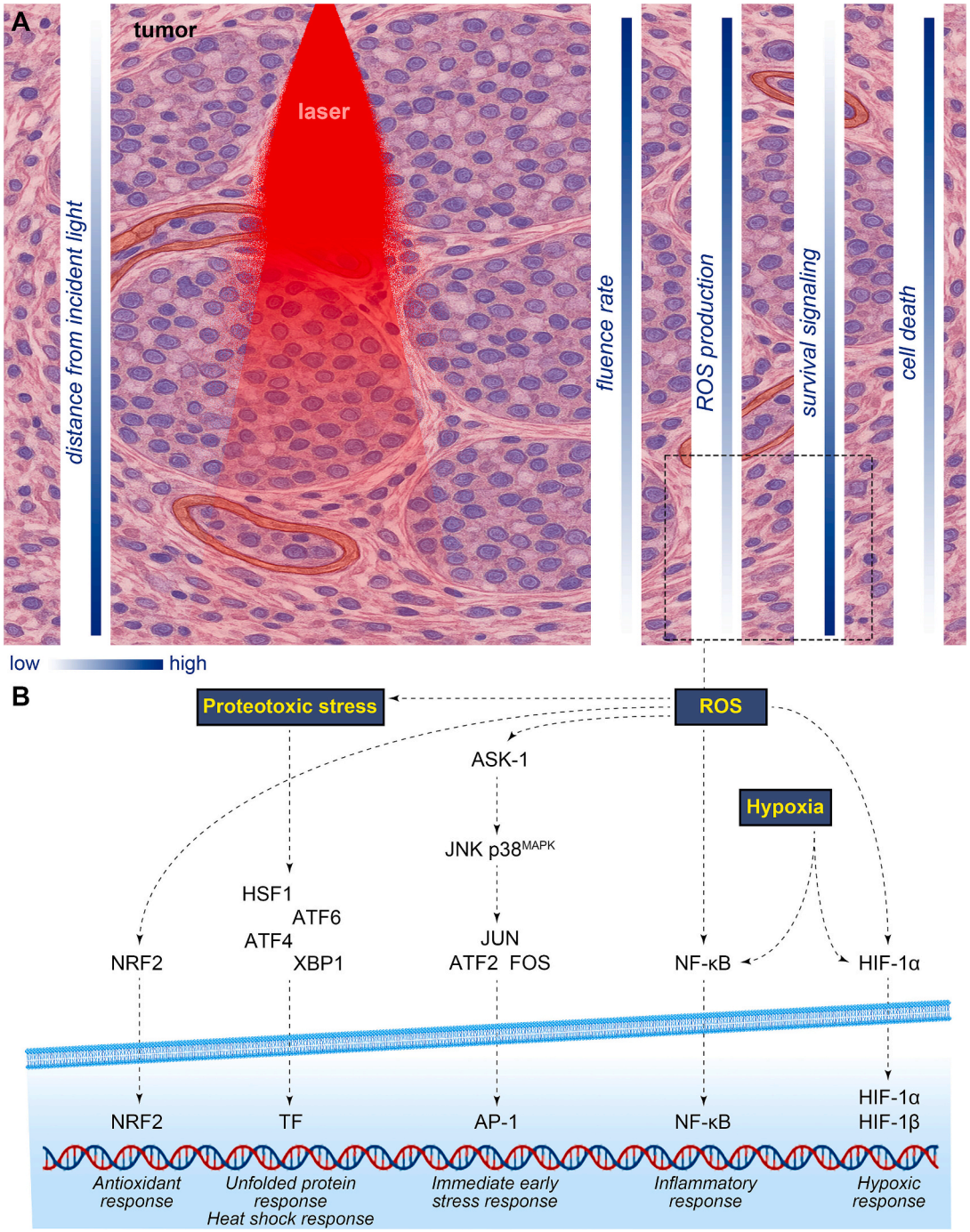

Fig. 1. Summary of laser-tissue interactions associated with PDT in relation to photophysical, photochemical, and biological effects that lead to survival signaling in cancer cells and consequent therapeutic recalcitrance. (**A**) Cross-section of a photosensitized tumor that is undergoing PDT, with the incident red laser light at the top of the cross-section. For the sake of the theoretical framework it is assumed that the tumor is homogeneously photosensitized and oxygenated. Five columns were drawn into the image that represent parameters that determine PDT efficacy, the effects of which are scaled low to high by the respective white-to-dark blue gradient bar placed in relation to the *z*-axial position of laser light (left column). More details are provided in the text (section 1.2). (**B**) Overview of the survival pathways that are activated by sublethally afflicted cells in the demarcated area (reviewed extensively in [28]). At the basis of every pathway lie ROS, which constitute the primordial trigger of every type of survival-promoting response that is eventually executed at the transcriptional level. The successful execution of survival pathways is diametrically opposed to photooxidative induction of cell death (**A**, two right columns), i.e., the chief objective of PDT.

reduced amount of ROS produced with depth inflicts a lower degree of biomolecule oxidation and hence less oxidative stress, allowing the cells to better cope with the relatively milder level of oxidative damage. These photophysical and photochemical hurdles can, albeit to a limited extent, be remediated by selecting PSs with absorption maxima that correspond to wavelengths of deeper penetrating (red) light [30]. Moreover, as described in this paper, pharmacological interventions can be implemented to obviate recovery from mild hyperoxidative stress in sublethally afflicted tumor regions. The biological barriers, i.e., poorly vascularized areas containing extensive desmoplastic tissue (Fig. 2A, B and e.g., [31]), are more challenging in terms of photosensitization inasmuch as PS molecules do not reach all of the target tissue, rendering PDT less effective or even therapeutically moot. This is a phenomenon that plagues all systemic therapies that target tumor tissue directly, not just PDT.

Hyperdense stroma, documented in for example hilar cholangiocarcinoma (Fig. 2A) and pancreatic ductal adenocarcinoma (Fig. 2B) [31,38] and in and of itself shown to debilitate parenchymal drug delivery [39–41], is responsible for raising intratissular (mechanical) pressure that collapses/shuts down microvessels. Correspondingly, these mechanical constraints have been evidenced in pancreatic ductal adenocarcinoma [40,42] and hilar cholangiocarcinoma [43]. Since blood vessels constitute the only conduits for intravenously administered PSs into a tumor, an absence or low density of intratumoral capillaries and post-capillary venules – through which administered compounds typically extravasate [44–46] – means that PSs exit the circulation at only a few loci and have to diffuse across large swathes of densely packed stromal tissue to reach remotely situated parenchyma. Consequently, intravenously administered PSs or drugs do not comprehensively accumulate in a tumor to confer cytotoxicity in all cancer cells. Even if some intratumoral accumulation of PS or drugs occurs, the distribution is commonly suboptimal as demonstrated for various types of nanoparticles in animal studies (Fig. 2C–G). At the whole body level, nanoparticle delivery to tumors appears to work well in mouse tumor models (Fig. 2C). At the tumor level, however, the distribution of nanoparticles tends to be heterogeneous and mainly confined to the tumor periphery (Fig. 2D and E). Nanoparticle penetration out of intratumoral blood vessels into the interstitium is often compromised by interstitial fluid pressure and dense extracellular matrix deposition (Fig. 2F–G). When these data are extrapolated to the clinical PDT setting, it is expected that photosensitization patterns are gradient-like and heterogeneous and leave large portions of tumor tissue insufficiently photosensitized or devoid of PS molecules. Consequently, only a fraction of the tumor will be lethally afflicted during illumination as per Fig. 1A. Sublethally affected tumor regions will contain cancer cells that have activated survival signaling (Fig. 1B), potentially leading to post-treatment tumor regrowth.

1.3. Photodynamic therapy-induced survival signaling and pharmacological remediation

Cancer cells that suffer non-lethal damage from the initial wave of direct and indirect PDT effects will attempt to recover by activating survival pathways [8,28,31,47,48] (Fig. 1B). These pathways are believed to form a biological basis for the resistance to PDT and eventual tumor regrowth [8,27]. Five main survival pathways have been outlined by the Photodynamic Therapy Study Group (Fig. 1B) [28] and subsequently proven to be activated by PDT [8,47]. The nuclear factor (erythroid-derived 2)-like 2 (NRF2) pathway, which is often constitutively hyperactivated in cancer cells, culminates in an antioxidant response that is further exacerbated by photoproduced ROS. ROS-activated proteotoxic stress gives rise to the unfolded protein and heat shock responses. Oxidative stress-activated ASK-1 results in the immediate early stress response. ROS also activate nuclear factor kappa-light-chain-enhancer of activated B cells (NF-κB) directly and indirectly (through hypoxia as a result of vascular shutdown), yielding an inflammatory response that mediates angiogenesis, stromal reconstruction and expansion, and proliferation of tumor cells, amongst others. ROS and hypoxia activate hypoxia-inducible factor 1α (HIF-1α), which regulates a hypoxic response by the transcription and translation of a multitude of survival-promoting genes (of the more than 500 genes that HIF-1α controls). Moreover, some of the survival pathways are inherent drivers of cancer development and may thus already be upregulated before PDT. Tumors with a profound desmoplastic signature tend to be hypoxic and may therefore constitutively upregulate HIF-1α. Consequently, distinct tumor types may possess an innately reduced susceptibility to PDT, depending on whether such resistance pathways have been engaged during tumorigenic development and sustenance [8,27,47]. The inhibition of survival signaling through pharmacological intervention in these pathways is therefore hypothesized to be conducive to therapeutic efficacy [27,28,31,48].

Research aimed at improving PDT outcomes embodies different approaches. Combinations of PDT and chemotherapy are most widely explored, which offer varying degrees of improved efficacy [49,50]. Research has further been performed on photo-activated chemotherapy, which couples a PS to a chemotherapeutic drug through a photocleavable linker. A prime example is ruthenium-based complexes that, in conjugated form, exhibit minimal toxicity but are rendered toxic following photodissociation of the PS [51]. An advantage of this approach is that chemotherapy can prolong the cytotoxic effects after PDT-induced hypoxia has rendered additional illumination ineffectual. Some chemotherapeutic drugs such as tirapazamine exploit PDT-induced hypoxia via their activation under low-oxygen conditions [52]. Another strategy is to enhance the post-PDT immune response by combining PDT with immunotherapy. Of particular note is the combination of PDT and immune checkpoint inhibitors, which enhance the post-PDT immune response through augmentation of cytotoxic T cell activity. This approach has proven quite effective in some clinical cases [53–55]. More modern options feature the use of an oxygen generator or donor, such as catalase or catalase mimetics, that convert endogenously produced H_2O_2 into H_2O and O_2, relieving tumor hypoxia to some degree and increasing O_2 levels for photochemical reactions during PDT [56,57]. Lastly, some studies focus on synergistically enhancing particular modes of cell death, such as ferroptosis, which is highly immunogenic. This is usually achieved through the combination with specific ferroptosis sensitizers, including some tyrosine kinase inhibitors and inhibitors of glutathione synthesis, or through co-administration of ferrous iron [56,58,59].

In terms of survival pathway inhibition, empirical proof-of-concept has been established for the HIF-1 pathway with liposomal zinc phthalocyanine and the selective HIF-1α inhibitor acriflavine [31,48]. Molecular inhibitors of the HIF-1 pathway [60] and the immediate early stress response [29] have been profiled in previous publications for purposes of developing fourth-generation PSs (i.e., second-generation PSs encapsulated in a (targeted) nanoparticulate delivery system with co-encapsulated small molecular inhibitors of survival signaling [27]).

1.4. Aim of the review

In this review, we home in on the oxidative and xenobiotic stress pathway mediated by NRF2, a basic leucine zipper (bZIP) transcription factor expressed by the NFE2 like bZIP transcription factor 2 (*NFE2L2*) gene. This master regulator of the antioxidant response to PDT is involved in the transcriptional upregulation of many target genes that

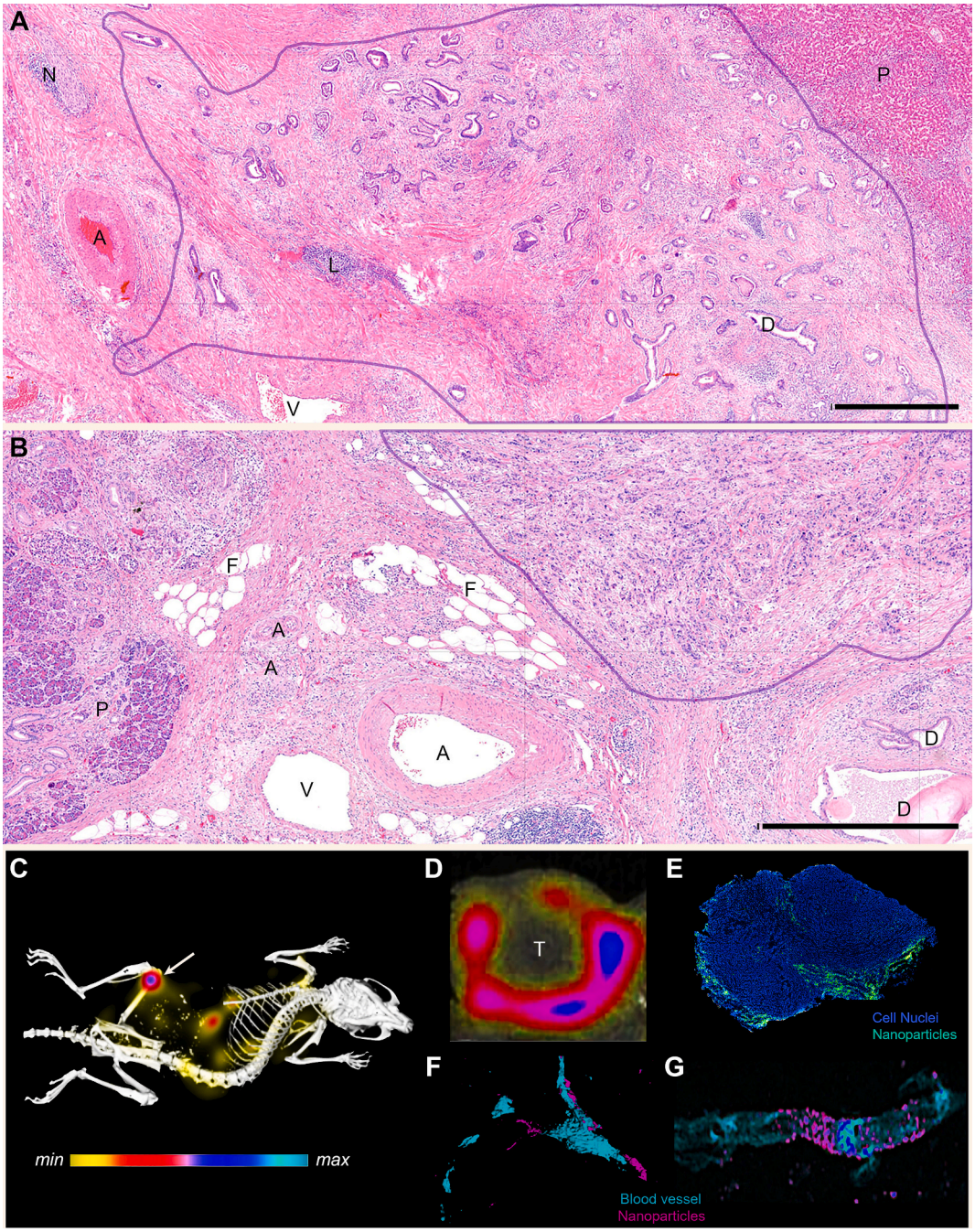

Fig. 2. Biological barriers to PS, drug, and nanocarrier delivery into solid tumors. Clinical examples of histological sections of (**A**) a hilar cholangiocarcinoma and (**B**) a pancreatic ductal adenocarcinoma, which reveal rich desmoplastic tissue in the tumors (delineated in purple) that is commonly poorly vascularized as shown previously for cholangiocarcinoma [31] and reported for pancreatic ductal adenocarcinoma [32,33]. Anatomical designations: A, artery; D, pre-existent bile or pancreatic duct; F, intrapancreatic adipose/fat tissue; L, lymphoid aggregate; N, nerve in hilum; P, pre-existent liver or pancreas parenchyma; V, vein. The large scale bar represents 1 mm, whereas the small scale bar on the left side of the main scale bar equates to 10 μm in width, i.e., the approximate diameter of capillaries and small post-capillary venules. (**C**) Micro-computed tomography-fluorescence tomography (μCT-FLT) image demonstrating the biodistribution and accumulation of Cy7-labeled polymeric micelles in orthotopic mammary (4T1) tumors (white arrow) following intravenous administration in female BALB/cAnNRj mice. (**D**) *In vivo* μCT-FLT image of a 4T1 tumor, zoomed in from panel (**C**) (region indicated with white arrow), showing the heterogeneous tumor distribution of Cy7-labeled polymeric micelles. (**E**) Fluorescence microscopy image taken of Cy7-labeled micelles that have accumulated in a mouse mammary (4T1) tumor (T in panel **D**) isolated and processed histochemically after sacrifice and tumor excision. (**F**) Two-photon microscopic images of fluorescently labeled liposome penetration in a human pancreatic (BxPC3) adenocarcinoma xenograft and (**G**) a 4T1 tumor allograft section. Images in (**C-G**) were compiled from data sets that have been published in [34–37] and are presented here in modified form to illustrate poor intratumoral penetration of drug mimetics (i.e., fluorescent probes) and nanoparticulate delivery systems. Panels (**C**) and (**E-G**) were reproduced with permission from Elsevier.

contain an antioxidant responsive element (ARE) sequence (5′-GTGACNNNGC-3′) [61]. The activation mechanisms of this pathway and its downstream effects are addressed as a backdrop to the synopsis provided on the role of NRF2 survival signaling in PDT. In addition, molecular inhibitors of the NRF2 signaling pathway are presented and their potential application in PDT of solid cancers is elaborated.

2. The NRF2 pathway

The canonical NRF2 pathway consists of 3 main components: (1) Kelch-like ECH-associated protein 1 (KEAP1), (2) NRF2, and (3) AREs. In this pathway, KEAP1 constitutes the sensor of oxidative stress, NRF2 is the activator of the stress response following dissociation from KEAP1 to which it is constitutively bound (Fig. 3A and B), and genes containing AREs encode proteins that directly combat oxidative and xenobiotic stress [62].

NRF2 is a bZIP transcription factor belonging to the Cap'n'collar subfamily of bZIP transcription factors and can form heterodimers with small musculoaponeurotic fibrosarcoma proteins (MAFs), which allows it to bind AREs and activate gene transcription [63]. NRF2 contains seven conserved NRF2-ECH homology (Neh) domains with different functions (ECH is erythroid cell-derived protein with Cap'n'collar homology, Fig. 3C). The first domain, Neh1, corresponds to the bZIP motif, which is necessary to interact with the MAFs. The Neh2 domain contains DLG and ETGE motifs that correspond to the two binding sites for KEAP1, facilitating the formation of a complex composed of one unit of NRF2 and two units of KEAP1. The presence of Ser40 in the Neh2 domain is essential for the release of NRF2 from KEAP1. Neh3 is responsible for recruiting the co-activator chromodomain helicase DNA binding protein 6 and is therefore essential for the transcriptional activity of NRF2, while Neh4 and Neh5 regulate the transactivation of NRF2 target genes by binding to CREB-binding protein. Neh6 has a binding domain for β-transducing repeat-containing protein (β-TrCP). Glycogen synthase kinase (GSK)-3β phosphorylates Ser335 and Ser338 in Neh6 and forms a complex with ubiquitin ligase β-TrCP independently of KEAP1. Lastly, Neh7 is a retinoid X receptor α binding domain through which NRF2 can dimerize and co-activate the retinoid X receptor α transcription factor [62,64–68].

Under normoxic conditions, NRF2 is retained in the cytoplasm by forming a complex with the oxidative stress sensor KEAP1, which is bound to the Neh2 domain of NRF2 (Fig. 3), thereby preventing its translocation to the nucleus (Fig. 4). KEAP1 is a substrate-adapter protein for the cullin 3 (Cul3)/RING-box protein 1-dependent E3 ubiquitin ligase complex that drives the ubiquitination and subsequent proteasomal degradation of NRF2 in the cytosol (Fig. 4) [69].

Under oxidative stress or an otherwise electrophilic environment, Cys151 in the BTB domain and two cysteine residues (Cys273 and Cys288) located in the NRF2 binding domain of KEAP1 (intervening region) are oxidized, inducing conformational and compositional changes in the KEAP1-CUL3 machinery that disable NRF2 degradation without necessarily disrupting KEAP1-NRF2 binding. Mechanistic experiments with prototypic inducers (sulforaphane, iodoacetamide probes) revealed that covalent modification of Cys151 weakens the KEAP1-CUL3 association, uncoupling the ligase from its substrate adaptor and preventing NRF2 polyubiquitination [70]. Complementary genetic experiments demonstrated that Cys273 and Cys288 are essential for the basal repressor function of KEAP1 in that C273A and C288A mutants failed to suppress NRF2 *in vivo* and blunted electrophile responsiveness [71,72]. While additional cysteines can participate (and distinct sets preferentially sense H_2O_2 versus electrophiles), the triad Cys151/Cys273/Cys288 provides the principal control points coupling thiol modification to the loss of CUL3-dependent NRF2 ubiquitination

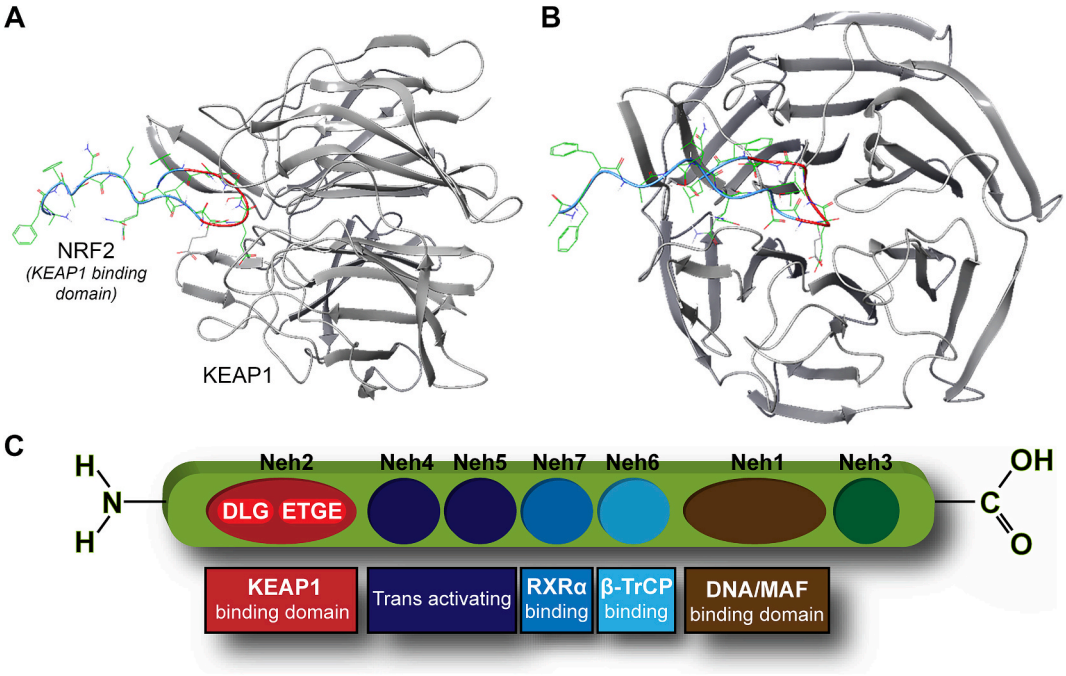

Fig. 3. Protein structure and functional domains of the transcription factor NRF2, which is the master regulator of the cellular antioxidant and xenobiotic stress response. In native state, NRF2 is bound to the redox sensor KEAP1 through a short stretch of the NRF2 sequence spanning amino acids 69 to 84 (**A**, **B**) until KEAP1 residues Cys273 and Cys288 in the NRF2 binding domain are oxidized by ROS. Presented here is the most detailed retrievable complex of NRF2 (light blue + red) with KEAP1 (grey), where NRF2 is represented by a protein fragment comprising a loop with two beta-sheet segments spanning 16 amino acids. The structural model was composed using information from the RCSB Protein Data Bank, in which the NRF2 protein is catalogued as 15–100 amino acid fragments, and AlphaFold3. More detailed information is provided in section S2 of the supporting document available in Mendeley Data (https://doi.org/10.17632/hw4286gycz.1). (**C**) Functionally, NRF2 is composed of seven NRF2-ECH homology (Neh1-7) domains; drawn here is a simple schematic. The main function of each domain is described in the box immediately below the respective encircled domain. Amino- and carboxy-terminal regions are depicted in the left ($–NH_2$) and right (–COOH) flanks of the protein, respectively.

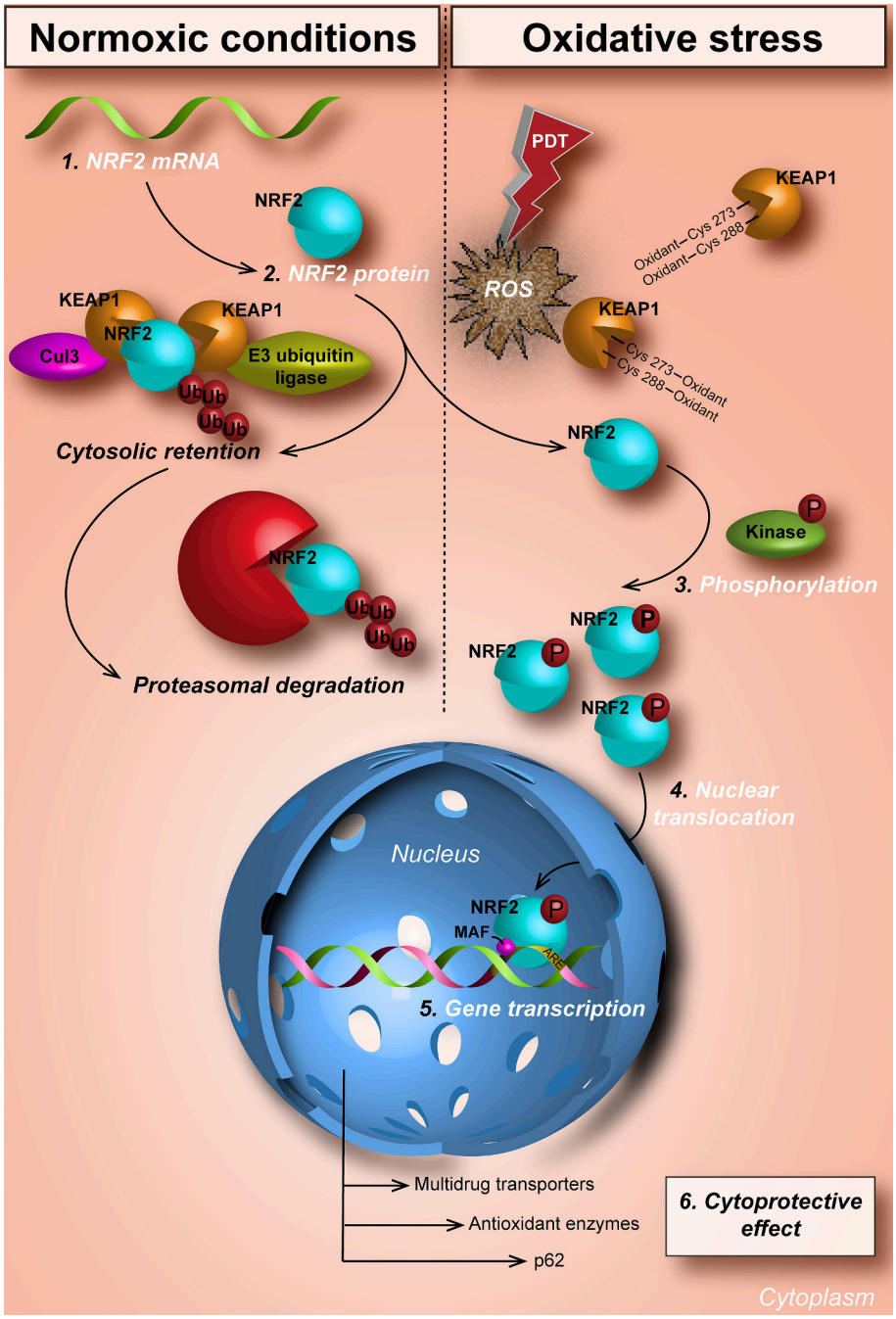

Fig. 4. NRF2 activity is modulated by intracellular oxygen tension. Under normoxic conditions (left side of the diagram), low levels of NRF2 are kept in the cytosol due to proteasomal degradation through polyubiquitination mediated by E3 ubiquitin ligases that recognize the NRF2-KEAP1-CUL3 complex as substrate. Under oxidative stress (right side of the diagram), KEAP1 is oxidized at cysteine residues 273 and 288, which triggers the disassembly of the NRF2-KEAP1-CUL3 complex. Consequently, NRF2 accumulates in the cytosol, where it is phosphorylated, and subsequently translocates to the nucleus, where it binds to AREs and activates the transcription of genes whose protein products regulate redox homeostasis, amongst other cytoprotective functions.

[73,74]. In this so-called floodgate/ubiquitination switch model, NRF2 is released and escapes from polyubiquitination and proteasomal degradation while E3 activity in KEAP1 is transiently inactivated and newly translated NRF2 is allowed to accumulate [64,70,75,76]. Elevated levels of cytosolic NRF2 are maintained by oxidation of Cys183 [77]. The final activation step involves the phosphorylation of NRF2 at Ser40 by protein kinase C, which enables its translocation to the nucleus [78]. However, Ser40 phosphorylation is not strictly required for NRF2 stabilization or ARE-driven transcription once ubiquitination is blocked, underscoring that the primary switch is redox-controlled E3 activity in the KEAP1 protein rather than obligate release [78]. Inside the nucleus, NRF2 complexes with proteins from the activator protein-1 (AP-1) family, mainly c-JUN and MAF, facilitating the binding of these complexes to ARE in the promoter regions of target genes [79,80]. More than 100 genes can be induced by NRF2, and their functions can be generally categorized into four groups: (1) resistance to oxidative stress; (2) antioxidant signaling; (3) drug metabolism and transport; and (4) intermediary metabolism [81,82]. Collectively, these data delineate a clear mechanistic link from oxidative/electrophilic modification of specific KEAP1 cysteines → conformational/complex remodeling that abrogates NRF2 ubiquitination → cytosolic accumulation and nuclear translocation of NRF2 → transcriptional activation of cytoprotective

programs that target oxidative stress and cytotoxicity imparted by xenobiotics. This cysteine-centric sensor architecture provides both sensitivity and specificity to redox cues while maintaining tight repression of NRF2 under homeostatic conditions [83,84].

With respect to the NRF2-regulated downstream biological processes, ROS detoxification is modulated via increased expression of antioxidant enzymes such as glutamate-cysteine ligase with a catalytic/modifier subunit (GCLC/M), glutathione S-reductase, heme oxygenase 1 (HO-1), superoxide dismutase (SOD), and aldo–keto reductases [85]. Xenobiotic detoxification is also regulated by NRF2 through activation of phase I, II, and III metabolic enzymes. For example, enzymes such as NAD(P)H quinone dehydrogenase 1 (NQO1; phase I); glutathione S-transferase (phase II); and ATP binding cassette subfamily of proteins such as ATP-binding cassette (ABC) transporters (also known as multidrug resistance-associated proteins (MRP); phase III) have ARE sequences in their promoter region [86,87]. A detailed list of genes induced by NRF2 is provided in [88].

Although the oxidation and structural alteration of KEAP1 form the basis for NRF2 activation and nuclear translocation, several other mechanisms can influence both NRF2 activation and inhibition. Similar to the oxidation of NRF2 Cys183 [82] and the phosphorylation of NRF2 Ser40 by protein kinase C [78], phosphorylation of NRF2 by p38α/β also promotes nuclear translocation. The latter occurs through mitogen-activated protein kinase/extracellular signal-regulated kinase (MAPK/ERK) signaling, which in turn can be mediated by the proteotoxic stress response. Conversely, NRF2 is negatively controlled by phosphatase and tensin homolog (PTEN) [89] and GSK-3β [90]. Currently, the exact relation between NRF2 and these diverse pathways remains to an extent uncharted, but multiple survival pathways [8] can intersect and overlap in oxidatively stressed cancer cells.

A dual role of NRF2 has recently been discovered. First, several studies demonstrated that NRF2 can act as a tumor suppressor in the early stages of carcinogenesis [91–93]. The tumor-suppressive effects result from activation of those genes that combat oxidative and xenobiotic stress, which consequently prevents DNA damage and thus delays mutagenesis [94,95]. NRF2 activity can be promoted with chemopreventive molecules such as curcumin, resveratrol, isothiocyanate, oltipraz, and sulforaphane as anticancer agents [96]. These compounds can interact with the cysteine residues in KEAP1, releasing NRF2 from KEAP1 to exert its tumor-suppressive impact. Contrastingly, an oncogenic function of NRF2 has also been discovered [97]. For example, NRF2 upregulation supports the proliferation and survival of Kirsten rat sarcoma viral oncogene homologue (KRAS)-transformed cells [98,99]. Constitutively activated NRF2 can result from (epi)genetic alterations in *NFE2L2* and/or in its negative regulator *KEAP1*, but also from persistent oxidative stress that typically prevails in a carcinogenic environment [91,100,101]. For more in-depth reading, an excellent review on the dual role of NRF2 in cancer was published by Wu et al. [102].

The most frequent genetic alterations that induce upregulation of *NRF2* are found in the *KEAP1* gene. Genetic analyses have shown that loss-of-function mutations in the NRF2 binding domain of KEAP1 prevent the negative regulation of NRF2 and that a heteroallelic mutation in *KEAP1* is sufficient to increase NRF2 activity [103,104]. Additionally, mutations that impair the interaction between KEAP1 and CUL3 (mutations in *CUL3* are frequently found in cancers [105–108]) can decrease proteasomal degradation of NRF2 [109,110]. It has been reported that DNA hypermethylation can decrease *KEAP1* expression. Gain-of-function mutations have also been detected in the *NFE2L2* gene, but these mutations are restricted to the Neh2 domain, which interferes with the binding to KEAP1 [111].

All the abovementioned mutations are prevalent in different types of cancer, underpinning the clinical relevance of NRF2. For example, lung squamous cell carcinomas frequently present with alterations in *NFE2L2*, *KEAP1*, and *CUL3* [112]. *KEAP1* mutations are also described in gastric-, hepatocellular-, colorectal-, breast-, and prostate carcinomas [113]. The genetically driven increase in NRF2 activity is positively correlated to poor survival and resistance to chemotherapy and radiotherapy [114,115].

3. NRF2 activation by PDT

3.1. NRF2 cytoprotection after PDT: The trigger-response paradox

The trigger-response paradox revolving around the NRF2 antioxidant response refers to the somewhat counterintuitive phenomenon where NRF2 confers cytoprotection and ensures cancer cell survival following PDT whilst the biological responders (i.e., the NRF2-induced proteins) take substantially longer to be synthesized than the time it takes the photoproduced ROS to react with biomolecules. Photochemically produced $^1O_2$ via the type II mechanism has a biological half-life ranging from less than a few μs in cells/biological milieu [116] to 10–16 μs in biomembranes [117,118], whereas $O_2^{\bullet-}$ from type I photochemical reactions generally reacts with biomolecules in the order of single-digit-to-tens of ms depending on the proximity and local density of SOD as well as pH [119–123]. Under physiological conditions, $O_2^{\bullet-}$ is dismutated to secondary and tertiary ROS derivatives [124,125] that have biological half-lives in the order of ns (Fenton reaction-produced hydroxyl radicals) [126] to the (sub-)s range (e.g., H_2O_2 and peroxynitrite) [127–132]. In contrast, following oxidative/electrophilic activation, NRF2 accumulates in nuclei within ~ 30 min [96]. After NRF2 binds AREs, target mRNAs rise within ~ 1–3 h and expand further by 12 h. Detectable protein accumulation typically follows by ~ 6–12 h, with many canonical proteins peaking between ~ 8–24 h depending on the gene, cell type, and stimulus [96,133–136]. The paradox therefore, lies in the considerably distinct timeframes of the incidence of hyperoxidative stress and the biological response to it.

The explanation is that NRF2 has no effect on the immediate events that occur upon PDT but confers protection in the latent stages, so long after the initial waves of photooxidative damage and activation of energy-driven cell death pathways. In that respect, the term 'antioxidant response' ascribed to NRF2 is rather a misnomer in the therapeutic context, notwithstanding that many tumors exhibit constitutively elevated NRF2 activity (and hence a pre-existent antioxidant response) due to aforementioned mutations in KEAP1 [137–140], NRF2 (gain of function) [111,138,141], and other upstream regulators [142]. Consequently, many antioxidant defenses (e.g., reduced glutatione (GSH), HO-1, NQO1) are already elevated in cancer cells before PDT begins [138,143]. PDT-induced ROS are therefore buffered immediately due to increased antioxidant capacity owing to NRF2 but otherwise unrelated to PDT. Correspondingly, disruption of the pre-existent antioxidant buffer has been shown to augment PDT efficacy [134,144].

Although initial ROS damage is immediate, sublethal damage results in cellular stress that activates different cellular responses. In the latent, PDT-induced NRF2 response, cells that have survived the initial ROS burst activate NRF2 [8,28,47] that in turn upregulates detox enzymes (e.g., NQO1, glutathione S-transferases) [135,145,146], glutathione synthesis (e.g., the catalytic and regulatory subunits of GCL) [147–149], drug efflux pumps (e.g., MRP1 and its gene *ABCC1*) [144,150–152], and proteasomal degradation as well as autophagy pathways [66,153–155] to aid in damage remediation and survival. These processes repair oxidized proteins and lipids, clear damaged mitochondria (via mitophagy), and cause the cell to adapt to redox stress. Moreover, NRF2 suppresses pro-inflammatory NF-κB pathways [156–158] and upregulates anti-inflammatory genes [159–161] through which immune cell recruitment is mitigated and tumor immune privilege post-PDT is maintained [28,159,162], contributing to long-term cell survival. Lastly, NRF2 can activate or stabilize other survival pathways induced by PDT (Fig. 1B) [8,28,47], including the HIF-1 pathway [163–167], and autoregulate by activating the phosphoinositide 3-kinase (PI3K)/RAC(Rho family)-alpha serine/threonine-protein kinase (Akt) pathway (which further boosts NRF2 activity) [168–171]. Taken together, although an antioxidant response is part of the mechanisms that NRF2

triggers following PDT, albeit in the sense of the removal of oxidation products rather than the neutralization of photoproduced ROS, many other processes instigated and controlled by NRF2 account for sublethally afflicted cancer cell survival. Pharmacological interference in the trigger pathways (not only NRF2; Fig. 1B) is hence warranted to optimize PDT outcomes, further underscored in the next section.

3.2. PDT-induced NRF2 activation and cytoprotection

A limited number of studies addressed the role of NRF2 and/or its targets in cancer in response to PDT. The following studies demonstrated that important processes regulated by NRF2 are implicated in the recovery of cellular redox homeostasis after PDT, allowing cancer cells to survive.

Ferino et al. [172] found a dose-dependent increase in NRF2 expression and ROS levels in pancreatic cancer (PANC-1) cells using the cationic porphyrin 5,10,15,20-tetrakis-(N-methyl-4-pyridyl)porphine (TMPyP4) (40 and 80 nM, white light, 7.2 J/cm^2). The inhibition of NRF2 with luteolin further increased the amount of ROS in the cells (due to a pharmacologically impaired antioxidant defense response rather than exacerbated oxidative stress) and also resulted in reduced expression of anti-apoptotic SNAIL while upregulating pro-apoptotic Raf kinase inhibitor protein.

Direct evidence of elevated NRF2 protein levels was provided in murine colon cancer (CT-26) cells photosensitized with the PS indocyanine green (20 μg/mL, 12 h incubation) and sequentially illuminated with a near-infrared laser (twice, 4-h interval, wavelength not specified) for 2 min at 2 W/cm^2. PDT of CT-26 cells that had been pre-treated with free TNYL peptides (selectively bind the EphB4 receptor that plays a role in tumor growth, angiogenesis, and metastasis [173,174]) resulted in lower intracellular ROS levels compared to non-pretreated but PDT-subjected control cells. The authors concluded that the reduced ROS levels were related to the overexpression of NRF2 in the NRF2-primed cells. They also investigated the levels of NRF2 targets NQO1, ABCG2, and HIF-1α. Significant increases were detected in NQO1 and ABCG2 [175], suggesting amplification of NRF2 signaling. The overexpression of NQO1 was also observed in human breast cancer (MCF-7) cells treated with methyl aminolevulinate-PDT (0.5 mM, 4 h incubation, 635 nm ± 17 nm, 1.6 mW/cm^2, cumulative radiant exposure of 2 J/cm^2). The authors attributed this overexpression to the activation of NRF2 by PDT [135].

ABCG2 can be induced by NRF2 and has been identified as a PDT-induced resistance factor in cultured human gastric cancer (NKPS) cells. 5-Aminolevulinic acid (5-ALA) was employed as PS, which is intracellularly metabolized to the photodynamically active protoporphyrin IX (PpIX) [176,177]. Downregulation of ABCG2 using ABCG2-specific siRNA in NKPS cells caused a 2.5-fold increase in intracellular concentration of PpIX. Additionally, after exposure to 630-nm light (~2 J/cm^2, 10 min), the ABCG2 knockdown cells exhibited a 3-fold increase in 5-ALA-PDT sensitivity (500 and 1,000 μM of 5-ALA incubated for 24 h). The sensitivity to 5-ALA-PDT was also increased by fumitremorgin C, a specific inhibitor of ABCG2 [178].

A study by Tian et al. investigating methyl pyropheophorbide A-PDT provided additional evidence for the role of ABCG2 in NRF2-based resistance in ovarian cancer cell lines A2780 and SKOV3. In response to PDT, NRF2 translocated from the cytoplasm to the nucleus and the expression of NRF2 increased, which was purportedly regulated via a MAPK-dependent mechanism. Furthermore, inhibiting NRF2 with siRNAs increased ROS levels and sensitivity to PDT and coincided with the downregulation of ABCG2. SKOV3 cells in particular, which exhibited strong resistance to PDT, had elevated levels of p-NRF2 (phosphorylated/activated) and ABCG2, further underscoring the role that antioxidants and efflux transporters play in NRF2-mediated resistance to therapy [179].

Choi et al. observed that shRNA-mediated NRF2-knockdown in human breast cancer (MDA-MB-231) cells and human colon cancer (HT-29) cells resulted in the downregulation of ABCG2. Subsequently, this led to enhanced cell death and increased levels of ROS generally and $^1O_2$ specifically following pheophorbide A-PDT (670 nm, 0.3 and 0.6 J/cm^2 for HT-29 and MDA-MB-231 cells, respectively). Similar results were achieved by direct inhibition of ABCG2. Combining both the knockdown of NRF2 and inhibition of ABCG2 using Ko143 greatly enhanced PDT-induced cell death. The inhibition of ABCG2 further eliminated the difference between NRF2 wild-type and knockdown cell lines in terms of cell death and pheophorbide A fluorescence levels in the cell. This suggests that ABCG2 plays a role in the accumulation of pheophorbide A and that NRF2 activation might augment the efflux of PS molecules [144].

Yoon et al. [113] investigated the efficacy of hexaminolevulinate, the hexenyl ester of 5-ALA, in the treatment of naive and doxorubicin-resistant MCF-7 cells. The doxorubicin-resistant cells exhibited a reduced oxidative stress response due to low levels of nuclear NRF2 protein as well as low levels of quinone oxidoreductase, HO-1, and GCL. As expected, these cells were more sensitive to hexaminolevulinate-PDT (4-h incubation with 5 μM hexaminolevulinate, LED 613–645 nm, 35 mW/cm^2, 5 J/cm^2) than naive MCF-7 cells with higher levels of NRF2. Moreover, following PDT the intracellular ROS levels were more elevated in the doxorubicin-resistant cells compared to naive MCF-7 cells, while GSH content was decreased. GSH is the most abundant intracellular antioxidant that aids in the maintenance of cellular redox homeostasis and detoxification of xenobiotics and is known to confer resistance to cancer therapies [180–184]. However, inducing overexpression of NRF2 in doxorubicin-resistant MCF-7 cells only marginally altered PDT sensitivity [113,183].

Li et al. [185] observed a light dose-dependent (between 0 and 3.6 J/cm^2) increase in NRF2 and HO-1 protein expression in HeLa cells after 5-ALA-PDT (0.25 mM, 635-nm laser; continuous output mode; irradiance of 20 mW/cm^2). The authors observed a further increase in NRF2 and HO-1 expression when combined with dihydroartemisinin, which contradictorily coincided with enhanced cell death. Dihydroartemisinin is an anticancer agent that was reported to reduce vascular endothelial growth factor (VEGF), HIF-1α, and NF-κB [172]. A possible explanation is that the cell death-promoting actions of dihydroartemisinin (suppression of VEGF/HIF-1α/NF-κB survival programs, iron-dependent ROS generation from its endoperoxide, and possible autophagy inhibition) raise oxidative and metabolic stress beyond the cytoprotective ceiling formed by elevated levels of NRF2 and HO-1. The observed NRF2/HO-1 upregulation likely represents a compensatory stress response that could not restore redox homeostasis once GSH was depleted by the PDT-induced ROS burst, mitochondria had depolarized, and efflux/repair pathways had become overwhelmed. Moreover, HO-1 can paradoxically liberate free iron, fueling Fenton chemistry [124,125] and ferroptosis-like damage [186–191], thereby amplifying lethality despite NRF2 activation. This is particularly pertinent in the context of dihydroartemisinin inasmuch as the compound's endoperoxide bridge is bioactivated by ferrous iron (Fe^{2+}) to generate alkoxy/oxygen-centered radicals [192–194], driving robust ROS production, GSH depletion, mitochondrial damage, and, at higher stress, ferroptosis-like lipid peroxidation [195–200]. Thus, dihydroartemisinin may override NRF2-mediated defenses, converting an adaptive antioxidant surge into an inadequate, ultimately pro-death response.

Hagiya et al. [86] showed that PDT with porphyrin substrates (100 μM 5-ALA, 10 μM PpIX, and 0.1 μM pheophorbide A, visible light, 90 min) increased transcript levels of *heme oxygenase 1* (*HMOX1*) and *ABCG2* in human hepatocellular carcinoma (HepG2) cells. Moreover, the involvement of NRF2 in the induction of *ABCG2* and *HMOX1* was assayed by the use of NRF2-specific siRNA. HepG2 cells in which NRF2 was knocked down expressed lower mRNA levels of *HMOX1* and *ABCG2* after PpIX-PDT [86].

The involvement of NRF2 in the induction of HO-1 at the mRNA and protein levels was also revealed in urinary bladder cancer (T24) cells after hypericin-PDT (75 and 125 nM, fluorescent lamp, 530–620 nm,

irradiance of 4.5 mW/cm^2, cumulative radiant exposure of 4 J/cm^2). Translocation of NRF2 to the nucleus was detected after PDT, leading to increased expression of HO-1. Moreover, when HO-1 expression was induced by pre-treatment with hemin, PDT became substantially less effective. Interestingly, it was observed that the nuclear translocation of NRF2 was blocked by inhibition of the p38^{MAPK} and PI3K pathways using the inhibitors PD169316 (1 μM) and LY294002 (10 μM), respectively. The results suggest that these two pathways mediate the nuclear accumulation of NRF2 after PDT [201], confirming the crosstalk between survival pathways (in this case, antioxidant response and immediate early stress response [28]).

Rubio et al. [66] reported a radiant exposure-dependent increase in NRF2 activity in PDT-subjected mouse embryonic fibroblasts (200 nM hypericin, irradiance of 4.5 mW/cm^2, cumulative radiant exposure ranging from 0.4 to 2 J/cm^2) using a gene-coupled NRF2 reporter. Moreover, it was demonstrated that NRF2 translocation to the nucleus was impaired in p38-deficient fibroblasts, which concomitantly resulted in reduced expression levels of HO-1 and p62 after 1.1 J/cm^2 of hypericin-PDT. The inhibition of p38 by PD169316 in wild-type fibroblasts caused a two-fold increase in ROS levels compared to untreated fibroblasts. In addition, p62, a target of NRF2, was also induced by hypericin-PDT. p62 can bind to KEAP1 and promote a noncanonical

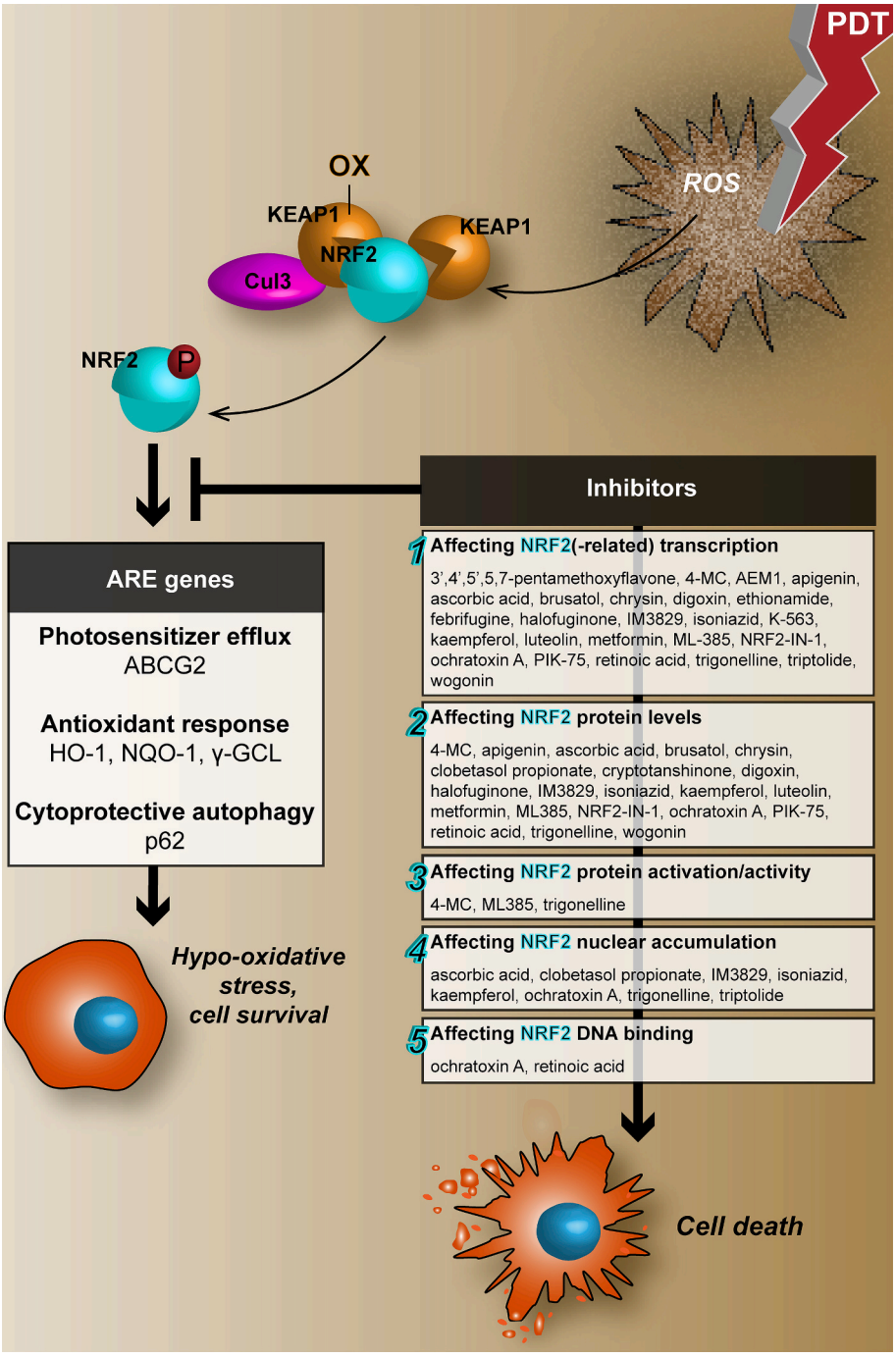

Fig. 5. Outline of possible NRF2 inhibition strategies to sensitize cancer cells to PDT. Inhibition of NRF2 can be achieved at multiple levels: 1) mRNA; 2) protein; 3) protein activation; 4) nuclear translocation; and 5) ARE sequence binding (see also Fig. 2, section 2). The cytoprotection enjoyed by cancer cells that (hyper)activate the NRF2 pathway as a hallmark of cancer and/or as a PDT-stimulated response can be subdued by pharmacological inhibition of NRF2 using inhibitors that are listed under each level of influence and addressed in sections 4.1-27.

pathway of NRF2 stabilization and its subsequent nuclear translocation, followed by transcription of ARE-driven genes. p62 is an autophagy adaptor protein that acts on protein aggregates that are destined for degradation by the autophagosome. Accordingly, the NRF2-p62 axis promoted cytoprotective autophagy by counteracting the proteotoxic stress induced by PDT [66]. Thus, these findings showed a protective role of the p38/NRF2/p62 pathway against ROS damage in cells treated with sublethal doses of PDT.

Finally, Weijer et al. [8,47] performed sublethal PDT on human extrahepatic biliary adenocarcinoma (Sk-ChA-1) cells using the second-generation PS zinc phthalocyanine delivered via neutral DPPC:DSPE-PEG liposomes (1.5 μM zinc phthalocyanine, 30-min incubation, 671 nm, 500 mW output power, cumulative radiant exposure of 15 J/cm^2). Similarly, PDT was performed on Sk-ChA-1 cells, human epidermoid carcinoma (A431) cells, human umbilical vein endothelial cells (HUVEC), and murine (RAW 264.7) macrophages with zinc phthalocyanine delivered by cationic DPPC:cholesterol:DC-cholesterol:DSPE-PEG liposomes (30 nM, 60-min incubation, 671 nm, 500 mW output power, cumulative radiant exposure of 15 J/cm^2). Whole-transcriptome microarray analysis was performed after PDT, and the data were superimposed on survival pathways that had been previously enumerated [28]. Concerning the NRF2-mediated antioxidant response

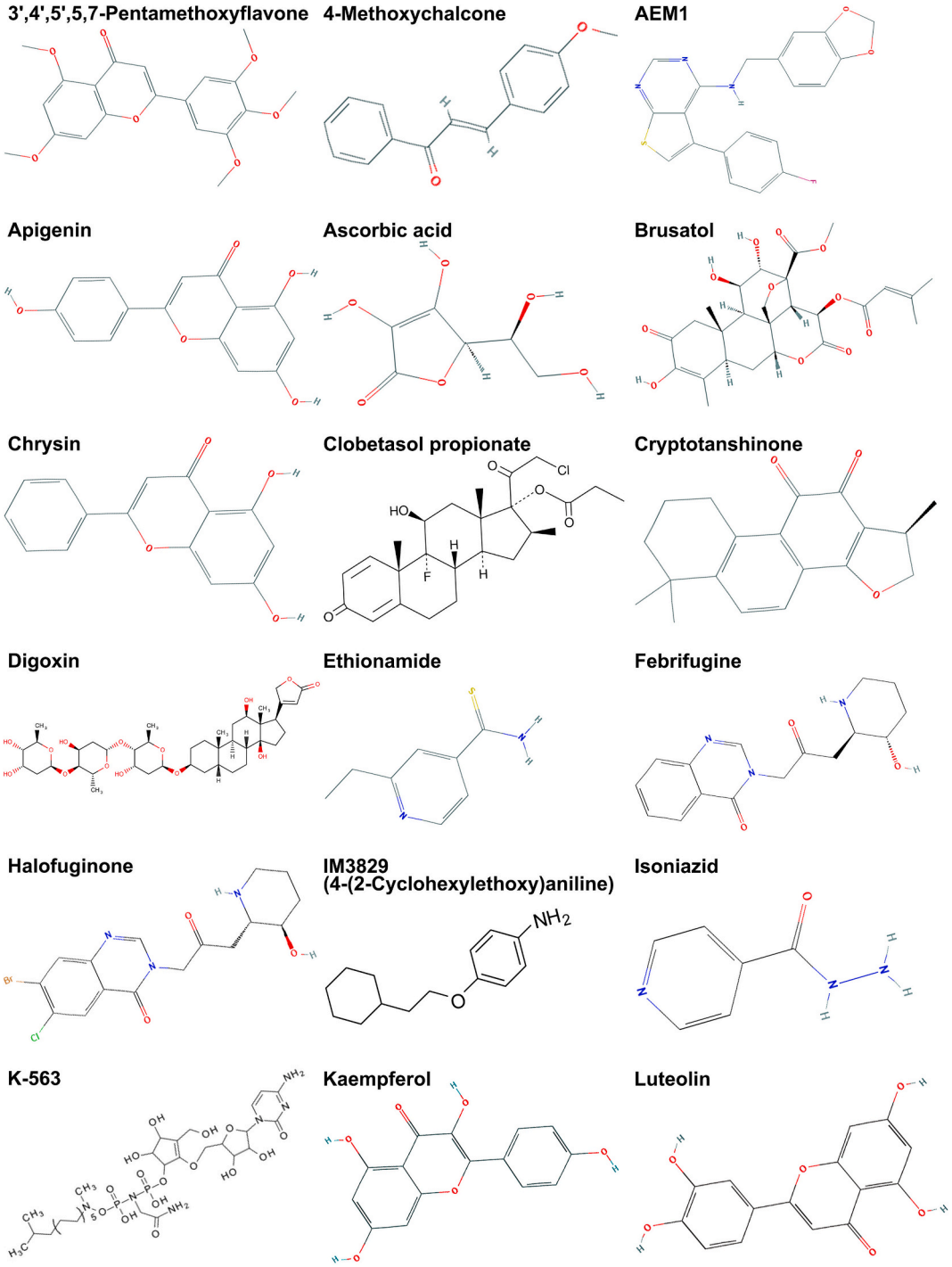

Fig. 6. Molecular structure of NRF2 pathway inhibitors. The chemical attributes, spectral properties, and pharmacokinetic and pharmacodynamic properties of the presented NRF2 pathway inhibitors are provided in the supporting information document (https://doi.org/10.17632/hw4286gycz.1).

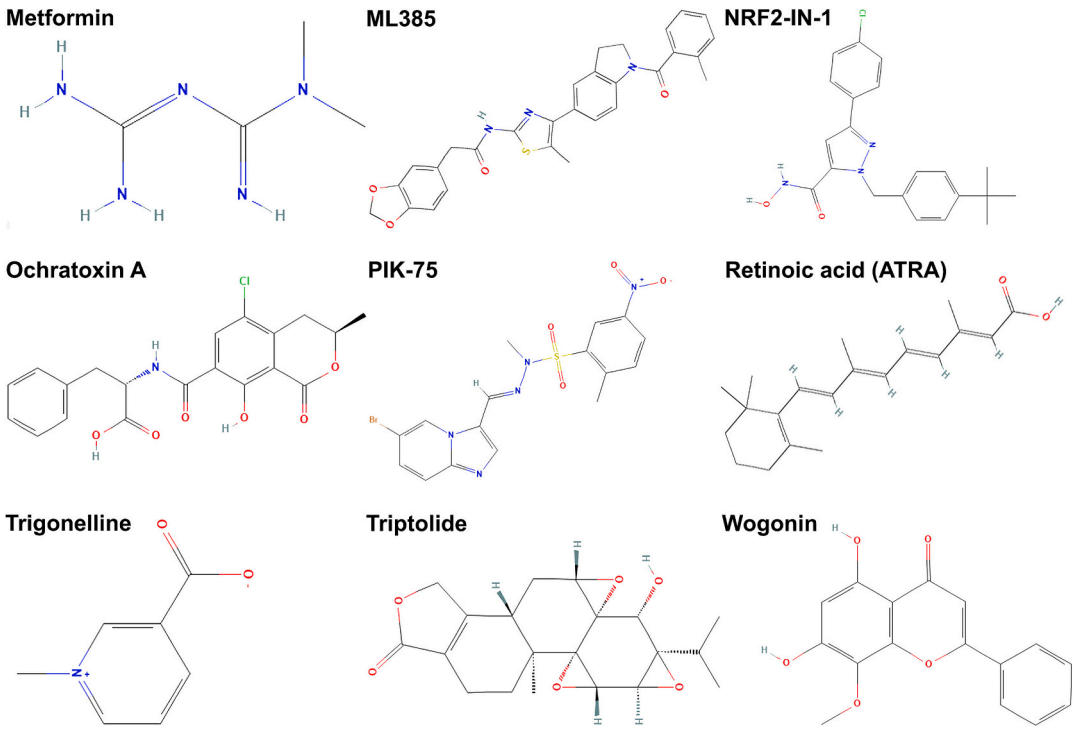

Fig. 6. (*continued*).

pathway, *HMOX1* (HO-1, upregulated, Sk-ChA-1, A431, RAW 264.7), *SRXN1* (sulfiredoxin 1, antioxidant synthesis/recycling, upregulated, Sk-ChA-1 and RAW 264.7), *JUN* (upregulated, Sk-ChA-1), *FOS* (upregulated, Sk-ChA-1), *ABCC3* (multidrug resistance, upregulated, Sk-ChA-1), *GSTP1* (glutathione S-transferase P1, antioxidant synthesis/recycling, upregulated, Sk-ChA-1), and *NQO2* (neutralization of toxins, upregulated, Sk-ChA-1) were dysregulated following PDT compared to dark toxicity controls, attesting to the activation of the antioxidant response survival pathway by PDT with lipophilic, membrane-intercalating PSs [47].

4. NRF2 inhibition to improve PDT efficacy

As NRF2 is upregulated in different types of cancer and its activity is induced by PDT, inhibition of the NRF2 pathway emerges as a promising strategy to increase the efficacy of PDT (Fig. 5) [179,202,203]. The combination of PS plus NRF2 pathway inhibitors may be delivered to cancer cells in a variety of ways, including nanoparticulate drug delivery systems, given the lipophilicity of many PSs. In this combinatorial approach, NRF2 inhibition would reduce the expression of genes involved in the antioxidant stress response, including those genes that regulate drug efflux and redox homeostasis. This is likely to elevate the intracellular retention of PS molecules and increase the sensitivity of cells to PDT-induced hyperoxidative stress, respectively.

Interventional modulation of NRF2 can occur by several mechanistic means, including but not limited to (1) the prevention of NRF2 nuclear translocation, (2) deterrence of DNA binding, (3) proteasomal clearance, and (4) (post-)transcriptional regulation. A non-exhaustive summary of small-molecular inhibitors of the NRF2 survival pathway that could be employed in conjunction with PDT is presented in Fig. 6 and Table 1 and discussed below. A summary of chemical, spectral, pharmacokinetics, and pharmacodynamics data is available from the Mendeley Data repository (https://doi.org/10.17632/hw4286gycz.1) and was created to aid pharmacologists, formulators, and analytical chemists in their research on these compounds.

Given the role of NRF2 in survival signaling under oxidative stress, pharmacological inhibition of the NRF2 pathway is expected to improve PDT outcomes. At this stage, however, limited research has been performed on NRF2 pathway inhibition as part of a PDT protocol. This review aims to spur research into combinatorial treatment modalities where the NRF2 inhibitors are used as adjuvants to improve the efficacy of PDT and to obtain a better understanding of the molecular mechanisms that govern the response of cancer cells to PDT in combination with these inhibitors. Accordingly, a non-exhaustive database of known NRF2 inhibitors was compiled, including inhibitors not tested in a PDT setting before, to facilitate the development of PDT-adjuvant therapeutic regimens.

4.1. 3′,4′,5′,5,7-Pentamethoxyflavone

3′,4′,5′,5,7-Pentamethoxyflavone (PMF), a flavonoid extracted from Rutaceae plants, suppressed the expression of NRF2 as well as its target genes (encoding GCLC, HO-1, and NQO1) and abrogated cisplatin resistance in human lung cancer (A549) cells. KEAP1 expression was increased by PMF in a dose-dependent manner while inhibiting ERK phosphorylation [204].

PMF further possesses anticancer and chemopreventive properties [206,207] and exhibits cytotoxic activity against urinary bladder cancer (T24) cells and ovarian cancer (TOV-21G) cells [207]. Cai et al. [206] demonstrated that PMF can inhibit the growth of cultured APC10.1 cells (a mouse-derived ApcMin/+ intestinal cell line), whilst *in vivo*, C57BL/6J Min/+ (ApcMin/+) mice fed PMF through their diet had reduced adenoma formation in their intestines. The authors further reported lowered levels of prostaglandin E_2 in human colorectal adenocarcinoma (HCA-7) cells treated with PMF, possibly due to interference in the activity of cyclooxygenase 1 and 2 enzymes by PMF binding, as was shown *in silico*. Prostaglandin E_2 mediates cancer cell progression [391] and also exhibits potential inhibitory activity towards glyceraldehyde 3-phosphate dehydrogenase [208], a critical protein in cancer biology that regulates numerous metabolic functions and cancer cell progression [392]. This interaction may have been indirect insofar as the binding of PMF to glyceraldehyde 3-phosphate dehydrogenase could not be confirmed by crystallography [208].

No studies have been conducted in combination with PDT. Drug

Table 1
Non-exhaustive summary of NRF2 inhibitors and mechanism of action, pharmacological and biological effects, test systems, and application in PDT. Data that have been collected mainly in the context of the NRF2 pathway are presented.

Name	Mechanism	Pharmacological effect	Biological effect	Test system	Notes	Tested in PDT
3′,4′,5′,5,7-Pentamethoxyflavone (PMF) [204–209]	Inhibition of ERK phosphorylation; inhibition of cyclooxygenase 1, cyclooxygenase 2, glyceraldehyde-3-phosphate dehydrogenase [204,206,208]	Downregulation of NRF2 and ARE-related genes; reduced prostaglandin E_2 levels [204,206]	Antiproliferative; anti-inflammatory; chemopreventative [204,206,207]	*In vitro*: A549, 293T, MCR-5, HepG2, T24, TOV-21G, HCA-7, APC10.1 cells *In vivo*: C57BL/6J Min/+ (ApcMin/+) mice [204,206,207]	Sensitized A549 cells to cisplatin [204]	No
4-Methoxychalcone [210–214]	Inhibition of Akt pathway phosphorylation; increased poly(ADP-ribose) polymerase γ DNA binding affinity [212,213]	Downregulation of *NFE2L2* mRNA and NRF2 protein levels, ARE-driven genes, adipogenic genes; upregulation of NRF2 activity; reversal of TNFα-mediated inhibition of adipogenesis [212,213]	Anti-inflammatory; cell type-dependent pro-oxidant and antioxidant activity [212,214]	*In vitro*: A549, HEK293, MDA-MB-231, 3T3-L1 cells [211–213]	Sensitizes A549 cells to cisplatin; protected HEK293 cells from cisplatin cytotoxicity by reducing ROS generation [212]	No
ARE expression modulator 1 [215]	Unknown mechanism of action	Downregulation of *NFE2L2* levels, ARE-related transcriptional activity (e.g., decreased levels of GSH), HO-1 protein levels (at 24 h); no effect on NRF2 protein levels [215]	Inhibition of tumor growth; antiproliferative [215]	*In vitro*: A549 (including a variant with an ARE-luciferase reporter gene), NIH/3T3 with ARE-luciferase reporter gene, NCI-H838, NCI-H460, 293T, HeLa, SH-SY5Y cells, lung primary fibroblast *In vivo*: male athymic nude mice (6 wk) bearing A549 xenografts [215]	ARE expression modulator 1 activities are selective for cell lines that harbor mutations which render NRF2 constitutively active; sensitizes cancer cells to chemotherapeutic agents such as doxorubicin, etoposide, and 5-fluorouracil; inhibits NRF2 activity only in cell lines with an NRF2-activating mutation [215]	No
Apigenin [216–227]	Inhibition of mammalian DNA polymerase, nuclear factor kappa-B kinase subunit α and β phosphorylation; DNA binding by enhancer of zeste 2 polycomb repressive complex 2 subunit; PI3K/Akt pathway phosphorylation; STAT1 phosphorylation [219–221,223,225,227]	Downregulation of *NFE2L2* mRNA and NRF2 protein levels, ARE-driven genes, p-mTOR, p62, HIF-1α, PD-L1; suppression of NF-κB/p65 activation; upregulation of miR-101; cleavage of caspase-3 and caspase-9; upregulation of ER stress-related proteins; upregulation of autophagy related 5, beclin-1, microtubule associated protein 1 light chain 3-II; phosphorylation of AMPK and Unc-51 like autophagy activating kinase 1 [216,220,221,223–225]	Antiproliferative, pro-apoptotic; inhibition of cell migration; inhibition of tumor growth; induction of autophagic cell death [216,220,221,225]	*In vitro:* A549, HepG2, HeLa, HCT116, MCF-7, DU145, BEL-7402 (including doxorubicin resistant variant), PC-3, 22Rv1, A375, A2058, RPMI-7951, AGS, SNU-638, NCI-N87, SNU-216, MKN7, MKN74, MRC-5, MDA-MB-463, MDA-MB-231, SK-BR-3, 4T1, and human mammary epithelial cells, peripheral blood mononuclear cell-derived dendritic cells, other cell lines reviewed in [216] *In vivo*: BALB/c nu/nu mice (5 wk) bearing BEL-7402 xenografts; athymic nude mice with PC-3 and 22Rv1 xenografts; BALB/c nu/nu mice (6 wk) with AGS xenografts; C57BL/6 mice (4–6 wk) bearing B16-F10 xenografts [219–221,223–225,227]	Apigenin is a hormetic drug and can upregulate NRF2 at low concentrations; apigenin was able to promote an anti-tumor immune response by suppressing PD-L1 expression in dendritic cells; sensitizes doxorubicin resistant BEL-7402 cells [223,225,226]	No
Ascorbic acid [228–237]	Reduction of nuclear translocation of NRF2 [229]	Downregulation of *NFE2L2* mRNA and NRF2 protein levels, ARE-driven genes; reduced Fas ligand and TNFα expression; catalysis of Fenton reaction (hydrogen peroxide	Antiproliferative; induction of mitochondrial damage [228,231–233,235]	*In vitro*: A549, PC-3, DU145, HeLa, SiHa, CC-33 A, HL-60, U937, 451Lu, EMT6, MCF-7, MDA-MB-468, MDA-MB-231, KCL-22 (imatinib-resistant), Huh-7, KM12C, SNU-C5 (including GLUT1-overexpressing subline), RKO, LoVo, SW620, SW480, DS-sarcoma cells	Can be both pro-oxidant and antioxidant depending on cellular specifics and biochemical milieu [233]	Yes [230,233–236]

(*continued on next page*)

Table 1 (*continued*)

Name	Mechanism	Pharmacological effect	Biological effect	Test system	Notes	Tested in PDT
		and hydroxyl radical production) [228–234]		*In vivo*: female BALB/c mice bearing EMT6 tumors; athymic (nude) mice (6 wk) bearing SNU-C5 and KM12C xenografts [228–237]		
Brusatol [203,238–250]	Induces ubiquitination of NRF2 and its proteasomal degradation; inhibition of global protein synthesis, especially short half-life proteins including NRF2; binding to Skp1 [239,242–246]	Transient downregulation of NRF2 and ARE-related gene and protein levels; inhibition of STAT3 activity and the PI3K/Akt/NF-κB pathway; blocking S-phase kinase-associated protein 1-S-phase kinase-associated protein 2 interaction [242,244,245,247–250]	Antiproliferative; inhibition of tumor growth; pro-apoptotic; inhibition of EMT [239,242,244,245,247–250]	*In vitro*: A549, UM-SCC-47, UD-SCC-2, JMAR, TuTu 167, LN686, YD-10B, HN-9, FaDu, HaCaT, DU145, SGC-7901, MIA PaCa-2, HCCLM3, HEp-2, K150 (also referred to as KYSE-150), Caco-2, SKOV3, HepG2, BEAS-2B, NCI-H1299, 293T, HeLa, MDA-MB-231, Ishikawa, SPEC-2, SK-N-AS, Raji, SU-DHL-4, LCL1, H929, HL-60, K562, NB-4, SU-DHL-10, RPMI-8226, MOLM14, C17, NPC43, NPC53, Hepa-1c1c7, NCI-H460, NCI-H1048, NCI-H441 cells, primary human hepatocytes and other cell lines reviewed in [246] *In vivo*: athymic nude mice (4–6 wk) bearing A549 xenografts; male nude mice (6 wk) with MIA PaCa-2 xenografts; NCr nude mice with HCCLM3 xenografts; male BALB/c mice with HEp-2 xenografts; BALB/c nu/nu mice (5–6 wk) bearing A549 xenografts; male NOD.CB17-Prkdc^{scid}/J (NOD/SCID) mice (6 wk) with MOLM14 xenografts [203,239,242–250]	Brusatol sensitizes A549, HeLa, and MDA-MB-231 cells to other chemotherapeutic drugs such as carboplatin, 5-fluorouracil, etoposide, and paclitaxel [244]	Yes [203]
Chrysin [226,251–259]	Inhibition of Akt phosphorylation; inhibition of the PI3K and ERK signaling pathways [254,255]	Downregulation of *NFE2L2* mRNA and NRF2 protein levels and ARE-driven genes (HO-1, NQO1) [255,256]	Antiproliferative; antimigratory; inhibition of tumor growth; pro-apoptotic [251,254,256]	*In vitro*: T98, U-251MG, U-87MG, NCTC clone 929, MCF-7, HeLa, MGC-803, BEL-7402 (doxorubicin-resistant) cells, male Sprague–Dawley rat hepatocytes *In vivo*: male BALB/c nu/nu mice (4–6 wk) bearing U-87MG xenografts [251,255–258]	Sensitizes doxorubicin-resistant cells [255]; can upregulate or downregulate NRF2 [226,257,259]	Yes (using porphyrin-conjugated derivatives of chrysin) [258]
Clobetasol propionate [260–263]	Interference with nuclear translocation of NRF2; promotion of β-TrCP-dependent proteasomal degradation in a glucocorticoid receptor- and GSK-3β-dependent manner, inhibition of CYP3A5 [260,261]	Downregulation of NRF2 and HIF-1α protein levels, ARE-related genes; increase in ROS levels [261,262]	Antiproliferative in KEAP1 mutant cell lines (loss of function) [261,263]	*In vitro*: WiL2-NS, A549 (including a variant with an ARE-luciferase reporter gene), NCI-H2228, NCI-H1299, NCI-H460, AsPC-1 (including CYP3A5 knockout), H6c7 cells, patient-derived organoids: PDM24/30/36/38/39/40/41/106/107/168/179 *In vivo*: BALB/c nu/nu mice (6–8 wk) bearing A549 xenografts *Clinical*: actinic keratosis patients [261–263]	Clobetasol propionate alone or in combination with rapamycin potently inhibits the growth of tumors harboring mutations in KEAP1 or both KEAP1 and liver kinase B1 *in vitro* and *in vivo*; reduces PDT-induced erythema [261,263]	Yes [263]
Cryptotanshinone [264–275]	Inhibition of the PI3K/Akt/mTOR/STAT3 signaling pathway [269–271]	Decrease in protein levels of NRF2, p-NRF2, MRP1, GCLC, GCLM, HO-1, NQO1, p-P38, p-JNK, p-ERK1/2; increase in protein levels of beclin 1, microtubule-associated proteins 1A/1B light chain 3, autophagy related 5 [269,271–273]	Anti-angiogenic; antiproliferative; anti-invasive; anti-glycolytic; pro-apoptotic; inhibition of tumor growth; anti-inflammatory; autophagy-inducing [265,269,272,273]	*In vitro*: A549 (including cisplatin-resistant subline), Chang Liver, BAEC, HT-1080, HT-29, HeLa, NCI-H1299, Huh-7, NCI-H1975, HFL1, PC-9, MHCC97-H, LPS-stimulated RAW 264.7 cells, Parkinson's patient-derived human-induced neuronal progenitor cells *In vivo*: male BALB/c nu/nu mice (4 wk)	Sensitizes and reverses recalcitrance to cisplatin or gefitinib; upregulated NRF2 activity in lipopolysaccharide-stimulated RAW 264.7 macrophages and Parkinson's patient-derived human-induced	No

(*continued on next page*)

Table 1 (*continued*)

Name	Mechanism	Pharmacological effect	Biological effect	Test system	Notes	Tested in PDT
				bearing Huh-7 xenografts; BALB/c nu/nu mice (3–4 wk) with NCI-H1975 and PC-9 xenografts [265,269,272–275]	neural progenitor cells [272–275]	
Digoxin [276–282]	Inhibition of PI3K/Akt/mTOR pathway phosphorylation; inhibition of Na^+/K^+-ATPase [279–281]	Downregulation of *NFE2L2* and ARE-related gene expression; reduction of NRF2 protein expression; inhibition of the HIF-1α pathway [276,279]	Induction of cell cycle arrest; inhibition of EMT [276,279,280]	*In vitro*: PANC-1, SW1990, A549, NCI-H1299, HCT116, HeLa, HepG2, MCF-7, A2780, MDA-MB-231, LL-02, H9c2, T-47D cells *In vivo*: female BALB/c nu/nu mice (6 wk) bearing SW1990 xenografts [276,279,280]	Pro-arrhythmic [282]	No
Ethionamide [283–286]	Unknown mechanism of action	Suppression of ARE-dependent transcriptional activity [286]	Decreased cell viability [286]	*In vitro*: THP-1, HepG2, U937, 3T3-L1, HaCaT cells [286]	Sensitizes THP-1 and U937 cells to arsenic trioxide [286]	No
Febrifugine [287–290]	Unknown mechanism of action	Suppression of ARE-dependent transcriptional activity; increased ROS production [287,288]	Cytotoxic effect; increased Th1 immune response [287]	*In vitro*: J774A.1, A549, NG108 *In vivo*: female BALB/c mice (4–6 wk) infected with *L. donovani*; ICR mice (4–5 wk) inoculated with *P. berghei*-infected erythrocytes [287–289]	–	No
Halofuginone [202,269,288,289,291–300]	Inhibition of SMAD3 phosphorylation downstream of the TGF-β signaling pathway; inhibition of prolyl-tRNA synthetase domain of glutamyl-prolyl-tRNA synthetase, leading to the accumulation of uncharged prolyl-tRNA which in turn stimulates general control nonderepressible 2 activity; inhibition of NF-κB, p65, and c-Fos nuclear translocation [288,293,295,297]	Downregulation of NRF2 protein levels, ARE-driven genes, NF-κB, AP-1, fibrotic proteins; increased proteasomal degradation of NRF2 through increased GSK-3β activity; inhibition of the TGF-β pathway; amino acid starvation; increased intracellular ROS production [202,288,292–297]	Antiproliferative; anti-angiogenic; antimigratory; antifibrotic; inhibition of tumor growth; pro-apoptotic [202,288,292–294,297,300]	*In vitro*: A549, KYSE70, BEAS-2B, NCC16-P11, ABC1, COR-L105, 22Rv1, SCL-1, HepG2, NCTC 1469, 293T, MCF-7, MDA-MB-231, J774, NG108 cells, T cells ($GCN2^{-/-}$ and WT), mouse embryo fibroblasts *In vivo*: male BALB/c nu/nu mice (6–8 wk) with A549 and KYSE70 xenografts; SKH-1 mice (8 wk) with cutaneous squamous cell carcinomas (established by subcutaneous co-injection of XL50 cells with NIH/3T3 fibroblasts); male SCID (CB17/Icr beige) mice with WISH-PC2, PC-3, and CWR22 xenografts; adult male Sprague Dawley rats; New Zealand white rabbits; ICR mice (4–5 wk) inoculated with *P. berghei*-infected erythrocytes *Clinical*: patients with refractory malignant solid tumors [202,288,289,292,294–300]	Febrifugine derivative; inhibition of prolyl-tRNA synthetase is ATP-dependent; exhibits gastro-intestinal toxicity in patients; subcutaneous administration was more toxic than oral administration in mice [202,289,293,299]	Yes [202]
4-(2-cyclohexylethoxy)aniline (IM3829) [115,301,302]	Inhibition of *NFE2L2* transcription and NRF2 nuclear translocation; decreased binding activity to ARE consensus sequences [115,302]	Downregulation of *NFE2L2* mRNA and NRF2 protein expression, downregulation of ARE-related protein expression [115,302]	Enhanced sensitivity to radiotherapy [115,301]	*In vitro*: A549, NCI-H1299, NCI-H460, HEK293 (expressing an ARE-luciferase reporter gene) cells *In vivo*: female athymic BALB/c nu/nu mice (5 wk) bearing H1299 and A549 xenografts [115,301]	Sensitizes cells to radiation-induced cell death [115,301]	No
Isoniazid [286,302–308]	Inhibition of NRF2 nuclear translocation by inhibition of ERK1 phosphorylation and downregulation of karyopherin β1 protein levels [303,304]	Increase in cytosolic NRF2 protein levels but decrease in nuclear NRF2 protein levels; upregulation of KEAP1 and caspase 9; downregulation of ARE-dependent mRNA levels; downregulation of PCNA protein levels [303,304]	Antiproliferative; pro-apoptotic; induction of oxidative stress; decreased cell viability [303,304]	*In vitro*: HepG2, THP-1, U937, PC-3, THLE-2, NIH/3T3-L1, HT-29, Hep3B cells *Ex-vivo*: mouse oocytes *In vivo*: BALB/c mice; female ICR mice; athymic nude mice bearing PC-3 xenografts [286,303–305]	Can sensitize cells to arsenic trioxide; negatively affects fertility (reduces oocyte maturation); tested in conjunction with photothermal therapy [286,307,308]	No [306]

(*continued on next page*)

Table 1 (*continued*)

Name	Mechanism	Pharmacological effect	Biological effect	Test system	Notes	Tested in PDT
K-563 [309]	Unknown molecular target and molecular mechanism	Reduced ARE-driven gene expression, GSH levels; increase in oxidative stress [309]	Antiproliferative [309]	*In vitro*: A549, BEAS-2B, LK-2, TGBC24TKB cells *In vivo:* male SCID mice (CB17/Icr- scid/scidJcl; 5 wk) bearing A549 xenografts [309]	K-563 has a synergistic effect on cisplatin and etoposide in inhibiting cell proliferation [309]	No
Kaempferol [310–316]	Reduces nuclear translocation of NRF2 [314,315]	Downregulation of *NFE2L2* mRNA and NRF2 protein levels; reduced expression of ARE-driven genes; reduced transglutaminase 2 expression; suppression of the Akt/mTOR pathway; increase in ROS levels [310,314–316]	Antiproliferative; inhibition of tumor growth; pro-apoptotic [310,314]	*In vitro*: A549, NCI-H460, PANC-1, MIA PaCa-2, Caco-2, HepG2 cells, primary mouse hepatocytes *Ex vivo*: rat liver microsomes *In vivo*: male BALB/c mice (4–6 wk) bearing PANC-1 xenografts; male ICR mice (5 wk) [310,314–316]	Can also upregulate NRF2 activity as a result of increased oxidative stress [310,316]	No
Luteolin [172,311,317–326]	Enhances *NFE2L2* mRNA degradation [317]	Downregulation of *NFE2L2* mRNA and NRF2 protein levels; reduced expression of ARE-driven genes (NQO1, HO-1, glutathione S-transferase α1/2 protein products); GSH depletion [317,318,322,324,326]	Antiproliferative; pro-apoptotic; inhibition of tumor growth [317,318,322–324]	*In vitro*: A549, A549 clones siNRF2-C27 and siGFP-C5, Caco-2, MCF-7, HT-29, SNU-407, FHC, HCT116 (oxaliplatin resistant variant), SW620 (oxaliplatin resistant variant), HepG2 (including ARE-luciferin transfected HepG2-C8), Hepa-1c1c7, RL-34, MDA-MB-231 cells *In vivo*: male C57BL/6 $Nrf2^{+/+}$ and $Nrf2^{-/-}$ mice (6 wk); female athymic nu/nu mice (6 wk) bearing A549 xenografts [317,318,320,322–326]	Increased protein levels of NRF2 downstream targets in some studies [325,327]; reduces resistance to anticancer drugs such as oxaliplatin, bleomycin, and doxorubicin in oxaliplatin-resistant colorectal cancer cell lines [317,318]; enhances anti-cancer potency of cisplatin in mice [322]; nanoparticulate luteolin is more effective in reducing *NFE2L2* transcript levels than free luteolin [324]	Yes [172]
Metformin [328–336]	Stimulation of AMPK activity; inhibition of Raf/ERK and PI3K/Akt/mTOR complex 1 pathways; inhibition of sirtuin 1-dependent deacetylation of NRF2 by p53-dependent upregulation of miR-34a [328–332]	Downregulation of *NFE2L2* and NRF2 protein levels, ARE-dependent gene transcription; upregulation of death receptor 5 and C/EBP homologous protein; elevation of nitrotyrosine levels and reduced inducible nitric oxide synthase and cyclooxygenase 2 expression (after tetrasulphonatophenyl porphyrin-PDT); reduced circulation of insulin and insulin receptor activity (in a clinical setting) [328,330–332,335]	Antiproliferative; inhibition of tumor growth [329,330,332,333]	*In vitro*: HepG2, HeLa, A549, H1299, NCI-H460, KLN205, BEAS-2B, MCF-7, MDA-MB-231(mutated p53), HCT116 (p53 knockout), SKOV3 ($p53^{-/-}$), MIA PaCa-2, AsPC-1 cells [329,330,332–334] *In vivo*: male Wistar rats (12 wk) bearing Walker-256 tumors; female BALB/c nu/nu mice (6–8 wk) with A549 xenografts; male Swiss nu/nu mice bearing MIA PaCa-2 and MIA PaCa-2/CAF9 xenografts [329,333,335] *Clinical*: patients with treatment-naive, early-stage breast cancer [331]	Increases susceptibility of wildtype p53 cancer cells to oxidative stress and TNF-related apoptosis inducing ligand-induced cell death; sensitizes NSCLC cells to epigallocatechin gallate through the suppression of the NRF2/HO-1 signaling pathway [330,332]	Yes [333–335]
ML385 [260,337–339]	Decreases NRF2 transcriptional activity by binding to the NRF2-ECH homology 1 domain, blocking the NRF2-MAF protein complex to regulatory DNA binding sequences [337]	Downregulation of ARE-related transcriptional activity and NRF2 protein levels [260,337]	Antiproliferative; inhibition of tumor growth [260,337,338]	*In vitro*: 4T1, A549 (expressing an ARE-luciferase reporter gene), H1437 (expressing an ARE-luciferase reporter gene), H838 (expressing an ARE-luciferase reporter gene), HEK293 (expressing an ARE-luciferase reporter gene), BEAS-2B, EBC-1, SUM159, NCI-H460 cells *In vivo*: male CD-1 athymic nude mice	Selective cytotoxicity in KEAP1 mutants (with gain of NRF2 function); chemosensitizer for paclitaxel, doxorubicin, and carboplatin [337]	Yes [339]

(*continued on next page*)

Table 1 (*continued*)

Name	Mechanism	Pharmacological effect	Biological effect	Test system	Notes	Tested in PDT
				bearing A549 and NCI-H460 xenografts; female BALB/c mice (4–5 wk) with 4T1 xenografts [337–339]		
NRF2-IN-1 [340,341]	Unknown mechanism of action	Downregulation of NRF2 protein levels and ARE-related gene expression; increased BAX, KEAP1, and cleaved caspase-3 protein levels; decrease of Bcl-2 protein expression [340,341]	Pro-apoptotic; antiproliferative; inhibition of tumor growth [340,341]	*In vitro*: HeLa, HL-60, THP-1, U937 cells *In vivo*: THP-1 xenografts on chicken egg chorioallantoic membrane; cardiac ischemia/reperfusion model in female Sprague-Dawley rats [340,341]	–	No
Ochratoxin A [172,342–349]	Possible mechanisms: inhibition of NRF2 nuclear translocation; inhibition of NRF2 DNA binding; epigenetic modifications (through inhibition of histone acetyltransferase and upregulation of histone deacetylase 3) preventing *NFE2L2* transcription; upregulation of miR-132 [345]	Downregulation of NRF2 protein levels and ARE-related gene expression [346–348]	Cytotoxic due to oxidative stress [172,347,349]	*In vitro*: PANC1, BxPC-3, LLC-PK1, NRK, RL-34, primary rat hepatocytes *In vivo*: male Fischer 344 rats [172,346,347,349]	Ochratoxin A is carcinogenic and can induce cell proliferation and tumor growth; exhibits hepato- and nephrotoxicity likely due to concentration-dependent upregulation of NF-κB and its downstream targets (particularly inducible nitric oxide synthase), which contributes to increased oxidative and nitrosative stress [343,349]	Yes [172]
PIK-75 [350,351]	Induces proteasomal degradation of NRF2; inhibition of p110α/β (catalytic subunits of PI3K) [350,351]	Downregulation of NRF2 protein levels and ARE-related gene expression [350]	Inhibition of tumor growth; pro-apoptotic; antiproliferative [350,351]	*In vitro*: A375, A549, AsPC-1, HeLa, MCF-7, ADR-RES, MIA PaCa-2 cells *In vivo*: male athymic nude mice (Foxn1nu; 6 wk) bearing MIA PaCa-2 cell xenografts; female BALB/c nu/nu mice with subcutaneous HeLa xenografts [350,351]	Sensitizes pancreatic cancer cells to gemcitabine [350]	No
Retinoic acid (ATRA) [352–363]	Inhibition of NRF2 binding to the ARE through activation of retinoic acid receptor α and its subsequent competitive and antagonistic binding to the ARE [352]	Downregulation of NRF2 protein levels and ARE-driven gene expression [352]	Antiproliferative [358,359]	*In vitro*: HL-60, NB4 (including ATRA-resistant R subline), HepG2, HEK293, MCF-7, Hepa-1c1c7, C2BBe1, Caov-3, SKOV3, THP-1, MOLM-13, KOCL-48, AREc32 (MCF-7 derived ARE-luciferase reporter cell line), SKBR3, HT-29, HCT116 cells, human primary hepatocytes, patient-derived primary acute myeloid leukemia cells *In vivo*: male CD-1 mice (9 wk); male C57BL/6 $Nrf2^{+/+}$ and $Nrf2^{-/-}$ mice (8 wk); female HSD athymic Foxn1nu mice (6–8 wk) bearing HT-29 xenografts; C3H/HeN mice bearing syngeneic SCCVII tumors *Clinical*: patients with acute promyelocytic leukemia, advanced stage small cell lung cancer, and various pediatric cancers [352,354,358–363]	High concentrations can promote NRF2 activity in response to oxidative stress; ATRA can differentiate myeloid-derived suppressor cells into mature cells [353,363]	Yes [361,362]
Trigonelline [364–369]	Suppression of NRF2 activation and nuclear import via epidermal growth factor	Downregulation of NRF2 protein levels, ARE-related gene expression, and proteasomal genes	Pro-apoptotic; antiproliferative [364,368]	*In vitro*: COLO 357, MIA PaCa-2, PANC-1, HPDE6c7, HT-29, A549, NCI-H460, NCI-H1299, L-132, HN-9, HN-3 cells *In vivo*: female SCID beige mice (8 wk)	Sensitizes HN-9 cells to cisplatin and artesunate; improves the responsiveness of NSCLC	No

(*continued on next page*)

Table 1 (*continued*)

Name	Mechanism	Pharmacological effect	Biological effect	Test system	Notes	Tested in PDT
	receptor pathway inhibition [364,366,367]	(proteasome 20S subunit alpha 4 and 5) [364,367,368]		bearing COLO 357 and PANC-1 xenografts; male BALB/c nu/nu mice (6 wk) with HN-9 xenografts [364,367–369]	cells to cisplatin and etoposide [364,369]	
Triptolide [260,370–381]	Possible mechanisms: increased nuclear export of NRF2 by stimulating exportin 1; increased nuclear translocation of NRF2; reduced expression of sirtuin 1 and inhibition of sirtuin 1-mediated nuclear accumulation of NRF2 [260,374,380]	Downregulation of *NFE2L2*, *HIF-1α*, *VEGFA*, *NF-κB* mRNA expression; inhibition of the NF-κB pathway; reduction in ARE-related genes; downregulation of sirtuin 3 expression leading to hyperacetylation of the genes of mitochondrial complex I and II; triggering of induced myeloid leukemia cell differentiation and protein expression [370,373–377]	Increased oxidative stress and mitochondrial dysfunction; anti-proliferative; pro-apoptotic; anti-metastatic; anti-angiogenic [375,378,379]	*In vitro*: Hs 578-T, MDA-MB-231, HUVECs, HL-60, K562, A549, NCI-H1299, NCI-H2009, NCI-H460, HCT116, HuCC-T1, QBC939, FRH0201, TM4, HepG2 cells *In vivo*: female nude mice (8 wk) bearing MDA-MB-231 xenografts; BALB/c nu/nu mice (6 wk) bearing A549 xenografts; male BALB/c nu/nu mice (7–8 wk) with orthotopic A549 xenografts; male BALB/c nu/nu mice (4–6 wk) with HuCC-T1 xenografts; BALB/c nu/nu mice bearing patient derived xenografts of hepatocellular carcinoma; Sprague-Dawley rats [370,373–375,377,378,380,381]	Poor water solubility; exhibits hematotoxicity and hepatotoxicity; liposomal encapsulation reduces toxicity; minnelide is a pro-drug of triptolide designed to overcome water solubility issues [375,378,379]	Yes [381]
Wogonin [382–390]	PI3K/Akt pathway suppression in a DNA-dependent protein kinase catalytic subunit-dependent manner [385,386]	Downregulation of *NFE2L2* mRNA and NRF2 protein levels and ARE-driven gene expression [385]	Antiproliferative; anti-angiogenic; antimigratory; pro-apoptotic [386]	*In vitro*: K562 (including multidrug resistant variant K562/A02), MCF-7, HepG2, SKOV3 (including cisplatin-resistant variant), OV-2008, 2008/C13*5, HEK293, AMC-HN-2/3/4/6/7/8/9/10 (including cisplatin-resistant variants for AMC-HN-4 and 9), SNU-1041/1066/1076, UM-SCC-1, THP-1, HCT116 cells, human oral keratinocytes, human oral fibroblasts, human skin keratinocytes *In vivo*: male BALB/c nu/nu mice (6 wk) bearing AMC-HN-4 and AMC-HN-9 xenografts; C57BL/6 mice (6–8 wk) with azoxymethane- and dextran sulfate sodium-induced colitis-associated cancer [385–390]	Sensitizes head and neck and ovarian cancer cells to cisplatin and reverses multidrug resistance in multiple cell lines; wogonin inhibited NF-κB and promoted NRF2 activation to decrease inflammation-induced injury and prevented the incidence and the development of colitis-associated cancer [386,387,389,390]	No

delivery systems have been described for PMF [393,394].

4.2. 4-Methoxychalcone

4-Methoxychalcone is a flavonoid synthesized by several plants that can inhibit NRF2-ARE transcriptional activity in A549 cells [212]. The inhibition seems to be correlated to decreased levels of phosphorylated Akt at Thr308. 4-Methoxychalcone significantly decreased ARE-luciferase activity at 21 μM in A549 cells.

Furthermore, treatment of A549 cells with 4-methoxychalcone enhanced the efficacy of cisplatin by increasing intracellular ROS production, although an opposite effect was observed in human embryonic kidney (HEK293) cells. In the latter, 4-methoxychalcone increased NRF2 activity through the upregulation of p-Akt (Ser473), thereby protecting these cells from cisplatin toxicity. The effects on the NRF2 pathway thus appear to be cell type-dependent [212]. A single study reported an absence of cytotoxic effects of 4-methoxychalcone in MDA-MB-231 cells, although further data on the cytotoxicity of this compound remain limited [211]. Additional pharmacodynamic properties of 4-methoxychalcone entail reversing the inhibitory effects of tumor necrosis factor (TNFα)-mediated adipogenesis via a peroxisome proliferator-activated receptor gamma (PPARγ)-dependent pathway in adipocytes [213] and antioxidant activity towards hydroxyl radicals [214].

Many of the biological effects of 4-methoxychalcone warrant further exploration and no studies have been conducted in combination with PDT.

4.3. ARE expression modulator 1

ARE expression modulator 1 is a small-molecular inhibitor that has been reported to downregulate NRF2 signaling in A549 cells *in vitro*, leading to modestly reduced cell proliferation and inhibition of cell proliferation under anchorage-independent growth conditions [215]. ARE expression modulator 1 priming additively sensitized A549 cells to the effects of doxorubicin, etoposide, and 5-fluorouracil in an NRF2 inhibition-dependent manner. Though the study could not determine the precise mechanism of action regarding the inhibition of NRF2, the process appears to require NRF2 to be constitutively activated.

In vivo, ARE expression modulator 1 was able to significantly inhibit tumor growth in A549 xenografts in 6-week-old male athymic nude mice when given an oral dose of 50 mg/kg twice a day. *In vivo* treatment with ARE expression modulator 1 did not result in the reduced expression of NRF2 but did result in the downregulation of downstream targets of NRF2, including *HMOX1*.

No studies have been conducted with ARE expression modulator 1 in combination with PDT.

4.4. Apigenin

Apigenin is a non-toxic, flavone-based PI3K/Akt pathway inhibitor that has been widely studied for its anti-cancer and anti-inflammatory properties [395–399]. The compound modulates various downstream targets in the PI3K/Akt pathway, most notably through inhibition of NRF2 and NF-κB and upregulation of various apoptotic proteins [395]. In terms of NRF2, apigenin is hormetic in that at low doses it upregulates NRF2 and thus imparts chemopreventive and anti-inflammatory effects, while at higher doses the drug inhibits NRF2 [226]. At higher doses apigenin also induces muscle relaxation and acts as a sedative [397]. Furthermore, apigenin enhances the efficacy of anti-cancer drugs such as 5-fluorouracil, cisplatin, cetuximab, doxorubicin, and sorafenib and minimizes chemotherapeutic toxicity in different types of cancer [395].

No studies have been conducted with apigenin in the framework of PDT, but studies on the combination of apigenin and doxorubicin have been performed in a PDT-induced signaling-pertinent context. Gao et al. [224] demonstrated that apigenin reverses drug resistance in doxorubicin-resistant hepatocellular carcinoma (BEL-7402/ADM) cells by inhibiting NRF2 activity via PI3K/Akt downregulation in a KEAP1-independent manner, which resulted in increased intracellular accumulation of doxorubicin and substantially enhanced the rate of apoptosis. This coincided with the downregulation of HO-1, aldo–keto reductase 1B10, and MRP5, which are fundamental to the xenobiotic and antioxidant responses. In another study by the same group, apigenin-mediated NRF2 inhibition was observed as a result of microRNA (miR)-101 upregulation [224]. Furthermore, apigenin inhibits the NF-κB [221,396] and HIF-1 pathways [220], thereby potentially enhancing tumor sensitivity to PDT [28,60]. Another possibly beneficial effect of apigenin is the downregulation of programmed death ligand 1 (PD-L1), as demonstrated in melanoma [225] and some breast cancer cell lines [227]. PD-L1 downmodulation renders cancer cells more susceptible to cytotoxic T cell clearance and therefore more amenable to the PDT-induced antitumor immune response [400]. A clinical trial has been registered (NCT00609310) studying apigenin's effect on tumor recurrence in resected colorectal carcinoma patients, although results have not been published since trial registration in 2008. Nanotechnological approaches have been described to increase cancer cell delivery and oncotherapeutic efficacy of apigenin [401].

4.5. Ascorbic acid

Ascorbic acid is commonly found in citrus fruits and taken as an oral food supplement. The phytochemical has also been researched as a chemotherapeutic agent and chemosensitizer, albeit with conflicting results [230,233,402]. With respect to NRF2, the combination treatment of ascorbic acid and imatinib restored drug sensitivity in imatinib-resistant leukemia (KCL-22/SR) cells, attributable to the impaired ability of NRF2 to bind DNA and corollary decrease in GCL mRNA and GSH protein levels [229]. Ascorbic acid further reduced NRF2 expression in combination with quercetin in prostate cancer (PC-3) cells, resulting in reduced enzymatic activity of GSH peroxidase, GSH reductase, and NQO1. A hormetic effect was observed in another line of prostate cancer (DU145) cells, where NRF2 expression increased at a dose of 200 μM ascorbic acid and 50 μM quercetin but decreased at a dose of 100 μM ascorbic acid and 75 μM quercetin [232]. Hormesis has been reported for ascorbic acid in terms of other cancer-related processes [403,404]. The activity of the abovementioned enzymes increased at the higher dose but remained at baseline levels at the lower dose [232]. In HeLa cells ascorbic acid (1–10 mM) caused a dose-dependent increase in ROS production and a decrease in NRF2 and p62 expression (HO-1 expression remained unaltered), sensitizing HeLa cells to cisplatin and doxorubicin [231].

In regard to PDT, the ascorbic acid-conjugated PS 5-(ethylamino)-9-diethylaminobenzo[a]phenothiazinium chloride was tested in glucose transporter 1-overexpressing cancer cells (KM12C and SNU-C5) *in vitro* (660-nm LED, 100 mW/cm^2) and *in vivo* (0.5 mg/kg/d, 660-nm laser, 2 W/cm^2, 10 min, cumulative radiant exposure of 1,200 J/cm^2, once every 5 days for 2 weeks) [236]. Ascorbic acid conjugation improved PS accumulation in cancer cells and the tumor due to the two one-electron oxidations of ascorbic acid into dehydroascorbic acid [405] by the tumor microenvironment and subsequent transport of dehydroascorbic acid into the cells by predominantly glucose transporter 1 and possibly other glucose transporter isoforms [402,406,407]. The exacerbated cellular loading of PS translated to greater PDT efficacy as a result of enhanced ROS generation and GSH depletion. Verteporfin-mediated PDT (1.8 nM, white light, 30 W daylight fluorescent bulbs and a UV light-removing surface, 2.2 mW/cm^2, 1.32–2.62 J/cm^2) in combination with ascorbic acid resulted in decreased survival of human leukemia (HL-60) cells, which exhibited an elevated redox state and a higher myeloperoxidase activity compared to human histiocytic lymphoma (U937) cells. This study demonstrated that ascorbic acid increased H_2O_2 production during verteporfin-PDT, which in turn resulted in a conversion to more reactive oxidants, such as hypochlorous acid, by myeloperoxidase [233]. Paradoxically, ascorbic acid also acted as a

cytoprotective agent in U937 cells, which had low redox levels and no demonstrable myeloperoxidase activity. The addition of 4-aminobenzoic acid hydrazide, a known inhibitor of the ROS-producing enzyme myeloperoxidase, to HL-60 cell cultures increased cell survival post-PDT, indicating that dampening of secondary ROS production directly translates to higher survival rates [233]. For further clarification, ascorbic acid is a hydrophilic antioxidant that can react with $^1O_2$ and produce the more innocuous H_2O_2, which could be neutralized/dismutated through peroxide-removing systems such as GSH and catalase [233]. Its antioxidant properties may in some cases ameliorate the extent of photo-induced hyperoxidative stress and reduce PDT-induced cell death [233]. In rat sarcoma (DS) cells treated with 5-ALA-PDT (0.5 mM, halogen lamp emitting from 420-1400 nm (Hydrosun PIRA-radiator, Hydrosun Medizintechnik), 70 mW/cm^2, cumulative radiant exposure of 19 J/cm^2), ascorbic acid reduced PDT effects on lipid and protein oxidation, expression of Fas ligand and TNFα, mitochondrial damage, and apoptosis-inducing factor release, resulting in reduced cell death [230]. Similarly, ascorbic acid reduced cell death in 5-ALA-treated human melanoma cells (0.5 mM, halogen lamp emitting wavelengths from 420-1400 nm (Hydrosun PIRA-radiator), 18 mW/cm^2, cumulative radiant exposure of 0.54–5.40 J/cm^2) [235].

It is important to note that the use of antioxidants such as ascorbic acid can bring about pleiotropic effects which can be either advantageous to PDT outcomes due to inhibition of NRF2 DNA binding or deleterious due to ROS neutralization [408]. Ascorbic acid can also act as a pro-oxidant through its interaction with transition metal ions, where it acts as a catalyst for the Haber-Weiss component of the Fenton reaction [409], thereby depending on e.g., the pool of labile iron that is present in certain types of cells [124], including pre-mutagenic somatic cells [410] and cancer cells [411]. This effect can synergize with PDT as exemplified in an experiment with Photofrin-treated mouse mammary carcinoma (EMT6) cells, revealing a surge in ROS after PDT in the presence of ascorbic acid. The elevation in ROS levels was caused by the PDT-induced release of transition metal ions, greatly augmenting the antitumor impact *in vitro* (5 μg/mL, 10 mW/cm^2, 635-nm semiconductor laser, cumulative radiant exposure of 0.6–2.4 J/cm^2) and *in vivo* (5 mg/kg, 135 mW/cm^2, 635 nm, cumulative radiant exposure of 65 J/cm^2) [234]. Moreover, ascorbate, the deprotonated form of ascorbic acid, facilitates HIF-1α depletion [412,413] owing to its redox cycling of ferric to ferrous iron that is required for HIF-1α hydroxylation and subsequent proteasomal removal [414,415]. Via this route, ascorbic acid inhibits HIF-1α-triggered survival signaling [28,60] and potentially compounds the effects of ascorbic acid-mediated NRF2 inhibition on reduced cancer cell survival. Nevertheless, as ascorbic acid triggers a plethora of different mechanisms that overlap with PDT-induced pathways, it is necessary to appreciate the physiological features of a tumor to gauge whether ascorbic acid would produce a yielding net effect treatment-wise.

4.6. Brusatol

A well-characterized NRF2 inhibitor is the natural product brusatol, a quassinoid compound extracted from the evergreen shrub *Brucea javanica* [242,244]. Brusatol's mechanism of action features some controversial aspects. Recent studies indicate that brusatol is an inhibitor of global protein synthesis and particularly reduces the expression of short half-life proteins such as NRF2 [243,246]. Initial findings in various human cell lines with different KEAP1 statuses revealed that brusatol amplifies KEAP1-mediated polyubiquitination and subsequent proteasomal degradation of NRF2 [244], which was contested in a later study showing that brusatol-induced NRF2 depletion does not require Keap1 activity [242]. However, this was shown in mouse hepatoma (Hepa-1c1c7) cells [242]. The exact mechanism notwithstanding, brusatol acts as a sensitizer to various anticancer therapies [203,416]. Brusatol enhances the toxicity of cisplatin, carboplatin, 5-fluorouracil, etoposide, and paclitaxel in A549, MDA-MB-231, and HeLa cells [244]. Brusatol also radiosensitizes A549 cells that were previously therapy-resistant due to the overexpression of NRF2, resulting in increased ROS accumulation, enhanced DNA damage, and ultimately cell death [416]. Other pharmacodynamic properties of brusatol that infringe on cancer cell metabolism and sustenance include the inhibition of signal transducer and activator of transcription (STAT)3 activity, i.e., abrogation of STAT3 phosphorylation at Tyr705 [247–249], PI3K/Akt/NF-κB pathway signaling [250], and S-phase kinase-associated protein 1-S-phase kinase-associated protein 2 interaction [245], altogether leading to reduced anti-apoptotic gene expression, proliferation, and epithelial-mesenchymal transition (EMT) propensity.

In terms of PDT, a recent paper by Tao et al. describes the incorporation of brusatol into PEGylated, folate-functionalized polydopamine nanoparticles containing surface-tethered chlorin e6 as PS and manganese dioxide as an oxygen generator to promote ROS production. Combining PDT (660-nm laser, 10-min illumination, 500 mW/cm^2) with photothermal therapy (hyperthermia, 808-nm laser, 10-min illumination, 1.5 W/cm^2) resulted in notably potentiated antitumor efficacy in both *in vitro* and *in vivo* models of pancreatic cancer (MIA PaCa-2) cells that entailed the inhibition of the NRF2 pathway and the heat shock response [203]. NRF2 inhibition by brusatol inactivated glutathione peroxidase 4 and ferritin heavy chain that in turn triggered ferroptotic cell death.

4.7. Chrysin

Chrysin is another flavonoid found in numerous plant extracts and honey. NRF2 overexpressing cells (BEL-7402/ADM) resistant to doxorubicin could be sensitized by combined treatment with chrysin. This downregulated the NRF2 and upstream PI3K/Akt and ERK pathways, resulting in the downregulation of downstream targets such as MRP5, HO-1, and aldo–keto reductase 1B10 at both mRNA and protein levels [255]. Furthermore, through the downregulation of NRF2/ERK signaling, chrysin was able to inhibit cell migration in glioblastoma (U251 and U87) cells and reduce cell viability in a concentration- and time-dependent manner. It similarly reduced tumor growth in immune-deficient BALB/c mice carrying U87 xenografts, showing little to no toxicity [256]. However, chrysin can also upregulate NRF2 expression, although the conditions under which this occurs have not yet been elucidated [226]. Examples include upregulation of NRF2 in rat hepatocytes and myocardial tissue of rats on a high-fat diet, conferring protection from oxidative stress [226,257,259].

Several chrysin-derivatives conjugated to porphyrin derivatives have been characterized and tested in PDT (12-W purple LED lamp, 10 min illumination) [258]. A number of these conjugated derivatives showed improved cytotoxicity compared to their unconjugated parent porphyrins. However, inhibition of NRF2 was not investigated with respect to these derivatives.

4.8. Clobetasol propionate

Clobetasol propionate is a glucocorticoid able to inhibit NRF2 by both blocking nuclear accumulation of activated NRF2 and stimulating GSK-3β- and β-TrCP-dependent proteasomal degradation [261]. Clobetasol propionate was able to inhibit cell proliferation in KEAP1-mutant cancer cell lines such as A549 but not in cell lines that expressed wild-type KEAP1. In addition to targeting NRF2, clobetasol propionate was able to downregulate HIF-1α in WiL2-NS non-secreting B lymphocytes [262]. Another target of clobetasol propionate is cytochrome P450 3A5 (CYP3A5). Clobetasol propionate inhibited the growth of pancreatic ductal adenocarcinoma-derived organoids that expressed high levels of CYP3A5 [417]. The inhibition of CYP3A5 sensitized the organoids to drugs that are CYP3A5 substrates, such as cisplatin. Similar to the anti-proliferative effect in KEAP1 mutant cell lines, clobetasol propionate either had a weak or no anti-proliferative effect when tested in cell lines or patient-derived organoids that did not express CYP3A5 or only had

low expression, indicating that the anti-tumor efficacy of clobetasol propionate is dependent on tumor specifics.

Topical combinatory treatment with clobetasol propionate (thin layer 0.05% Dermovate; GlaxoSmithKline Pharma A/S, Broendby, Denmark) and methyl aminolevulinate-PDT (methyl aminolevulinate 16%; cream Metvix; Galderma Nordic AB, Uppsala, Sweden; red light-emitting diode (Aktilite 128; PhotoCure ASA, Oslo, Norway), illuminated at 580–670 nm (peak at 630 nm) for approximately 9 min with a total radiant exposure of 37 J/cm^2) was applied for the treatment of multiple actinic keratosis on the face or scalps of patients, where the treatment area was divided in two symmetrical sections for PDT-only and combinatory treatment. Clobetasol propionate significantly reduced PDT-induced erythema compared to the PDT-only treatment. However, no significant change in regard to 3-month complete response rate was detected [263].

4.9. Cryptotanshinone

Cryptotanshinone, a quinoid diterpene isolated from the root of *Salvia miltiorrhiza*, has a broad range of biological activity affecting different pathways that contribute to its anti-inflammatory and anti-cancer properties [271]. It was able to downregulate NRF2, reversing resistance to gefitinib and cisplatin in a number of different non-small cell lung cancer (NSCLC) cell lines [272,275]. Cryptotanshinone also downregulates the Akt, STAT3, and NF-κB pathways and suppresses p38, c-Jun N-terminal kinase (JNK), and ERK1/2 phosphorylation in a dose-dependent manner [272,273,275]. However, some studies also showed cryptotanshinone upregulating NRF2, providing cytoprotective functions in human induced neuronal progenitor cells made by reprogramming fibroblasts isolated from a Parkinson's disease patient [274], and reducing inflammatory signaling in lipopolysaccharide-stimulated RAW 264.7 macrophages [273]. The circumstances affecting its activity on NRF2 are not explored, but possibly could be dependent on the metabolic status or disease type, although none of these examples concern cancer.

No studies have been conducted in combination with PDT.

4.10. Digoxin

Digoxin is a cardiac glycoside used to treat congestive heart failure through the inhibition of Na^+/K^+-ATPase but is also being tested in clinical trials as an anticancer drug [281]. A study on gemcitabine-resistant pancreatic cell lines found that digoxin decreased *NFE2L2* expression, downregulating NRF2 pathway activity [279]. This allowed for the resensitization of gemcitabine-resistant SW1990 and PANC-1 cell lines in a KEAP1-independent manner, with evidence pointing towards the attenuation of PI3K/Akt signaling. Digoxin also inhibited EMT in NSCLC (A549 and HT1299) cells by blocking the PI3K/Akt/mechanistic target of rapamycin kinase (mTOR) pathway by reducing p-Akt and inducing apoptosis in A549 cells and autophagy in A549 and H1299 cells [280]. Digoxin is also known to be an inhibitor of the HIF-1 pathway, which is another survival pathway activated by PDT [28,60,276].

No studies have been conducted in combination with PDT.

4.11. Ethionamide

Ethionamide is an anti-tuberculosis drug with a chemical structure that is similar to that of isoniazid (section 4.15). This inhibitor suppressed the transcription of NRF2 target genes, thereby sensitizing human acute monocytic leukemia (THP-1) cells to arsenic trioxide toxicity, resulting in ethionamide concentration-dependent augmentation of arsenic trioxide-mediated inhibition of cell proliferation that was partially NRF2-dependent [286].

No studies have been conducted in combination with PDT.

4.12. Febrifugine

Febrifugine is an antimalarial drug (quinazolinone alkaloid) isolated from *Dichroa febrifuga* that has also been tested against visceral leishmaniasis [287], which increases ROS levels and induces cytotoxicity whilst stimulating a Th1 immune response in BALB/c mice infected with *L. donovani*. In A549 cells it was shown to inhibit NRF2 activity, but the mechanism of action has not been uncovered [288]. Halofuginone (section 4.13) is a derivative of febrifugine [288].

No studies have been conducted in combination with PDT.

4.13. Halofuginone

Halofuginone is a febrifugine (section 4.12) analog with a wide range of beneficial activities in malaria, cancer, and inflammatory and autoimmune diseases [293]. With respect to cancer, it is able to reduce angiogenesis and metastasis by inhibiting the transforming growth factor (TGF)-β pathway by targeting SMAD family member 3 phosphorylation, downregulating fibrosis-promoting proteins such as collagen and matrix metalloproteinase (MMP)2, and reducing tumor stroma [293]. Halofuginone is also an inhibitor of NRF2, with several studies showing halofuginone downregulating NRF2 activity, reflected by reduced protein levels of p-ERK1/2, ERK1/2, and p-Akt [202,288,292,294,295].

Halofuginone was able to sensitize treatment-resistant cancer cells to cisplatin, doxorubicin, and cabazitaxel as a result of NRF2 reduction [288,292]. Reduction of NRF2 seems to occur through the inhibition of protein synthesis by amino acid starvation [288]. Another study also found that an increase in uncharged prolyl-tRNA resulted in the expression of general control nonderepressible 2 that stimulated GSK-3β-dependent proteasomal degradation of NRF2 [295].

In addition to inhibiting NRF2, halofuginone was also able to deactivate NF-κB and AP-1 signaling [296,297], which are part of the inflammatory and immediate early stress response, respectively [28]. A study using methylcholanthrene-induced malignant fibrous histiocytoma in rats found that halofuginone inhibited angiogenesis, which coincided with reduced tumor growth and extended survival. A phase I clinical study in patients with advanced solid tumors found that halofuginone exhibited gastrointestinal toxicity in the form of nausea and vomiting within 30 min to 1 h after oral administration using a dose of 2 mg/day, requiring the addition of prophylactic anti-emetics [299]. Furthermore, while no hepatotoxicity was observed in blood values, several patients experienced bleeding complications for which a causal relation with halofuginone could not be excluded.

Halofuginone enhanced 5-ALA-PDT (red LED light (633 nm) at 15 mW/cm^2, 1.8 J/cm^2) in cutaneous squamous cell carcinoma (SCL-1 cells), reducing clonogenicity and migration through the reduced accumulation of NRF2 [202]. It was further demonstrated that a daily dose of 2 μg (i.p.) of halofuginone enhanced 5-ALA-PDT (power density of 80 mW/cm^2, 19.2 J/cm^2) in a mouse model of cutaneous squamous cell carcinoma (XL50 co-injected with NIH/3T3 fibroblasts), resulting in complete clearance of the tumor, whereas single agent treatment with either 5-ALA or halofuginone only slowed tumor growth [202].

4.14. IM3829

4-(2-Cyclohexylethoxy)aniline or IM3829 is an aniline-based compound that inhibits NRF2 nuclear translocation and reduces *NFE2L2* expression in a concentration-dependent manner, leading to the downregulation of downstream targets of NRF2 [115]. IM3829 was used to sensitize radioresistant lung cancer cell lines A549, NCI-H1299, and NCI-H460, increasing the extent of radiation-induced apoptosis. IM3829 enhanced tumor growth reduction when combined with radiotherapy in nude mice bearing A549 or NCI-H1299 xenografts. IM3829 exhibited no clear cytotoxicity on its own or had any observable toxic effects on the treated mice [115].

No studies have been conducted in combination with PDT.

4.15. Isoniazid

Isoniazid is an antibiotic drug used for the treatment of tuberculosis and is also proposed as an anticancer drug. Isoniazid can inhibit NRF2 activity by blocking the nuclear translocation of NRF2 via karyopherin β1 and ERK1 inhibition [303,304]. Isoniazid was able to sensitize THP-1 cells to arsenic trioxide [286]. Treatment with isoniazid also increased ROS levels, reduced GSH, blocked DNA synthesis, and negatively affected mitochondrial functioning, leading to induction of apoptosis in HepG2, THLE-2, and Hep3B cells and mouse oocytes [303,304,307]. DNA synthesis was blocked by the disruption of the mitotic spindle morphology, which was shown in a study on the effect of isoniazid on mouse fertility, resulting in reduced oocyte maturation and the number of offspring [307]. Another study also found evidence of hepatotoxicity in HepG2 cells, which coincided with a decrease in levels of proliferator cell nuclear antigen (PCNA), which has an important role in DNA replication. Hepatotoxicity was confirmed in adult BALB/c mice that had received isoniazid [304].

Isoniazid has not been tested in PDT. However, a study used conjugation of isoniazid to the fluorescent dye MHI-148 to specifically target mitochondria in prostate cancer cells through inhibition of oncogene monoamine oxidase A by isoniazid. MHI-148 is a PS, and combining PDT with isoniazid in this manner has been proposed for prostate cancer [305]. Isoniazid was also tested in combination with photothermal therapy through conjugation to the fluorescent dye ZW800-1, combining image-guided photothermal effects of ZW800-1 with the anti-tumor potential of isoniazid, resulting in a synergistic reduction in tumor growth in HT-29 xenografts in mice compared to the respective singular treatments [308].

4.16. K-563

K-563 is a novel inhibitor of the NRF2 pathway isolated from Streptomyces. The exact molecular target is not known, as the inhibitor does not affect NRF2 expression or nuclear translocation [309]. However, K-563 did result in the downregulation of NRF2 downstream target genes, reduced GSH levels, and a concentration-dependent increase in ROS formation. Furthermore, K-563 exerted an inhibitory effect on the proliferation of both lung cancer (A549 and LK-2) cells and gallbladder cancer (TGBC24TKB) cells. K-563 also inhibited the proliferation of normal lung epithelial cells (BEAS-2B), albeit not to the same extent. In addition, K-563 exerted a synergistic effect with cisplatin and etoposide in inhibiting cell proliferation [309].

No studies have been conducted in combination with PDT.

4.17. Kaempferol

Kaempferol, a natural flavonoid extracted from plants, was found to decrease the proliferation of NSCLC (A549, NCI-H460) cells by inhibiting the NRF2-mediated antioxidant response [314]. However, kaempferol has also been reported as an inducer of NRF2 expression. Wang et al. [310] demonstrated that kaempferol increased ROS-mediated apoptosis in *in vitro* and *in vivo* pancreatic cancer models by inhibiting transglutaminase 2. Inasmuch as apoptosis is triggered by increased oxidative stress, NRF2 is activated in the process. In the case of colorectal adenocarcinoma (Caco-2) cells, exposure to 10 μM kaempferol increased the expression of NRF2 and its targeted genes, while kaempferol neutralized NRF2 activation upon co-exposure with the potent NRF2 inducer benzo[a]pyrene [316]. Similarly, kaempferol suppressed *tert*-butylhydroquinone-induced nuclear translocation of NRF2 in HepG2 cells [315].

To date, no studies have been published on the combination of this flavonoid and PDT.

4.18. Luteolin

Luteolin, a natural flavonoid derived from various plant extracts, was shown to decrease NRF2-induced ARE-driven gene expression by stimulating *NFE2L2* mRNA degradation, thereby reducing NRF2 protein expression [172,317,326]. Increased sensitization to oxaliplatin, bleomycin, and doxorubicin was observed in A549 cells exposed to luteolin (i.e., 2-fold reduction in the IC_{50}) [317]. Oxaliplatin-resistant colorectal cancer cells (HCT116 and SW620) were re-sensitized to oxaliplatin by luteolin [318]. Luteolin has also been shown to reduce NRF2 *in vivo*. Wild-type mice (C57BL/6) treated daily with luteolin (40 mg/kg, gavage) for 14 days showed a reduction in protein levels of NQO1, HO-1, and GSH compared to non-treated mice, while no effect was observed in C57BL/6 $Nrf2^{-/-}$ transgenic mice [318]. This demonstrates that luteolin acts directly on NRF2. Moreover, a synergistic effect against cancer cells was observed in A549 xenograft-bearing mice treated with cisplatin (5 mg/kg, i.p.) and luteolin (40 mg/kg, gavage) every other day for 32 days [322]. Controversially, luteolin was also shown to increase the expression of NRF2 and downstream genes in cancer cells [323,325]. Kang et al. found that luteolin activates an antioxidant response in the human colon cancer cell lines HT-29 and SNU-407 by epigenetically activating the *NFE2L2* gene [323].

Given the successful tumor inhibition *in vivo*, new drug delivery systems have been developed for luteolin. When loaded into phytosomes, luteolin sensitized MDA-MB-231 cells to doxorubicin [324] and induced higher suppression of NRF2 and its downstream target genes compared to the free drug [324].

In terms of PDT, luteolin was found to increase the toxicity of the cationic PS porphyrin TMPyP4 by decreasing the NRF2-mediated antioxidant response. The combination of TMPyP4 (40 nM TMpyP4, 7.2 J/cm^2) and luteolin (20 μM) induced a stronger reduction in cell viability than each component separately [172].

4.19. Metformin

The antidiabetic drug metformin has been shown to indirectly downregulate *NFE2L2* gene expression by interfering with sirtuin 1 expression in MCF-7 cancer cells through upregulation of miR-34a in a wild-type p53-dependent manner [332]. Metformin has also been linked to the inhibition of signaling pathways upstream of the NRF2 pathway [329–331]. The treatment of HepG2, HeLa, and A549 cells with 1–5 mM metformin for 24 h reduced ERK1/2 phosphorylation and inhibited HO-1 expression. The highest metformin concentration increased the sensitization of HeLa cells to paclitaxel [330]. Untreated/naive breast cancer patients treated with 500 mg of metformin three times daily after diagnostic biopsy until surgery showed reduced phosphorylation of ERK1 and AMP-activated protein kinase (AMPK) [331].

The efficacy of metformin in combination with PDT was recently studied in a heterotypic 3D culture model of pancreatic cancer. These models exhibited elevated redox activity and overexpressed cyclooxygenase 2 and HO-1. Metformin ameliorated the redox activity in the microtumors and abrogated resistance to verteporfin-PDT (0.25 μM, 1-h incubation, 690 nm, irradiance of 150 mW/cm^2, radiant exposure of 1–50 J/cm^2) and oxaliplatin (tested dose range of 10–1,000 μM) [333]. Male Wistar rats (3-months old) bearing breast (Walker 256) carcinosarcomas were shown to benefit from a combinatorial treatment of tetrasulfophenyl-porphyrin-mediated PDT and metformin. In combination with 5-ALA PDT (0.6, 1.2, 2.5, 5 mM, illuminated between 1–10 J/cm^2 using a 630-nm laser), metformin at concentrations of 1 or 5 mM enhanced cytotoxicity and induced autophagic and apoptotic cell death in KLN205 lung cancer cells [334]. Administration of metformin before or after illumination was equally effective in reducing cyclooxygenase 2 expression and enhancing apoptosis in cancer cells [335]. Moreover, co-administration of metformin with PSs via nanoparticles has been shown to enhance PDT efficacy by reducing mitochondrial respiration in cancer cells and hence increasing oxygen availability for photochemical

reactions [418,419].

4.20. ML385

ML385 is a small molecule that blocks NRF2 transcriptional activity by binding directly to the Neh1 domain of NRF2 (Fig. 3), thereby interfering with the binding of the NRF2-MAF protein complex to regulatory DNA binding sequences. This has been shown in various NSCLC cell lines harboring KEAP1 mutations *in vitro* [337]. In addition, ML385 reduced mRNA levels of multiple antioxidant target genes and inhibited tumor growth in xenograft models using KEAP1-mutant NSCLC cells (in combination with carboplatin) [337]. Also, in dipeptidyl peptidase-4-treated murine breast cancer (4T1) cells, ML385 attenuated NRF2 expression and NRF2-responsive gene levels [338].

The combination of ML385 and PDT has been studied in a breast cancer model [339]. 4T1 tumor-bearing mice were treated with ML385 (30 mg/kg, gavage) and etoposide (10 mg/kg), a heat shock protein (HSP)60 inhibitor, 1 day prior to treatment with poly(ethylene oxide)-b-poly(methacrylic acid) nanoparticles functionalized with the PS cobalt tungstate. The tumors were illuminated with an 808-nm laser (1.0 W/cm^2) for 10 min at 1 h post-injection. The combination of ML385 and etoposide prevented tumor regrowth after 10 days, which did occur in the PDT-only treatment group. These results support the hypothesis that cells are more sensitive to PDT when NRF2 is inhibited by ML385. Unfortunately, there was no group included in which the mice were pre-treated with ML385 only, followed by PDT. Consequently, it is not possible to determine what the individual contributions of ML385 and etoposide were in preventing tumor regrowth. As with PDT, the cytotoxic effect of radiotherapy can also be counteracted by the activation of the NRF2 pathway in cancer cells. One study has shown that inhibition of NRF2 activation by ML385 sensitized breast cancer stem cells to radiotherapy [420], which is an indirect indication that these cells would also be more sensitive to PDT after pre-treatment with ML385.

4.21. NRF2-IN-1

Pyrazolyl hydroxamic acid derivative 1-(4-(*tert*-butyl)benzyl)-3-(4-chlorophenyl)-N-hydroxy-1H-pyrazole-5-carboxamide, or NRF2-IN-1, is an inhibitor of NRF2 and may be a promising agent in the treatment of acute myeloid leukemia, as NRF2 is persistently activated in this tumor. NRF2-IN-1 had a profound growth-inhibitory effect in the acute myeloid leukemia cell lines THP-1, HL-60, and U937. A similar anti-growth effect was observed in a chicken embryo model [341]. NRF2-IN-1 induced apoptotic cell death, which could be ameliorated by upregulating NRF2. Apoptosis coincided with decreased B-cell lymphoma 2 (Bcl-2), and Bcl-2 associated X apoptosis regulator (BAX) protein levels, indicating that mitochondria-dependent apoptotic signaling contributed to NRF2-IN-1-induced apoptosis [341]. The exact mechanism by which NRF2-IN-1 interferes with the NRF2 pathway is not fully understood. One study found that NRF2-IN-1 elevated levels of KEAP1 in a cardiac ischemia/reperfusion model [340], which might explain the NRF2 inhibitory effects of NRF2-IN-1.

Studies in combination with PDT have not yet been conducted.

4.22. Ochratoxin A

Ochratoxin A is a toxic secondary metabolite produced by several fungal species of *Aspergillus* and *Penicillium*, and a common food-contaminating mycotoxin. Ochratoxin A causes nephrotoxicity and renal tumors in a variety of animal species, although the health effects in humans are less characterized [421].

Ochratoxin A inhibits the expression of *NFE2L2* genes in porcine kidney tubular cells, normal rat kidney epithelial cells, and in primary hepatocyte cultures [346,347]. Four different mechanisms have been ascribed to ochratoxin A in terms of NRF2 inhibition: (1) impairment of NRF2 nuclear translocation; (2) blocking of NRF2 DNA binding; (3) induction of epigenetic changes that affect NRF2 transcription; and (4) upregulation of miR-132 targeting *NFE2L2* [345]. The reduction of *NFE2L2* expression resulted in oxidative DNA damage *in vitro*, which was confirmed in kidneys *in vivo* [347]. The oxidative stress could be prevented with inducers of NRF2 activity. Moreover, the oxidative stress induced by exposure to ochratoxin A could be prevented by NRF2 activators [347]. The incubation of PANC-1 cells with a combination of 10 or 20 μM of ochratoxin A with 40 nM of the cationic porphyrin TMPyP4 (cumulative light dose of 7.2 J/cm^2) inhibited cell viability more than the porphyrin alone (~ 30%), further supporting the hypothesis that, when NRF2 is inhibited by ochratoxin A, cells are more sensitive to PDT [172].

4.23. PIK-75

PIK-75, known as a PI3K/DNA-dependent protein kinase catalytic subunit (DNA-PKcs) inhibitor, is an imidazopyridine that selectively inhibits the p110α subunit of PI3K [351]. Duong et al. demonstrated in human pancreatic cancer (AsPC-1 and MIA PaCa-2) cells that PIK-75 indirectly reduced NRF2 protein levels and mRNA expression of *HMOX1* and *MRP5*, and increased the susceptibility of these cells to gemcitabine [350]. They further evaluated the combinatory effect of gemcitabine and PIK-75 in immunocompromised mice bearing subcutaneous AsPC-1 or MIA PaCa-2 xenografts. Mice were treated by i.p. injection twice a week with 20 mg/kg of gemcitabine and five times a week with PIK-75 (2 mg/kg). The latter to ensure the inhibitory effects on NRF2. Co-administration of PIK-75 resulted in a significant reduction in tumor growth compared to gemcitabine alone, demonstrating the synergistic effect of PIK-75 with chemotherapy [350].

Studies in combination with PDT have not yet been conducted.

4.24. Retinoic acid

(All-trans) Retinoic acid, available under the name tretinoin for the treatment of acne or acute promyelocytic leukemia, has been found to inhibit NRF2-mediated activation of ARE genes along with other activators of retinoic acid receptors [352]. Activated retinoic acid receptor α competes with NRF2 for ARE binding and prevents NRF2 from binding to ARE, thereby hindering the transcription of NRF2-related genes [352]. Treatment of leukemia cells with arsenic trioxide and all-trans retinoic acid induced more toxicity than arsenic trioxide alone via retinoic acid receptor α activation and consequent NRF2 blockage [360]. Mutation of retinoic acid receptor α was shown to interfere with the inhibitory effect of retinoic acid and therefore an assessment of the tumor mutational profile can help predict resistance to retinoic acid [360]. Conversely, a higher toxic concentration of retinoic acid has been suggested to promote NRF2 activity in response to oxidative stress [363].

Pretreatment with retinoic acid before fimaporfin-based PDT resulted in improved therapeutic outcomes in several breast and colon cancer cell lines (SKBR3, HCT116, and HT-29) *in vitro* (LumiSource, PCI Biotech, Oslo, Norway; no data on wavelength; 0.58 J/cm^2, 0.87 J/cm^2, and 1.16 J/cm^2) [362]. However, in an HT-29 xenograft model (5 mg/kg systemic or 20 μg intratumoral administration, 652 nm, irradiance of 90 mW/cm^2, cumulative light dose of 15 and 10 J/cm^2), retinoic acid yielded non-significant tumor growth delay relative to the PDT-only group. Nevertheless, 2 of 5 mice in the retinoic acid-PDT group achieved a complete response, while this was the case for none of the animals in the monotherapy groups (PDT or retinoic acid). Additionally, a PDT vaccination study found that, after mice had been inoculated using chlorin e6-PDT treated squamous cell carcinoma (SCCVII) cells (30-min PS incubation, 665 ± 10 nm (150-W quartz tungsten halogen lamp), radiant exposure of 1 J/cm^2), retinoic acid treatment further improved survival time after injection with viable SCCVII cells present in the vaccinated mice [361]. They attributed this effect to retinoic acid differentiating myeloid-derived suppressor cells into mature myeloid

cells, thereby reducing the tolerogenic tumor microenvironment and improving the antitumor immune response [353,361].

4.25. Trigonelline

Trigonelline, a natural alkaloid extracted from raw coffee beans, has been found to reduce NRF2 nuclear translocation in several cell lines while not affecting *NFE2L2* transcription [364,367,368]. Moreover, the compound blocks NRF2 activation and nuclear translocation by inhibiting the epidermal growth factor receptor pathway [364,368]. Reduced nuclear accumulation of NRF2 in PANC-1 and COLO 357 xenografts treated with 0.02 mg/kg trigonelline increased sensitivity to etoposide [368]. The combination of trigonelline with artesunate, an anti-malarial drug that induces cell death via ROS production, reversed cisplatin resistance and reduced tumor growth in a head and neck cancer model (artesunate: 50 mg/kg daily, trigonelline: 50 mg/kg daily) [369].

Hitherto no studies have been conducted in combination with PDT.

4.26. Triptolide

Triptolide is a natural compound derived from the root of the *Tripterygium wilfordii* Hook. f. plant that is used in traditional Chinese medicine [379]. It possesses both anti-inflammatory and anti-cancer properties and has been shown to induce apoptosis and reduce proliferation, metastasis, and angiogenesis in various types of cancer [422–429].

Triptolide has been shown to inhibit NRF2, but there is some inconsistency in the manner by which this occurs. In HL-60 and K562 cells, which have been made resistant to doxorubicin and imatinib, respectively, through overexpression of HIF-1α and NRF2, triptolide reduced NRF2 expression and resensitized the resistant cells by reducing the transcription of both genes [373]. Contrastingly, triptolide did not reduce NRF2 expression in A549 cells but instead stimulated the nuclear export of NRF2 via chromosome region maintenance 1 (also known as exportin 1), thereby preventing NRF2 target gene expression and enhancing cisplatin-induced apoptosis. Triptolide also increased oxidative stress and was able to inhibit tumor growth in A549 xenografts [374]. Another study found both an increased expression of NRF2 and increased nuclear translocation of NRF2 in triptolide-treated p53 knockout HCT116 cells [375]. The authors contended that this upregulation was in response to increased levels of oxidative stress caused by triptolide's disruption of mitochondrial function, owing to downregulation of several key complexes (I and II) of the electron transport chain through targeting of sirtuin 3. Another proposed mechanism is via inhibition of sirtuin 1 expression and the interaction between sirtuin 1 and NRF2, which in mouse Sertoli (TM4) cells led to a reduction in NRF2 nuclear accumulation and ARE-activity [380]. This implies that triptolide can have varying different biological effects and molecular targets between different tissue types and metabolic states. Furthermore, triptolide exhibited adverse events in clinical trials, particularly hepatological and nephrological toxicity [379], which compromises its clinical utility. Clinical translation is further complicated by the molecule's slight lipophilicity (Fig. 6), necessitating chemical modification or encapsulation into an aqueous solution-compatible carrier system. Several derivatives and (nano)formulations have been investigated to circumvent toxicity and optimize the pharmacokinetics, including the development of the pro-drug minnelide that is rapidly converted into triptolide in the bloodstream [376]. Triptolide-loaded liposomes have also been designed and showed reduced toxicity whilst improving tumor specificity and cytotoxicity *in vivo* [378].

Triptolide has the potential to target several pathways relevant for cancer cell survival in PDT through its ability to inhibit VEGFA, HIF-1α [373], HSP70, and NF-κB [376], i.e., mediators of survival signaling and tumor growth [28]. Triptolide has been investigated in conjunction with PDT through co-delivery with liposomal Ce6, improving tumor growth inhibition after 4 cycles of treatment (i.v. dose of 0.04 mg/kg Ce6 and 0.4 mg/kg triptolide, 650 nm laser, irradiance of 0.5 W/cm^2, 10 min illumination following 24 h after administration) compared to single-agent therapy in a patient-derived hepatocellular carcinoma tumor model and reducing triptolide's systemic toxicity [381].

4.27. Wogonin

Wogonin, a flavonoid extracted from the root of *Scutellaria baicalensis*, was found to inhibit the transcription of the *NFE2L2* gene in MCF-7 and K562/A02 cells [385,387]. The inhibitory effect of wogonin on NRF2 is accomplished indirectly via suppression of the PI3K/Akt pathway in a DNA-PKcs-dependent manner [385,386], and has been shown to reverse multidrug resistance in different cell lines [386,387,389]. Mice subcutaneously implanted with cisplatin-resistant head and neck cancer (AMC-HN4 and AMC-HN9) cells have been shown to benefit from the combination of chemotherapy with wogonin. Mice treated with 5 mg/kg cisplatin once per week and 50 mg/kg wogonin once per day (both i.p.) exhibited reduced NRF2 expression in cancer cells and decreased tumor growth compared to cisplatin-only treated mice [389]. Furthermore, the synergistic effect of wogonin with doxorubicin has been successfully tested in a drug-resistant leukemia model [385]. As reported for other models, the NRF2 inhibitors had to be administered frequently and at high doses (40 mg/kg, once every other day). Similar to chrysin (section 4.7) and apigenin (section 4.4), wogonin has also been shown to promote NRF2 activity [390] and therefore might have a dual role dependent on the cell transcriptional profile.

The compound has not been investigated in combination with PDT.

4.28. Notes on in vitro cytotoxicity testing

Many of the *in vitro* cell viability assays that were employed in the studies referenced in section 4.1 through 4.27 entail short-term viability assays, which include MTT/MTS/XTT, WST-1/WST-8 (CCK-8), resazurin/AlamarBlue, ATP-luminescence (CellTiter-Glo), LDH release, and trypan blue/PI exclusion assays. However, these assays often correlate poorly with clonogenic survival after PDT and other cytotoxic stresses. Metabolic or membrane integrity readouts can misclassify cells that are alive/metabolically active yet destined to die via delayed apoptosis/mitotic catastrophe or permanently growth-arrested (cytostatic) cells as 'viable' [430]. In contrast, the clonogenic assay measures a cell's ability to undergo unlimited proliferation post-insult and is therefore the gold standard for *in vitro* cytotoxicity/viability testing, integrating early and delayed lethal events and distinguishing cytostasis from true cell kill [431,432]. The cytotoxicity information presented in the preceding sections should therefore be contextualized to assay propriety and future *in vitro* analyses with respect to PDT and molecular adjuvants should be performed using the highest-standard test methods.

5. Interaction between inhibitors and NRF2 and KEAP1

5.1. Direct inhibitor-NRF2 interactions

The nature of the interactions between the inhibitors listed in section 4 and the NRF2 protein was appraised to determine target selectivity of the inhibitors. Of all the inhibitors addressed, only ML385 has been shown to directly interact with NRF2. High-throughput screening identified ML385 as a specific NRF2 inhibitor that directly binds to the Neh1 domain (CNC-bZIP) (Fig. 3C) of NRF2. This binding was shown to inhibit NRF2–MAFG complex formation and DNA binding at ARE sequences (section 2), suppressing downstream gene expression [337].

All other inhibitors do not interact with NRF2 directly but inhibit its activity indirectly via mechanisms summarized in Table 1. The biological consequences of the indirect inhibition are also listed in Table 1. For example, brusatol (section 4.6) was originally described as an NRF2 inhibitor but acts indirectly by broadly inhibiting protein synthesis or

enhancing ubiquitination and subsequent proteasomal degradation of NRF2 [242,433]. Retinoic acid (section 4.24) inhibits NRF2 indirectly through epigenetic regulation in the absence of direct DNA methylation or histone modification [434]. Retinoids such as all-trans retinoic acid activate retinoic acid receptor α, prompting it to form complexes with NRF2 that hinder the protein's ability to bind to AREs, thereby diminishing its transcriptional activity [352].

5.2. Inhibitor-KEAP1 interactions

As alluded to in section 2, the redox sensor KEAP1 resides in the cytosol, where it binds newly synthesized NRF2 under basal (unstressed) cellular conditions through a "hinge-and-latch" interaction. The high-affinity ETGE motif from NRF2 provides a hinge, while the low-affinity DLG motif serves as a latch within the Kelch domain of KEAP1 [435,436]. In this configuration and under these circumstances, NRF2 is directed for poly-ubiquitination by the CUL3-RBX1 ligase and subsequently degraded by the proteasome, thus maintaining low NRF2 levels [435,437,438]. Furthermore, KEAP1 is tethered to the actin cytoskeleton, effectively anchoring the NRF2–KEAP1 complex in the cytoplasm and further limiting NRF2 translocation to the nucleus [439]. Accordingly, it was postulated that the blocking of the NRF2-KEAP1 association by inhibitor-KEAP1 complexation in its stead would disrupt NRF2 homeostasis in favor of cancer cell survival (i.e., an undesired pharmacological outcome) insofar as NRF2 would no longer be poly-ubiquitinated and proteasomally degraded and could migrate to the nucleus to mediate transcription of ARE genes. This is particularly problematic in a post-PDT molecular landscape, where de novo NRF2 synthesis is strongly upregulated [66,144,201,440,441] and where inhibitor blockade of KEAP1 could exacerbate survival signaling [8,47] by keeping NRF2 decomplexed from KEAP1. The interactions between the inhibitors and KEAP1 were therefore studied by molecular docking analysis.

A systematic approach was used to gauge the interactive strength of abovementioned inhibitors towards KEAP1 directly. First, the structure of NRF2 was enumerated as described in Fig. 3A and B and in the associated supporting information (https://doi.org/10.17632/hw4286gycz.1). Next, model compounds 8IVG and 6QMC that emulate NRF2′s KEAP1 binding region (represented by the 16 amino-acid spanning protein fragment of NRF2; Fig. 3A, B red structure), and more specifically the Glu78-Phe83 loop, were docked into the KEAP1 binding cavity as positive controls. The eventual docking grid was constructed based on the centroid coordinates of the ligand from model compound 8IVG. Twenty docking solutions were generated for each compound. The best solutions were selected based on the scoring function value and the clustering of poses within the active KEAP1 cavity. The scoring function value was determined by Glide ligand efficiency (measures binding efficiency normalized by ligand size; higher absolute Glide ligand efficiency values (more negative) represents better binding efficiency per atom [442]) and Glide score (estimates the binding affinity between a ligand and its protein target; more negative Glide scores signal stronger predicted binding affinity, where –10 kcal/mol is typically considered excellent, while –5 kcal/mol is considered moderate [443]). Shape similarity was also scored from 0.000 (no similarity) to 1.000 (identical). More detailed methodological accounting is provided in section S5.2 in the supporting document (https://doi.org/10.17632/hw4286gycz.1).

The results of the calculations are summarized in Table 2. The inhibitors NRF2-IN-1, ochratoxin A, luteolin, apigenin, and wogonin showed excellent clustering, optimal ligand efficiency scores, highly negative Glide score values, and similar pharmacophoric characteristics to control compounds 1 and 2. Molecular docking results of the 4 highest ranked compounds are presented in Fig. 7. Accordingly, when selecting an NRF2 inhibitor to combine with PDT, it is advisable that these strongly interacting compounds should be given lower priority. More detailed results are presented in section S5.2 in the supporting document (https://doi.org/10.17632/hw4286gycz.1).

Table 2
Results of molecular docking of investigated compounds into the KEAP1 active cavity. Control metrics: "Stars" denote the quality of docking solution clustering, where 3 indicates maximal clustering with 90% of docking solutions having a root mean square deviation (RMSD) less than 1.5 Å; 2 represents an RMSD between 1.5 and 3.5 Å for 60% of docking solutions; and 1 signifies an RMSD greater than 3.5 Å, with no more than 20% of solutions clustering together. Ligand efficiency metrics: values of ≥ -0.200 indicate low binding efficiency; -0.200 to -0.249 represent moderate efficiency; -0.249 to -0.400 denote high efficiency; and ≤ -0.401 suggest excessive affinity (often indicative of toxic compounds or PAINS). Glide score: compounds with a high affinity for the active cavity are associated with values of ≤ -5.501 kcal/mol. Moderate activity is represented by values between -5.001 and -5.5 kcal/mol. Values above -5.0 kcal/mol indicate low or inactive compounds. Particular attention should be paid to structures where all metrics support interaction. These compounds satisfy all criteria for high-affinity ligands for KEAP1 and suggest possible avoidance as post-PDT inhibitors of the NRF2 survival pathway.

Rank	Stars	Title	Glide ligand efficiency (kcal/mol/atom)	Glide score (kcal/mol)	Shape similarity
1	3	Control 1 (8IVG)	−0.304	−7.897	0.996
2	3	Control 2 (6QMC)	−0.350	−6.652	0.942*
3	3	NRF2-IN-1	−0.280	−7.568	0.821
4	3	ochratoxin A	−0.253	−7.086	0.846
5	3	ML385	−0.177	−6.546	0.528
6	3	AEM1	−0.217	−5.848	0.797
7	3	luteolin	−0.268	−5.623	0.722
8	3	apigenin	−0.278	−5.558	0.702
9	3	wogonin	−0.264	−5.550	0.708
10	3	4-methoxychalcone	−0.286	−5.146	0.704
11	3	trigonelline	−0.500**	−5.001	0.349
12	3	retinoic acid	−0.213	−4.677	0.625
13	3	clobetasol propionate	−0.118	−3.766	0.599
14	2	brusatol	−0.160	−5.933	0.542
15	2	ethionamide	−0.532**	−5.854	0.401
16	2	kaempferol	−0.274	−5.744	0.722
17	2	PMF	−0.186	−5.035	0.722
18	2	chrysin	−0.265	−5.028	0.631
19	2	ascorbic acid	−0.406	−4.870	0.358
20	1	halofuginone	−0.242	−5.803	0.717
21	1	K-563	−0.105	−5.777	0.215
22	1	cryptotanshinone	−0.251	−5.524	0.608
23	1	febrifugine	−0.250	−5.509	0.705
24	1	triptolide	−0.184	−4.787	0.690
25	1	isoniazid	−0.478**	−4.783	0.405
26	1	PIK-75	−0.177	−4.779	0.791
27	1	IM3829	−0.265	−4.232	0.595
28	1	metformin	−0.276	−2.481	0.337

* −0.642 relative to Control 1.
** Potentially toxic compound.

6. Discussion and future perspectives

PDT has progressively become a viable treatment option for superficial and easily accessible tumors [444–449], where cure rates in the upper 80% to even more than 90% have been achieved for certain types of cancer (mainly skin cancers) [450–455]. The treatment modality has also been investigated for highly lethal, therapy-recalcitrant tumors, including cholangiocarcinoma [456–460] and pancreatic cancer [461–463], where several studies have reported superior outcomes relative to gold standard chemotherapy [460,464]. Despite the clinical successes, PDT is not curative when it concerns tumors located in deeper situated organs, which include the aforementioned biliary and pancreatic malignancies.

One of the prime reasons for the suboptimal outcomes, despite being superior to conventional treatments, is that sublethally afflicted cancer cells activate survival pathways that enable them to cope with

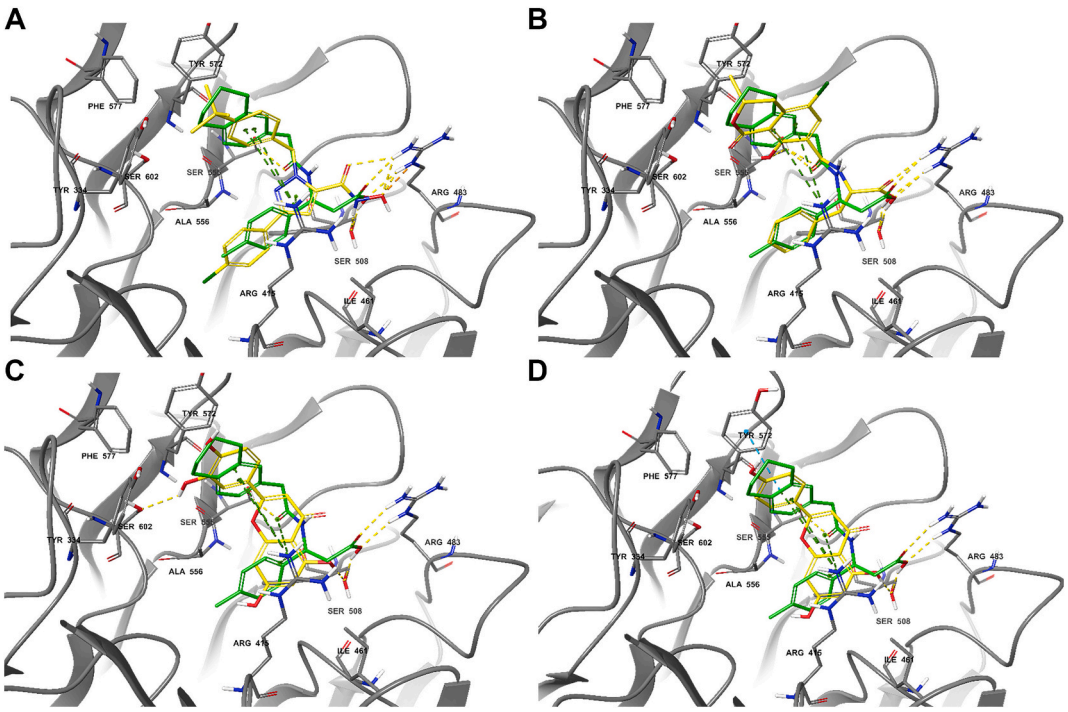

Fig. 7. Molecular docking results of the most strongly binding compounds in the NRF2 binding cavity of KEAP1. The structures of NRF2-IN-1 (**A**), ochratoxin A (**B**), luteolin (**C**), and apigenin (**D**) (yellow) were superimposed onto compound 2 (green), a mimetic of the NRF2 loop structure (Fig. 3A and B, red) that was used as a positive control. Dotted lines represent hydrogen bonds (yellow), π-π stacking (cyan), and π-cation interactions (green).

hyperoxidative stress and overcome the impact of treatment. This is especially the case in bulkier and highly vascularized tumors, where the distal tumor regions (relative to the incident light) suffer from low photon densities and hence insufficient ROS production [27,29,30]. Cancer cells in these areas are amenable to activate survival pathways comprising the hypoxic response (HIF-1α), inflammatory response (NF-κB), immediate early stress response (AP-1), proteotoxic stress response, heat shock response, and the antioxidant response (NRF2) [28,30]. Activation of these survival pathways by PDT has been experimentally demonstrated in cancer cells as well as endothelial cells (which line intratumoral vasculature) and macrophages (immune cells in the tumor microenvironment) [8,31,47,48]. Libraries of small-molecular inhibitors of the HIF-1α pathway [60] and the immediate early stress response [29] have been assembled, and empirical proof-of-concept on the basis of these libraries was provided for the selective HIF-1α inhibitor acriflavine [31,48] as well as the hypoxic cytotoxin tirapazamine [52]. Moreover, non-targeted and targeted drug delivery systems have been formulated for the intravenous delivery of third-generation PSs (e.g., nanoencapsulated PSs zinc- and aluminum phthalocyanine) [8,9,465–471] and fourth-generation PSs (e.g., nanoencapsulated PSs zinc phthalocyanine with co-encapsulated inhibitors of PDT-induced biological response pathways) [31,48,52]. Accordingly, this work serves as an investigational drug reference platform for the development of NRF2-targeted third-generation and fourth-generation PSs.

When selecting an inhibitor for co-administration or co-encapsulation as part of a PDT regimen, several factors should be considered. First, the chemical properties (available at: https://doi.org/10.17632/hw4286gycz.1) are key in determining whether (co–)encapsulation of the inhibitor will be necessary – an aspect that tailors to the practical utility and feasibility of the research and development (R&D) trajectory. Drugs with a logP of ≥ 4 typically require formulation into an aqueous buffer-compatible delivery system such as liposomes or micelles, while those that can partition into both aqueous and lipophilic compartments (logP of $\sim$ 1–3) are generally more cumbersome to encapsulate into stable formulations. Drugs with a logP of ≤ 0 can be administered in free form or encapsulated into, for instance, the aqueous compartment of liposomes. Second, it is advisable to select an inhibitor that inherently possesses anti-cancer properties, preferably by targeting multiple pathways (e.g., anti-proliferative, anti-metastatic, pro-apoptotic, etc.), next to acting as a survival pathway inhibitor, which hypothetically would translate to a 'multiple whammy' effect on cancer cells. This would render the PDT treatment into a multi-prong therapeutic approach, which is what we have consistently advocated in the framework of optimal cancer treatment [30,472]. In this regard, some interesting examples from Table 1 include apigenin, brusatol, chrysin, cryptotanshinone, halofuginone, kaempferol, luteolin, NRF2-IN-1, PIK-75, triptolide, and wogonin. Third, the drug itself should not confer notable toxicity to the organism upon intravenous administration. For instance, triptolide has very potent anti-cancer properties (LC_{50} in the low nM range) but is rather toxic to humans, with case reports of people dying from accidental poisoning following ingestion of triptolide-containing honey [473]. Unless the inherent systemic toxicity of such compounds can be mitigated (e.g., through encapsulation or targeted delivery), the practical utility will remain limited.

A more general concern with respect to NRF2 inhibition during PDT is how the intervention with adjuvants and the combined treatment regimen affects healthy tissue. Estimating potential off-target effects is currently difficult, given the novelty of NRF2 inhibition in PDT and the lack of clinical research in combined PDT treatment regimens. The NRF2 inhibitors that are currently employed in the clinical setting are used for purposes other than NRF2 inhibition *per se* and are therefore known to exert NRF2-unrelated pharmacodynamic effects. Generally, PDT tissue specificity is achieved through a combination of preferential tumor tissue photosensitization (e.g., through the enhanced permeability and retention effect) as well as selective illumination. Still, damage to healthy tissue is a risk factor if said tissue has been photosensitized and is located in the path of light during treatment [474,475]. Moreover, non-selective accumulation of NRF2 inhibitors might exacerbate damage to healthy tissue if the inhibitors reduce the ability of healthy cells to resist oxidative stress. Some inhibitors might exhibit altered pharmacodynamic behavior in healthy tissues, such as chrysin, or, in the case of clobetasol propionate, only work in cells carrying a KEAP1 mutation

[226,257,259]. These traits impart greater tissue specificity and hence beneficial therapeutic sequelae. However, these features do not apply to all inhibitors. As with every new field, future pre-clinical and clinical studies are warranted.

In addition to the NRF2 inhibitors described above, which chiefly target protein expression levels or activity of NRF2, stimulate its proteasomal degradation, block nuclear translocation, or interfere with its downstream transcriptional regulation (Fig. 5), future strategies aimed at modulating the antioxidant response may also focus on protein methylation processes. This is a young but exciting oncotherapeutic niche, where protein arginine methylation of non-histone proteins has emerged as a potential therapeutic target [476]. The arginine methylation of non-histone proteins is a form of post-translational modification that can regulate the localization and activity of various signaling molecules, and the aberrant activity of this by protein arginine methyltransferases (PRMT) is linked with cancer hallmarks such as unrestricted proliferation, inflammatory signaling, metastasis, and suppression of programmed cell death [477]. As a result, the overexpression of these PRMTs is often associated with poor prognosis in various types of cancer [477]. For example, high expression of PRMT1 or PRMT5 is associated with worse relapse-free survival in several types of breast cancer [478]. Therefore, targeting PRMT1 and PRMT5 is a promising therapeutic strategy for cancer, with several inhibitors already having entered clinical trials [478].

PRMT1 is the main PRMT found in mammals and is most notably known to catalyze the methylation of histone 4 at arginine 3 (H4R3), as well as several non-histone substrates including NRF2 [479]. The monomethylation of NRF2 at arginine 437 (R437) has been shown to regulate NRF2 transcriptional activity during the antioxidative response [480]. R437 is situated within the Neh1 domain of Nrf2 (Fig. 3) that is responsible for both heterodimerization with MAF and the binding of NRF2 to its target genes [481]. The enzyme responsible for this methylation is PRMT1. The methylation of NRF2 at R437 by PRMT1 produced a moderate increase in transcriptional activity [480], with the overall effect of R437 mono-methylation being an increased protection against cell death. PRMT5, in contrast, inhibits NRF2 by methylating KEAP1 at R596, stabilizing the KEAP1 protein by protecting it from ubiquitination [482].

To date, there is no specific PRMT1 inhibitor in clinical use, and the closest therapeutic effector is CTS-2190, a type I PRMT inhibitor [483] intended for the treatment of patients with advanced or metastatic solid tumors and currently undergoing phase I/II clinical trials. Another type I PRMT inhibitor, GSK3368715, was discontinued primarily due to a lack of clinical efficacy and a high rate of thromboembolic events in a phase I study [484]. Several inhibitors at the preclinical stage are also available. These include, among others, MS023, a type I PRMT1 inhibitor targeting PRMT1/3/4/6/8 that shows anti-proliferation properties in patient-derived clear cell renal cell carcinoma (IC_{50} in the range of 0.4 to 6 μM), with the inhibition of PRMT1 resulting in disruption of DNA repair pathways and cell cycle arrest as a result of accumulating double-strand DNA breaks [485,486]. Another study also observed cell cycle arrest, elevated transcript expression of apoptosis-related genes, and genes involved in the adaptive immune response (particularly increased expression of MHC class II-related genes) in patient-derived multiple myeloma cells [487]. It is important to reiterate the significance of the innate and adaptive immune system in long-term tumor control [488–492]. Another example is TC-E-5003, which is a selective PRMT1 inhibitor. TC-E-5003 shows anti-tumor effects when tested against a panel of cancer cell lines as well as *in vivo* tumor growth inhibition [493]. A study also found that PRMT1 inhibition using TC-E-5003 resulted in moderate inhibition of NF-κB and AP-1 signaling [494], both of which are considered survival pathways in PDT [28], resulting in reduced inflammatory signaling induced by lipopolysaccharide and orchestrated by macrophages. It remains to be explored whether this ability can be reproduced in cancer, especially in combination with PDT.

To date, none of the PRMT inhibitors have been investigated for their effect on NRF2. Similarly, no studies have combined PDT and PRMT inhibitors of any type. However, the published studies do point towards a potential synergy with PDT, first by their anti-proliferative effects, second by their effect on PDT-induced survival signaling, and third by the ability to enhance immunogenicity [495]. Therefore, the use of PRMT inhibitors opens up a study direction centered on combinational therapy with PDT.

6.1. Preclinical and translational caveats and challenges

It should be noted that the translation of NRF2 inhibition strategies into clinical practice does not come without challenges. Limitations such as incomplete understanding of tumor-specific NRF2 pathway dynamics in patients, potential systemic toxicity of inhibitors, and the complexity of tumor heterogeneity may affect treatment outcomes and should be carefully considered in future studies. Another important aspect to consider in future R&D efforts is proper benchmarking in preclinical studies. Third- and fourth-generation PSs are being developed to improve existing therapeutic options for a particular cancer type. Accordingly, it would serve that purpose to benchmark the efficacy of an experimental treatment regimen to a clinically employed PDT protocol as well as non-PDT treatment options such as gold standard chemotherapy (e.g., gemcitabine + cisplatin). The goal would be to develop interventions that are superior to currently employed clinical modalities and to demonstrate this empirically, treating this goal as a key performance indicator.

The therapeutic window for NRF2 inhibition in PDT is constrained by stage-dependent biology of NRF2. In established malignancies, where NRF2 is frequently hyperactivated by KEAP1 loss or oncogenic signaling, NRF2 drives redox buffering and drug efflux, blunting ROS-mediated killing. In this context, transient NRF2 suppression around light exposure can potentiate PDT. Corroboratively, NRF2 knockdown increased intracellular ROS and significantly enhanced pheophorbide-a PDT cytotoxicity in multiple cancer lines, validating NRF2 as a resistance node that can be exploited therapeutically [144]. More similar examples were provided in section 3.2. By contrast, in premalignant or early-stage tissues, NRF2 is tumor-suppressive. Nrf2-deficient mice exhibit markedly higher susceptibility to chemical carcinogenesis with loss of phase 2 cytoprotective enzyme induction, indicating that basal NRF2 activity limits initiation and early progression [496]. Thus, broad NRF2 inhibition in early lesions risks exacerbating genotoxic stress and promoting tumorigenesis, arguing against routine use in that setting. Compounding this, many advanced tumors harbor constitutive NRF2 activation through KEAP1 mutations, which supports survival and therapy resistance [497] and further justifies selective, time-locked NRF2 blockade in PDT regimens directed at such tumors. Practically, this duality mandates biomarker-guided stratification (KEAP1/NRF2 status), spatiotemporally restricted delivery (e.g., tumor-targeted nanocarriers), and brief *peri*-PDT inhibition to amplify intratumoral oxidative injury without eroding physiological cytoprotection offered by NRF2 in normal or premalignant epithelium. In sum, NRF2 inhibition can widen the therapeutic index of PDT in resistant cancers, but it may be contraindicated early in carcinogenesis, where NRF2 acts as a guardian against malignant transformation.

Although targeting NRF2 to potentiate PDT is mechanistically attractive, it is imperative to take into account the fact that NRF2 fulfills a physiological cytoprotective role in healthy tissues. NRF2 orchestrates basal and inducible antioxidant, detoxification, and proteostasis programs in multiple organs. Blockade or attenuation of NRF2 by systemically infused inhibitors predictably sensitizes healthy cells to oxidative and electrophilic injury, which may provoke non-trivial pathogenic consequences [498,499] that include amplification of pro-inflammatory responses and collateral tissue damage. For instance, brusatol suppresses global protein synthesis and accelerates NRF2 loss secondarily to rapid downregulation of many short-lived proteins beyond NRF2, which could result in non-selective toxicity. Even selective NRF2 inhibitors such as

ML385 affect other signaling nodes by ancillary pathway intersection (e.g., the PI3K/mTOR pathway), potentiating on-target/off-tumor risk [244,246,337]. Off-target risk mitigation is particularly important in light of poor tumor selectivity of systemically administered unformulated inhibitors, which necessitates the employment of (functionalized) nanoparticulate delivery systems such as ligand-targeted liposomes [469] and polymeric micelles [467,468] that can be advanced in design to co-deliver PS and NRF2 inhibitor spatiotemporally to the tumor (i.e., fourth-generation PSs [31,48]) while sparing normal tissues [27,500,501]. When formulating fourth-generation PSs it is important to understand the issues related to delivery and toxicity mismatch emanating from nanoparticles containing hydrophilic, inherently toxic small-molecular inhibitors and lipophilic photoactivatable PSs. These orthogonal ADMET traits could hinder co-encapsulation, co-biodistribution, synchronized tumor uptake, and toxicity profiles that in turn may give rise to subtherapeutic intratumoral drug ratios [500,502,503]. Drug-containing nanoparticles often behave differently when injected systemically versus when added to cell culture medium. The particles may suffer from destabilization by blood constituents, which could prompt premature drug release and corollary abrogation of therapeutic efficacy. Notable examples include nanoformulated curcumin [504] and micelles containing the second-generation PS zinc phthalocyanine [467]. Lastly, our understanding of the non-canonical roles of NRF2 in e.g., metabolic rewiring (glycolysis, glutaminolysis), immune modulation, and autophagy crosstalk [505–507] is incomplete. Indiscriminate inhibition of the NRF2 pathway could perturb oncoimmunological metabolism and stress adaptation in unpredictable ways that are not *per se* conducive to therapeutic outcome and/or patient safety. Taken together, while NRF2 inhibition + PDT is a rational illuminosensitization strategy, practically implementable progress hinges on tumor-selective, well-characterized inhibitors, co-delivery systems that harmonize PS and inhibitor pharmacology, and preferably biomarker-driven patient selection to balance efficacy with protection of normal tissue homeostasis [28].

Finally, during the R&D trajectory, it is important to consider potentially deleterious longer-term effects of novel therapies. One such side effect that should be considered when implementing NRF2 inhibitors as therapeutic adjuvants is the promotion of EMT and subsequent metastasis. Pharmacological NRF2 inhibition during PDT can modulate EMT programs in ways that cut both ways for progression and metastasis. PDT-generated ROS can activate TGF-β signaling and promote EMT traits in that blocking NRF2 will amplify ROS, potentially exacerbating TGF-β/Notch-driven EMT unless those axes are co-controlled. In epithelial models, ROS → NRF2 → Notch signaling is required for TGF-β1-induced EMT. Silencing NRF2 or quenching ROS attenuates Notch activation and EMT marker switching, implicating NRF2 as a facilitator of EMT in certain contexts. Thus, inhibiting NRF2 could suppress EMT where NRF2 is upstream of TGF-β/Notch, but it could also enhance EMT by unleashing ROS-TGF-β signaling when the antioxidant brake function of NRF2 is removed [508,509]. NRF2 can also stabilize hybrid epithelial/mesenchymal phenotypes that favor collective migration. NRF2 knockdown in human NSCLC (H1975) and human transitional cell papilloma (RT4) cells destabilizes this state and reduces collective motility, suggesting that NRF2 inhibition might diminish cooperative invasion in tumors relying on hybrid EMT. Conversely, in other cancers, NRF2 was shown to promote EMT and anoikis resistance via SNAIL1, implying that NRF2 blockade could limit dissemination [510–512]. Moreover, NRF2 can attenuate TGF-β-induced EMT (e.g., by restraining SNAIL) so that indiscriminate inhibition may de-repress EMT and increase tumor aggressiveness in those settings. Because PDT itself can induce EMT, the net effect of NRF2 inhibition on metastatic potential will depend on the baseline EMT wiring (TGF-β/Notch/HIF status) of the treated tumor and EMT mode (hybrid versus full) [513–515]. Practically, pairing transient, *peri*-PDT NRF2 inhibition with TGF-β/Notch/HIF blockade and monitoring EMT markers (E-cadherin, vimentin, ZEB1/SNAIL) constitutes an option to leverage cytotoxic gain while minimizing pro-metastatic drift. Admittedly, such overly complex therapeutic interventions with joint monitoring protocols may not always be practically feasible and demand a robust SWOT analysis before clinical actualization.

7. Conclusions

The NRF2 pathway is a complex cytoprotective mechanism through which cancer cells can cope with high levels of oxidative stress and unbalanced redox homeostasis. This pathway is persistently activated in various cancer types but can also be activated by cancer cells subjected to PDT for survival. The NRF2 pathway is therefore an attractive target for therapeutic approaches to sensitize cancer cells to PDT. Although numerous NRF2 inhibitors have been identified, the inhibitors have either not or only sporadically been investigated in combination with PDT. Future research should focus on exploring the inhibition of the NRF2 pathway as a way to enhance PDT efficacy, and further on the toxicity and therapeutic mechanisms of these drugs in combination with PDT. Benchmarking to existing, clinically employed modalities for the cancer type of interest is warranted to observe and safeguard the greater purpose of the R&D trajectory while harboring target selectivity and patient safety aspects of the novel modalities.

Funding information

This work was supported by grants from the Dutch Cancer Foundation (KWF project # 10666), a Zhejiang Provincial Foreign Expert Program Grant, Zhejiang Provincial Key Natural Science Foundation of China (#Z20H160031), Zhejiang Provincial Basic Public Welfare Research Project (LGD21H300001), the Science and Technology Bureau of Jiaxing (No. 2019AY32012), and a grant for the establishment of the Jiaxing Key Laboratory for Photonanomedicine and Experimental Therapeutics to MH. LPF was supported by a grant from the Fundacao de Amparo a Pesquisa do Estado de Sao Paolo – FASEP (Sao Paolo State Research Support Foundation, grant # CNPJ 43.828.151/0001–45) and BM was supported by the Fundação para a Ciência e a Tecnologia (FCT) grant SFRH/BD/140283/2018. LW was supported by Jiaxing Medical Key Subject Funding of Zhejiang Province (2023-ZC-013). YSK was funded by the Academy of Medical Sciences (grant number SGL027/1011). ML and JT were supported by a PhD scholarship from the Chinese Scholarship Council (CSC #202108330069 and #202308320054, respectively). The article was prepared within the framework of the project "International academic cooperation" HSE University (MAG, YBP, MH).

Research data for this article

All data compiled for this article can be made available upon request to MH.

CRediT authorship contribution statement

Daniel J. de Klerk: Writing – review & editing, Writing – original draft, Visualization, Validation, Software, Methodology, Investigation, Formal analysis, Data curation. **Mark J. de Keijzer:** Writing – review & editing, Writing – original draft, Visualization, Validation, Software, Methodology, Investigation, Formal analysis, Data curation. **Leonardo P. Franchi:** Writing – review & editing, Writing – original draft, Validation, Methodology, Investigation, Funding acquisition, Formal analysis, Data curation. **Jiahao Tian:** Writing – review & editing, Writing – original draft, Validation, Investigation, Funding acquisition, Data curation. **Maxim A. Gureev:** Writing – review & editing, Writing – original draft, Visualization, Software, Methodology, Investigation, Formal analysis, Data curation, Conceptualization. **Yingnan Ge:** Writing – review & editing, Validation, Investigation, Data curation. **Bárbara Mesquita:** Writing – review & editing, Writing – original draft,

Validation, Investigation, Formal analysis. **Gideon E. Saelman:** Writing – review & editing, Writing – original draft, Validation, Investigation, Formal analysis, Data curation. **Isis Van herteryck:** Writing – review & editing, Validation, Investigation, Data curation. **Lionel M. Dias:** Writing – review & editing, Writing – original draft, Validation, Investigation, Data curation. **Lianne R. de Haan:** Writing – review & editing, Visualization, Validation. **Mingjuan Li:** Writing – review & editing, Validation, Funding acquisition. **Lenka N.C. Boyd:** Writing – review & editing, Validation. **Tessa Y.S. Le Large:** Writing – review & editing, Validation. **Elisa Giovannetti:** Writing – review & editing, Supervision, Resources, Project administration. **Geert Kazemier:** Writing – review & editing, Supervision, Resources, Project administration. **Perry D. Moerland:** Writing – review & editing, Project administration, Methodology. **Yunlei Li:** Writing – review & editing, Validation, Methodology. **Andrew P. Stubbs:** Writing – review & editing, Supervision, Resources, Project administration, Methodology. **Mathias Devreese:** Writing – review & editing, Validation, Supervision, Resources, Project administration, Methodology. **Yuri B. Porozov:** Writing – review & editing, Writing – original draft, Visualization, Validation, Supervision, Software, Resources, Project administration, Methodology, Investigation, Funding acquisition, Data curation, Conceptualization. **Joanne Verheij:** Writing – review & editing, Writing – original draft, Visualization, Resources, Methodology, Investigation, Formal analysis. **Twan Lammers:** Writing – review & editing, Writing – original draft, Visualization, Resources, Methodology, Investigation, Formal analysis. **Yazan S. Khaled:** Writing – review & editing, Resources, Project administration, Funding acquisition. **Byron Baron:** Writing – review & editing, Writing – original draft, Validation, Resources, Project administration, Methodology, Investigation, Data curation, Conceptualization. **Lingfeng Wu:** Writing – review & editing, Project administration, Funding acquisition. **Michal Heger:** Writing – review & editing, Writing – original draft, Visualization, Validation, Supervision, Software, Resources, Project administration, Methodology, Investigation, Funding acquisition, Formal analysis, Data curation, Conceptualization.

Declaration of competing interest

The authors declare that they have no known competing financial interests or personal relationships that could have appeared to influence the work reported in this paper.

Acknowledgement

Tony Kleijn and Azeem Ullah are acknowledged for providing feedback on the manuscript.

References

[1] K. Plaetzer, et al., Photophysics and photochemistry of photodynamic therapy: fundamental aspects, Lasers Med. Sci. 24 (2) (2009) 259–268.
[2] N.M. Candido, et al., Combining photodynamic therapy and chemotherapy: improving breast cancer treatment with nanotechnology, J. Biomed. Nanotechnol. 14 (5) (2018) 994–1008.
[3] L.P. Franchi, et al., In vitro effects of photodynamic therapy induced by chloroaluminum phthalocyanine nanoemulsion, Photodiagnosis Photodyn. Ther. 16 (2016) 100–105.
[4] L.P. Franchi, et al., The redox function of apurinic/apyrimidinic endonuclease 1 as key modulator in photodynamic therapy, J. Photochem. Photobiol. B 211 (2020) 111992.
[5] A.C. Tedesco, et al., Cholesterol-rich nanoemulsion (LDE) as a novel drug delivery system to diagnose, delineate, and treat human glioblastoma, Mater Sci Eng C Mater Biol Appl 123 (2021) 111984.
[6] E.R. Stadtman, Protein oxidation and aging, Science 257 (5074) (1992) 1220–1224.
[7] D. Borchman, et al., The dual effect of oxidation on lipid bilayer structure, Lipids 27 (4) (1992) 261–265.
[8] R. Weijer, et al., Multi-OMIC profiling of survival and metabolic signaling networks in cells subjected to photodynamic therapy, Cell. Mol. Life Sci. 74 (6) (2017) 1133–1151.
[9] L.M. Dias, et al., Attritional evaluation of lipophilic and hydrophilic metallated phthalocyanines for oncological photodynamic therapy, J. Photochem. Photobiol. B 216 (2021) 112146.
[10] D. Kessel, Apoptosis, paraptosis and autophagy: death and survival pathways associated with photodynamic therapy, Photochem. Photobiol. 95 (1) (2019) 119–125.
[11] D. Kessel, N.L. Oleinick, Cell death pathways associated with photodynamic therapy: an update, Photochem. Photobiol. 94 (2) (2018) 213–218.
[12] M.A. Weston, M.S. Patterson, Measurement of intracellular oxygen concentration during photodynamic therapy in vitro, Photochem. Photobiol. 90 (4) (2014) 878–888.
[13] V.H. Fingar, Vascular effects of photodynamic therapy, J. Clin. Laser Med. Surg. 14 (5) (1996) 323–328.
[14] A.P. Castano, P. Mroz, M.R. Hamblin, Photodynamic therapy and anti-tumour immunity, Nat. Rev. Cancer 6 (7) (2006) 535–545.
[15] A.D. Garg, et al., DAMPs and PDT-mediated photo-oxidative stress: exploring the unknown, Photochem. Photobiol. Sci. 10 (5) (2011) 670–680.
[16] D.V. Krysko, et al., Immunogenic cell death and DAMPs in cancer therapy, Nat. Rev. Cancer 12 (12) (2012) 860–875.
[17] P.S. Thong, et al., Photodynamic-therapy-activated immune response against distant untreated tumours in recurrent angiosarcoma, Lancet Oncol. 8 (10) (2007) 950–952.
[18] B.W. Henderson, et al., Interaction of photodynamic therapy and hyperthermia: tumor response and cell survival studies after treatment of mice in vivo, Cancer Res. 45 (12 Pt 1) (1985) 6071–6077.
[19] M. Karwicka, et al., Effects of photodynamic therapy with redaporfin on tumor oxygenation and blood flow in a lung cancer mouse model, Sci. Rep. 9 (1) (2019) 12655.
[20] C. Nwogu, et al., Porfimer sodium versus PS785 for photodynamic therapy (PDT) of lung cancer xenografts in mice, J. Surg. Res. 263 (2021) 245–250.
[21] J.C. Cacaccio, et al., Photodynamic therapy in combination with doxorubicin is superior to monotherapy for the treatment of lung cancer, Biomedicines 10 (4) (2022) 857.
[22] C.S. Shim, et al., Prospective study of the effectiveness of percutaneous transhepatic photodynamic therapy for advanced bile duct cancer and the role of intraductal ultrasonography in response assessment, Endoscopy 37 (5) (2005) 425–433.
[23] R. Lindberg-Larsen, H. Solvsten, K. Kragballe, Evaluation of recurrence after photodynamic therapy with topical methylaminolaevulinate for 157 basal cell carcinomas in 90 patients, Acta Derm. Venereol. 92 (2) (2012) 144–147.
[24] H.O. Alsaab, et al., Progress in clinical trials of photodynamic therapy for solid tumors and the role of nanomedicine, Cancers (Basel) 12 (10) (2020) 2793.
[25] S.L. Jacques, How tissue optics affect dosimetry of photodynamic therapy, J. Biomed. Opt. 15 (5) (2010) 051608.
[26] T. Sheng, et al., Reactive oxygen species explicit dosimetry to predict local tumor growth for Photofrin-mediated photodynamic therapy, Biomed. Opt. Express 11 (8) (2020) 4586–4601.
[27] R. Weijer, et al., Enhancing photodynamic therapy of refractory solid cancers: combining second-generation photosensitizers with multi-targeted liposomal delivery, J Photochem Photobiol C: Photochem Rev 23 (2015) 103–131.
[28] M. Broekgaarden, et al., Tumor cell survival pathways activated by photodynamic therapy: a molecular basis for pharmacological inhibition strategies, Cancer Metastasis Rev. 34 (4) (2015) 643–690.
[29] D.J. de Klerk, et al., Strategies for improving photodynamic therapy through pharmacological modulation of the immediate early stress response, Methods Mol. Biol. 2451 (2022) 405–480.
[30] M. Korbelik, M. Heger, A.W. Girotti, Participation of lipids in the tumor response to photodynamic therapy and its exploitation for therapeutic gain, J. Lipid Res. 66 (2) (2025) 100729.
[31] R. Weijer, et al., Inhibition of hypoxia inducible factor 1 and topoisomerase with acriflavine sensitizes perihilar cholangiocarcinomas to photodynamic therapy, Oncotarget 7 (3) (2016) 3341–3356.
[32] T. Ueda, et al., Neovascularization in pancreatic ductal adenocarcinoma: Microvessel count analysis, comparison with non-cancerous regions and other types of carcinomas, Oncol. Rep. 9 (2) (2002) 239–245.
[33] M. Erkan, et al., Cancer-stellate cell interactions perpetuate the hypoxia-fibrosis cycle in pancreatic ductal adenocarcinoma, Neoplasia 11 (5) (2009) 497–508.
[34] I. Biancacci, et al., Optical imaging of the whole-body to cellular biodistribution of clinical-stage PEG-b-pHPMA-based core-crosslinked polymeric micelles, J. Control. Release 328 (2020) 805–816.
[35] I. Biancacci, et al., Repurposing tamoxifen for tumor microenvironment priming and enhanced tumor-targeted drug delivery, Adv Ther (Weinh) 6 (11) (2023) adtp.202300098.
[36] D. Mockel, et al., CCL2 chemokine inhibition primes the tumor vasculature for improved nanomedicine delivery and efficacy, J. Control. Release 365 (2024) 358–368.
[37] B. Theek, et al., Sonoporation enhances liposome accumulation and penetration in tumors with low EPR, J. Control. Release 231 (2016) 77–85.
[38] L. Bolm, et al., Alignment of stroma fibers, microvessel density and immune cell populations determine overall survival in pancreatic cancer-an analysis of stromal morphology, PLoS One 15 (7) (2020) e0234568.
[39] K.P. Olive, et al., Inhibition of Hedgehog signaling enhances delivery of chemotherapy in a mouse model of pancreatic cancer, Science 324 (5933) (2009) 1457–1461.

[40] P.P. Provenzano, et al., Enzymatic targeting of the stroma ablates physical barriers to treatment of pancreatic ductal adenocarcinoma, Cancer Cell 21 (3) (2012) 418–429.
[41] S. Aoki, et al., Placental growth factor promotes tumour desmoplasia and treatment resistance in intrahepatic cholangiocarcinoma, Gut 71 (1) (2022) 185–193.
[42] M.A. Jacobetz, et al., Hyaluronan impairs vascular function and drug delivery in a mouse model of pancreatic cancer, Gut 62 (1) (2013) 112–120.
[43] A. Thelen, et al., Microvessel density correlates with lymph node metastases and prognosis in hilar cholangiocarcinoma, J. Gastroenterol. 43 (12) (2008) 959–966.
[44] S.K. Hobbs, et al., Regulation of transport pathways in tumor vessels: role of tumor type and microenvironment, Proc. Natl. Acad. Sci. U. S. A. 95 (8) (1998) 4607–4612.
[45] H. Hashizume, et al., Openings between defective endothelial cells explain tumor vessel leakiness, Am. J. Pathol. 156 (4) (2000) 1363–1380.
[46] W.L. Monsky, et al., Augmentation of transvascular transport of macromolecules and nanoparticles in tumors using vascular endothelial growth factor, Cancer Res. 59 (16) (1999) 4129–4135.
[47] R. Weijer, et al., Low-power photodynamic therapy induces survival signaling in perihilar cholangiocarcinoma cells, BMC Cancer 15 (1) (2015) 1014.
[48] M. Broekgaarden, et al., Inhibition of hypoxia-inducible factor 1 with acriflavine sensitizes hypoxic tumor cells to photodynamic therapy with zinc phthalocyanine-encapsulating cationic liposomes, Nano Res. 9 (6) (2016) 1639–1662.
[49] E.C. Aniogo, B.P.A. George, H. Abrahamse, Phthalocyanine induced phototherapy coupled with Doxorubicin; a promising novel treatment for breast cancer, Expert Rev. Anticancer Ther. 17 (8) (2017) 693–702.
[50] A. El-Hussein, et al., A review of chemotherapy and photodynamic therapy for lung cancer treatment, Anticancer Agents Med Chem. 21 (2) (2021) 149–161.
[51] L. Conti, et al., Combination of light and Ru(II) polypyridyl complexes: recent advances in the development of new anticancer drugs, Coord. Chem. Rev. 469 (2022) 214656.
[52] M. Broekgaarden, et al., Photodynamic therapy with liposomal zinc phthalocyanine and tirapazamine increases tumor cell death via DNA damage, J. Biomed. Nanotechnol. 13 (2) (2017) 204–220.
[53] Y. Zhao, et al., Combination of phototherapy with immune checkpoint blockade: theory and practice in cancer, Front. Immunol. 13 (2022) 955920.
[54] J. Zhu, et al., Photodynamic therapy may salvage chemotherapy failure in gastric cancer: a case report and a literature review, Photodiagnosis Photodyn. Ther. 46 (2024) 104038.
[55] E.P. Maswikiti, et al., Case Report: a novel chemotherapy-free regimen combined with photodynamic therapy, target therapy, and immunotherapy in a geriatric male with huge recurrent scalp and facial angiosarcoma: a report of an extremely rare case and literature review, Front. Immunol. 16 (2025) 1556493.
[56] Y. Chen, et al., Iron-based MOF with Catalase-like activity improves the synergistic therapeutic effect of PDT/ferroptosis/starvation therapy by reversing the tumor hypoxic microenvironment, J Nanobiotechnology 22 (1) (2024) 705.
[57] X. Wang, et al., A versatile gas-generator promoting drug release and oxygen replenishment for amplifying photodynamic-chemotherapy synergetic anti-tumor effects, Biomaterials 276 (2021) 120985.
[58] Y.P. Huang, et al., Surufatinib combined with photodynamic therapy induces ferroptosis to inhibit cholangiocarcinoma in vitro and in tumor models, Front. Pharmacol. 15 (2024) 1288255.
[59] Y. Kojima, et al., Induction of ferroptosis by photodynamic therapy and enhancement of antitumor effect with ferroptosis inducers, J. Gastroenterol. 59 (2) (2024) 81–94.
[60] M.J. de Keijzer, et al., Inhibition of the HIF-1 survival pathway as a strategy to augment photodynamic therapy efficacy, Methods Mol. Biol. 2451 (2022) 285–403.
[61] T. Yamadori, et al., Molecular mechanisms for the regulation of Nrf2-mediated cell proliferation in non-small-cell lung cancers, Oncogene 31 (45) (2012) 4768–4777.
[62] J. Zhu, et al., An overview of chemical inhibitors of the Nrf2-ARE signaling pathway and their potential applications in cancer therapy, Free Radic. Biol. Med. 99 (2016) 544–556.
[63] K. Taguchi, M. Yamamoto, The KEAP1-NRF2 system in cancer, Front. Oncol. 7 (2017) 85.
[64] P. Canning, F.J. Sorrell, A.N. Bullock, Structural basis of Keap1 interactions with Nrf2, Free Radic. Biol. Med. 88 (Pt B) (2015) 101–107.
[65] A. Kobayashi, et al., Oxidative stress sensor Keap1 functions as an adaptor for Cul3-based E3 ligase to regulate proteasomal degradation of Nrf2, Mol. Cell Biol. 24 (16) (2004) 7130–7139.
[66] N. Rubio, et al., p38(MAPK)-regulated induction of p62 and NBR1 after photodynamic therapy promotes autophagic clearance of ubiquitin aggregates and reduces reactive oxygen species levels by supporting Nrf2-antioxidant signaling, Free Radic. Biol. Med. 67 (2014) 292–303.
[67] D.D. Zhang, Mechanistic studies of the Nrf2-Keap1 signaling pathway, Drug Metab. Rev. 38 (4) (2006) 769–789.
[68] D.D. Zhang, et al., Keap1 is a redox-regulated substrate adaptor protein for a Cul3-dependent ubiquitin ligase complex, Mol. Cell Biol. 24 (24) (2004) 10941–10953.
[69] L. Baird, et al., Regulatory flexibility in the Nrf2-mediated stress response is conferred by conformational cycling of the Keap1-Nrf2 protein complex, Proc. Natl. Acad. Sci. U. S. A. 110 (38) (2013) 15259–15264.
[70] G. Rachakonda, et al., Covalent modification at Cys151 dissociates the electrophile sensor Keap1 from the ubiquitin ligase CUL3, Chem. Res. Toxicol. 21 (3) (2008) 705–710.
[71] T. Yamamoto, et al., Physiological significance of reactive cysteine residues of Keap1 in determining Nrf2 activity, Mol. Cell Biol. 28 (8) (2008) 2758–2770.
[72] E. Kansanen, et al., Electrophilic nitro-fatty acids activate NRF2 by a KEAP1 cysteine 151-independent mechanism, J. Biol. Chem. 286 (16) (2011) 14019–14027.
[73] T. Suzuki, et al., Molecular mechanism of cellular oxidative stress sensing by keap1, Cell Rep. 28 (3) (2019) 746–758 e4.
[74] H.K. Bryan, et al., The Nrf2 cell defence pathway: Keap1-dependent and -independent mechanisms of regulation, Biochem. Pharmacol. 85 (6) (2013) 705–717.
[75] A.L. Eggler, et al., Modifying specific cysteines of the electrophile-sensing human Keap1 protein is insufficient to disrupt binding to the Nrf2 domain Neh2, Proc. Natl. Acad. Sci. U. S. A. 102 (29) (2005) 10070–10075.
[76] A.T. Dinkova-Kostova, R.V. Kostov, P. Canning, Keap1, the cysteine-based mammalian intracellular sensor for electrophiles and oxidants, Arch. Biochem. Biophys. 617 (2017) 84–93.
[77] A. Kobayashi, et al., Oxidative and electrophilic stresses activate Nrf2 through inhibition of ubiquitination activity of Keap1, Mol. Cell Biol. 26 (1) (2006) 221–229.
[78] H.C. Huang, T. Nguyen, C.B. Pickett, Phosphorylation of Nrf2 at Ser-40 by protein kinase C regulates antioxidant response element-mediated transcription, J. Biol. Chem. 277 (45) (2002) 42769–42774.
[79] K. Itoh, et al., An Nrf2/small Maf heterodimer mediates the induction of phase II detoxifying enzyme genes through antioxidant response elements, Biochem. Biophys. Res. Commun. 236 (2) (1997) 313–322.
[80] R. Venugopal, A.K. Jaiswal, Nrf2 and Nrf1 in association with Jun proteins regulate antioxidant response element-mediated expression and coordinated induction of genes encoding detoxifying enzymes, Oncogene 17 (24) (1998) 3145–3156.
[81] I. Bellezza, et al., Nrf2-Keap1 signaling in oxidative and reductive stress, Biochim. Biophys. Acta, Mol. Cell Res. 1865 (5) (2018) 721–733.
[82] W. Li, A.N. Kong, Molecular mechanisms of Nrf2-mediated antioxidant response, Mol. Carcinog. 48 (2) (2009) 91–104.
[83] N. Wakabayashi, et al., Protection against electrophile and oxidant stress by induction of the phase 2 response: fate of cysteines of the Keap1 sensor modified by inducers, Proc. Natl. Acad. Sci. U. S. A. 101 (7) (2004) 2040–2045.
[84] T. Suzuki, J. Takahashi, M. Yamamoto, Molecular Basis of the KEAP1-NRF2 Signaling Pathway, Mol. Cells 46 (3) (2023) 133–141.
[85] C.D. Klaassen, S.A. Reisman, Nrf2 the rescue: effects of the antioxidative/electrophilic response on the liver, Toxicol. Appl. Pharmacol. 244 (1) (2010) 57–65.
[86] Y. Hagiya, et al., Nrf2-dependent induction of human ABC transporter ABCG2 and heme oxygenase-1 in HepG2 cells by photoactivation of porphyrins: biochemical implications for cancer cell response to photodynamic therapy, J. Exp. Ther. Oncol. 7 (2) (2008) 153–167.
[87] D. Ross, Quinone reductases multitasking in the metabolic world, Drug Metab. Rev. 36 (3–4) (2004) 639–654.
[88] J.D. Hayes, A.T. Dinkova-Kostova, The Nrf2 regulatory network provides an interface between redox and intermediary metabolism, Trends Biochem. Sci 39 (4) (2014) 199–218.
[89] K. Sakamoto, et al., Role of the tumor suppressor PTEN in antioxidant responsive element-mediated transcription and associated histone modifications, Mol. Biol. Cell 20 (6) (2009) 1606–1617.
[90] A.K. Jain, A.K. Jaiswal, GSK-3beta acts upstream of Fyn kinase in regulation of nuclear export and degradation of NF-E2 related factor 2, J. Biol. Chem. 282 (22) (2007) 16502–16510.
[91] C. Geismann, et al., Cytoprotection “gone astray”: Nrf2 and its role in cancer, Onco Targets Ther 7 (2014) 1497–1518.
[92] J.D. Hayes, et al., Cancer chemoprevention mechanisms mediated through the Keap1-Nrf2 pathway, Antioxid. Redox Signal. 13 (11) (2010) 1713–1748.
[93] M.K. Kwak, T.W. Kensler, Targeting NRF2 signaling for cancer chemoprevention, Toxicol. Appl. Pharmacol. 244 (1) (2010) 66–76.
[94] J.K. Kundu, Y.J. Surh, Nrf2-Keap1 signaling as a potential target for chemoprevention of inflammation-associated carcinogenesis, Pharm. Res. 27 (6) (2010) 999–1013.
[95] C.R. Zhao, Z.H. Gao, X.J. Qu, Nrf2-ARE signaling pathway and natural products for cancer chemoprevention, Cancer Epidemiol. 34 (5) (2010) 523–533.
[96] C.A. Houghton, R.G. Fassett, J.S. Coombes, Sulforaphane and other nutrigenomic Nrf2 activators: can the clinician's expectation be matched by the reality? Oxid. Med. Cell. Longev. 2016 (2016) 7857186.
[97] H. Kitamura, H. Motohashi, NRF2 addiction in cancer cells, Cancer Sci. 109 (4) (2018) 900–911.
[98] G.M. DeNicola, et al., Oncogene-induced Nrf2 transcription promotes ROS detoxification and tumorigenesis, Nature 475 (7354) (2011) 106–109.
[99] B. Kong, et al., Overview on how oncogenic Kras promotes pancreatic carcinogenesis by inducing low intracellular ROS levels, Front. Physiol. 4 (2013) 246.
[100] R. Barbano, et al., Aberrant Keap1 methylation in breast cancer and association with clinicopathological features, Epigenetics 8 (1) (2013) 105–112.
[101] N. Chen, et al., Nrf2 expression in endometrial serous carcinomas and its precancers, Int. J. Clin. Exp. Pathol. 4 (1) (2010) 85–96.
[102] S. Wu, H. Lu, Y. Bai, Nrf2 in cancers: a double-edged sword, Cancer Med. 8 (5) (2019) 2252–2267.

[103] B.E. Hast, et al., Cancer-derived mutations in KEAP1 impair NRF2 degradation but not ubiquitination, Cancer Res. 74 (3) (2014) 808–817.
[104] T. Suzuki, J. Maher, M. Yamamoto, Select heterozygous Keap1 mutations have a dominant-negative effect on wild-type Keap1 in vivo, Cancer Res. 71 (5) (2011) 1700–1709.
[105] A. Ooi, et al., CUL3 and NRF2 mutations confer an NRF2 activation phenotype in a sporadic form of papillary renal cell carcinoma, Cancer Res. 73 (7) (2013) 2044–2051.
[106] J.A. Hellyer, et al., Impact of KEAP1/NFE2L2/CUL3 mutations on duration of response to EGFR tyrosine kinase inhibitors in EGFR mutated non-small cell lung cancer, Lung Cancer 134 (2019) 42–45.
[107] V.D. Martinez, et al., Unique pattern of component gene disruption in the NRF2 inhibitor KEAP1/CUL3/RBX1 E3-ubiquitin ligase complex in serous ovarian cancer, Biomed Res. Int. 2014 (2014) 159459.
[108] M. Zhao, et al., Cullin3 deficiency shapes tumor microenvironment and promotes cholangiocarcinoma in liver-specific Smad4/Pten mutant mice, Int. J. Biol. Sci. 17 (15) (2021) 4176–4191.
[109] I. Ganan-Gomez, et al., Oncogenic functions of the transcription factor Nrf2, Free Radic. Biol. Med. 65 (2013) 750–764.
[110] K. Taguchi, H. Motohashi, M. Yamamoto, Molecular mechanisms of the Keap1-Nrf2 pathway in stress response and cancer evolution, Genes Cells 16 (2) (2011) 123–140.
[111] T. Shibata, et al., Cancer related mutations in NRF2 impair its recognition by Keap1-Cul3 E3 ligase and promote malignancy, Proc. Natl. Acad. Sci. U. S. A. 105 (36) (2008) 13568–13573.
[112] Y. Zhang, et al., Mutations and expression of the NFE2L2/KEAP1/CUL3 pathway in chinese patients with lung squamous cell carcinoma, J. Thorac. Dis. 8 (7) (2016) 1639–1644.
[113] J.H. Yoon, et al., The enhanced anti-cancer effect of hexenyl ester of 5-amino-laevulinic acid photodynamic therapy in adriamycin-resistant compared to non-resistant breast cancer cells, Lasers Surg. Med. 44 (1) (2012) 76–86.
[114] M.B. Sporn, K.T. Liby, NRF2 and cancer: the good, the bad and the importance of context, Nat. Rev. Cancer 12 (8) (2012) 564–571.
[115] S. Lee, et al., An effective strategy for increasing the radiosensitivity of Human lung Cancer cells by blocking Nrf2-dependent antioxidant responses, Free Radic. Biol. Med. 53 (4) (2012) 807–816.
[116] M. Przygoda, et al., Cellular mechanisms of singlet oxygen in photodynamic therapy, Int. J. Mol. Sci. 24 (23) (2023) 16890.
[117] T. Maisch, et al., The role of singlet oxygen and oxygen concentration in photodynamic inactivation of bacteria, Proc. Natl. Acad. Sci. U. S. A. 104 (17) (2007) 7223–7228.
[118] G. Szewczyk, K. Mokrzynski, T. Sarna, Generation of singlet oxygen inside living cells: correlation between phosphorescence decay lifetime, localization and outcome of photodynamic action, Photochem. Photobiol. Sci. 23 (9) (2024) 1673–1685.
[119] K.K. Griendling, et al., Measurement of reactive oxygen species, reactive nitrogen species, and redox-dependent signaling in the cardiovascular system: a scientific statement from the american heart association, Circ. Res. 119 (5) (2016) e39–e75.
[120] J. Fujii, T. Homma, T. Osaki, Superoxide radicals in the execution of cell death, Antioxidants (Basel) 11 (3) (2022) 501.
[121] T. Sousa, et al., How abundant are superoxide and hydrogen peroxide in the vasculature lumen, how far can they reach? Redox Biol. 58 (2022) 102527.
[122] C.C. Winterbourn, Reconciling the chemistry and biology of reactive oxygen species, Nat. Chem. Biol. 4 (5) (2008) 278–286.
[123] Y. Wang, et al., Superoxide dismutases: dual roles in controlling ROS damage and regulating ROS signaling, J. Cell Biol. 217 (6) (2018) 1915–1928.
[124] M.J. Reiniers, et al., Reactive oxygen and nitrogen species in steatotic hepatocytes: a molecular perspective on the pathophysiology of ischemia-reperfusion injury in the fatty liver, Antioxid. Redox Signal. 21 (7) (2014) 1119–1142.
[125] R.F. van Golen, T.M. van Gulik, M. Heger, Mechanistic overview of reactive species-induced degradation of the endothelial glycocalyx during hepatic ischemia/reperfusion injury, Free Radic. Biol. Med. 52 (8) (2012) 1382–1402.
[126] S. Di Meo, P. Venditti, Evolution of the knowledge of free radicals and other oxidants, Oxid. Med. Cell. Longev. 2020 (2020) 9829176.
[127] A. Ledo, et al., In vivo hydrogen peroxide diffusivity in brain tissue supports volume signaling activity, Redox Biol. 50 (2022) 102250.
[128] B.A. Wagner, et al., An assay for the rate of removal of extracellular hydrogen peroxide by cells, Redox Biol. 1 (1) (2013) 210–217.
[129] C.M. Andrés, et al., Chemistry of hydrogen peroxide formation and elimination in mammalian cells, and its role in various pathologies, Stresses 2 (2022) 256–274.
[130] A. Denicola, J.M. Souza, R. Radi, Diffusion of peroxynitrite across erythrocyte membranes, Proc. Natl. Acad. Sci. U. S. A. 95 (7) (1998) 3566–3571.
[131] M.N. Möller, A. Denicola, Diffusion of peroxynitrite, its precursors, and derived reactive species, and the effect of cell membranes, Redox Biochemistry and Chemistry 9 (2024) 100033.
[132] R. Radi, Oxygen radicals, nitric oxide, and peroxynitrite: Redox pathways in molecular medicine, Proc. Natl. Acad. Sci. U. S. A. 115 (23) (2018) 5839–5848.
[133] M. Gao, et al., Antioxidant components of naturally-occurring oils exhibit marked anti-inflammatory activity in epithelial cells of the human upper respiratory system, Respir. Res. 12 (1) (2011) 92.
[134] D. Nowis, et al., Heme oxygenase-1 protects tumor cells against photodynamic therapy-mediated cytotoxicity, Oncogene 25 (24) (2006) 3365–3374.
[135] M.J. Lamberti, et al., Synergistic enhancement of antitumor effect of beta-Lapachone by photodynamic induction of quinone oxidoreductase (NQO1), Phytomedicine 20 (11) (2013) 1007–1012.
[136] T. Pecchillo Cimmino, et al., Formyl-peptide receptor 2 signaling modulates SLC7A11/xCT expression and activity in tumor cells, Antioxidants (Basel) 13 (5) (2024) 552.
[137] B. Padmanabhan, et al., Structural basis for defects of Keap1 activity provoked by its point mutations in lung cancer, Mol. Cell 21 (5) (2006) 689–700.
[138] T. Shibata, et al., Genetic alteration of Keap1 confers constitutive Nrf2 activation and resistance to chemotherapy in gallbladder cancer, Gastroenterology 135 (4) (2008) 1358–1368, e1–4.
[139] P. Zhang, et al., Loss of Kelch-like ECH-associated protein 1 function in prostate cancer cells causes chemoresistance and radioresistance and promotes tumor growth, Mol. Cancer Ther. 9 (2) (2010) 336–346.
[140] B.L. Probst, et al., Cancer cell growth is differentially affected by constitutive activation of NRF2 by KEAP1 deletion and pharmacological activation of NRF2 by the synthetic triterpenoid, RTA 405, PLoS One 10 (8) (2015) e0135257.
[141] M.J. Kerins, A. Ooi, A catalogue of somatic NRF2 gain-of-function mutations in cancer, Sci. Rep. 8 (1) (2018) 12846.
[142] K. Lisek, et al., Mutant p53 tunes the NRF2-dependent antioxidant response to support survival of cancer cells, Oncotarget 9 (29) (2018) 20508–20523.
[143] V.I. Sayin, et al., Activation of the NRF2 antioxidant program generates an imbalance in central carbon metabolism in cancer, Elife 6 (2017) e28083.
[144] B.H. Choi, et al., The sensitivity of cancer cells to pheophorbide a-based photodynamic therapy is enhanced by Nrf2 silencing, PLoS One 9 (9) (2014) e107158.
[145] M.J. Lamberti, et al., NQO1 induction mediated by photodynamic therapy synergizes with beta-Lapachone-halogenated derivative against melanoma, Biomed. Pharmacother. 108 (2018) 1553–1564.
[146] M.J. Dabrowski, et al., Glutathione S-transferase P1-1 expression modulates sensitivity of human kidney 293 cells to photodynamic therapy with hypericin, Arch. Biochem. Biophys. 449 (1–2) (2006) 94–103.
[147] S.C. Lu, Glutathione synthesis, Biochim. Biophys. Acta 1830 (5) (2013) 3143–3153.
[148] S. Shi, et al., Homologous-targeting biomimetic nanoparticles for photothermal therapy and Nrf2-siRNA amplified photodynamic therapy against oral tongue squamous cell carcinoma, Chem. Eng. J. 388 (2020) 124268.
[149] S. Shui, et al., Non-enzymatic lipid peroxidation initiated by photodynamic therapy drives a distinct ferroptosis-like cell death pathway, Redox Biol. 45 (2021) 102056.
[150] J. Kralova, et al., Glycol porphyrin derivatives and temoporfin elicit resistance to photodynamic therapy by different mechanisms, Sci. Rep. 7 (2017) 44497.
[151] K. Ibbotson, J. Yell, P.T. Ronaldson, Nrf2 signaling increases expression of ATP-binding cassette subfamily C mRNA transcripts at the blood-brain barrier following hypoxia-reoxygenation stress, Fluids Barriers CNS 14 (1) (2017) 6.
[152] I. de Souza, et al., High levels of NRF2 sensitize temozolomide-resistant glioblastoma cells to ferroptosis via ABCC1/MRP1 upregulation, Cell Death Dis. 13 (7) (2022) 591.
[153] W.K. Martins, et al., Autophagy regulation and photodynamic therapy: insights to improve outcomes of cancer treatment, Front. Oncol. 10 (2020) 610472.
[154] J. Steffen, et al., Proteasomal degradation is transcriptionally controlled by TCF11 via an ERAD-dependent feedback loop, Mol. Cell 40 (1) (2010) 147–158.
[155] Z. Sha, A.L. Goldberg, Proteasome-mediated processing of Nrf1 is essential for coordinate induction of all proteasome subunits and p97, Curr. Biol. 24 (14) (2014) 1573–1583.
[156] E.H. Kobayashi, et al., Nrf2 suppresses macrophage inflammatory response by blocking proinflammatory cytokine transcription, Nat. Commun. 7 (2016) 11624.
[157] W. Li, et al., Activation of Nrf2-antioxidant signaling attenuates NFkappaB-inflammatory response and elicits apoptosis, Biochem. Pharmacol. 76 (11) (2008) 1485–1489.
[158] G.H. Liu, J. Qu, X. Shen, NF-kappaB/p65 antagonizes Nrf2-ARE pathway by depriving CBP from Nrf2 and facilitating recruitment of HDAC3 to MafK, Biochim. Biophys. Acta 1783 (5) (2008) 713–727.
[159] S. Saha, et al., An overview of Nrf2 signaling pathway and its role in inflammation, Molecules 25 (22) (2020) 5474.
[160] X. Li, et al., Heme oxygenase-1 protects against neutrophil-mediated intestinal damage by down-regulation of neutrophil p47phox and p67phox activity and O2- production in a two-hit model of alcohol intoxication and burn injury, J. Immunol. 180 (10) (2008) 6933–6940.
[161] L. Wang, C. He, Nrf2-mediated anti-inflammatory polarization of macrophages as therapeutic targets for osteoarthritis, Front. Immunol. 13 (2022) 967193.
[162] W. Wang, et al., A NRF2 regulated and the immunosuppressive microenvironment reversed nanoplatform for cholangiocarcinoma photodynamic-gas therapy, Adv Sci (weinh) 11 (14) (2024) e2307143.
[163] H.R. Potteti, et al., Nrf2 mediates hypoxia-inducible HIF1alpha activation in kidney tubular epithelial cells, Am. J. Physiol. Renal Physiol. 320 (3) (2021) F464–F474.
[164] S. Lee, et al., Impairment of HIF-1alpha-mediated metabolic adaption by NRF2-silencing in breast cancer cells, Redox Biol. 24 (2019) 101210.
[165] X. Jin, et al., Enhancer-bound Nrf2 licenses HIF-1alpha transcription under hypoxia to promote cisplatin resistance in hepatocellular carcinoma cells, Aging (Albany NY) 13 (1) (2020) 364–375.
[166] J. Zheng, et al., Overactivated NRF2 induces pseudohypoxia in hepatocellular carcinoma by stabilizing HIF-1alpha, Free Radic. Biol. Med. 194 (2023) 347–356.
[167] T.H. Kim, et al., NRF2 blockade suppresses colon tumor angiogenesis by inhibiting hypoxia-induced activation of HIF-1alpha, Cancer Res. 71 (6) (2011) 2260–2275.

[168] I. Pitha-Rowe, et al., Synthetic triterpenoids attenuate cytotoxic retinal injury: cross-talk between Nrf2 and PI3K/AKT signaling through inhibition of the lipid phosphatase PTEN, Invest. Ophthalmol. Vis. Sci. 50 (11) (2009) 5339–5347.
[169] D. Liu, et al., Activation of AKT pathway by Nrf2/PDGFA feedback loop contributes to HCC progression, Oncotarget 7 (40) (2016) 65389–65402.
[170] W. Xu, et al., Role of PI3K/Akt-mediated Nrf2/HO-1 signaling pathway in resveratrol alleviation of zearalenone-induced oxidative stress and apoptosis in TM4 cells, Toxins (basel) 14 (11) (2022) 733.
[171] J.M. Shin, et al., Nrf2 negatively regulates melanogenesis by modulating PI3K/Akt signaling, PLoS One 9 (4) (2014) e96035.
[172] A. Ferino, V. Rapozzi, L.E. Xodo, The ROS-KRAS-Nrf2 axis in the control of the redox homeostasis and the intersection with survival-apoptosis pathways: implications for photodynamic therapy, J. Photochem. Photobiol. B 202 (2020) 111672.
[173] M. Koolpe, et al., EphB receptor-binding peptides identified by phage display enable design of an antagonist with ephrin-like affinity, J. Biol. Chem. 280 (17) (2005) 17301–17311.
[174] S. Bhatia, et al., Inhibition of EphB4-Ephrin-B2 signaling reprograms the tumor immune microenvironment in head and neck cancers, Cancer Res. 79 (10) (2019) 2722–2735.
[175] W. Li, et al., Overcoming photodynamic resistance and tumor targeting dual-therapy mediated by indocyanine green conjugated gold nanospheres, J. Control. Release 258 (2017) 171–181.
[176] S. Bagdonas, et al., Phototransformations of 5-aminolevulinic acid-induced protoporphyrin IX in vitro: a spectroscopic study, Photochem. Photobiol. 72 (2) (2000) 186–192.
[177] H.S. de Bruijn, et al., Increase in protoporphyrin IX after 5-aminolevulinic acid based photodynamic therapy is due to local re-synthesis, Photochem. Photobiol. Sci. 6 (8) (2007) 857–864.
[178] Y. Hagiya, et al., Pivotal roles of peptide transporter PEPT1 and ATP-binding cassette (ABC) transporter ABCG2 in 5-aminolevulinic acid (ALA)-based photocytotoxicity of gastric cancer cells in vitro, Photodiagnosis Photodyn. Ther. 9 (3) (2012) 204–214.
[179] S. Tian, et al., Enhancement of the effect of methyl pyropheophorbide-a-mediated photodynamic therapy was achieved by increasing ROS through inhibition of Nrf2-HO-1 or Nrf2-ABCG2 signaling, Anticancer Agents Med Chem. 17 (13) (2017) 1824–1836.
[180] M.M. Silva, et al., The balance between NRF2/GSH antioxidant mediated pathway and DNA repair modulates cisplatin resistance in lung cancer cells, Sci. Rep. 9 (1) (2019) 17639.
[181] M.A. Fath, et al., Enhancement of carboplatin-mediated lung cancer cell killing by simultaneous disruption of glutathione and thioredoxin metabolism, Clin. Cancer Res. 17 (19) (2011) 6206–6217.
[182] J. Hong, et al., Targeting glutamine metabolism enhances responses to platinum-based chemotherapy in triple-negative breast cancers (TNBC), Genes Dis 9 (6) (2022) 1408–1411.
[183] A. Bansal, M.C. Simon, Glutathione metabolism in cancer progression and treatment resistance, J. Cell Biol. 217 (7) (2018) 2291–2298.
[184] M. Zhao, et al., GSH-dependent antioxidant defense contributes to the acclimation of colon cancer cells to acidic microenvironment, Cell Cycle 15 (8) (2016) 1125–1133.
[185] Z. Li, et al., Dihydroartemisinin administration improves the effectiveness of 5-aminolevulinic acid-mediated photodynamic therapy for the treatment of high-risk human papillomavirus infection, Photodiagnosis Photodyn. Ther. 33 (2021) 102078.
[186] M.Y. Kwon, et al., Heme oxygenase-1 accelerates erastin-induced ferroptotic cell death, Oncotarget 6 (27) (2015) 24393–24403.
[187] L.C. Chang, et al., Heme oxygenase-1 mediates BAY 11-7085 induced ferroptosis, Cancer Lett. 416 (2018) 124–137.
[188] O. Adedoyin, et al., Heme oxygenase-1 mitigates ferroptosis in renal proximal tubule cells, Am. J. Physiol. Renal Physiol. 314 (5) (2018) F702–F714.
[189] R. Wei, et al., Tagitinin C induces ferroptosis through PERK-Nrf2-HO-1 signaling pathway in colorectal cancer cells, Int. J. Biol. Sci. 17 (11) (2021) 2703–2717.
[190] Y.T. Lv, et al., HO-1 activation contributes to cadmium-induced ferroptosis in renal tubular epithelial cells via increasing the labile iron pool and promoting mitochondrial ROS generation, Chem. Biol. Interact. 399 (2024) 111152.
[191] J. de Oliveira, M.B. Denadai, D.L. Costa, Crosstalk between heme oxygenase-1 and iron metabolism in macrophages: implications for the modulation of inflammation and immunity, Antioxidants (basel) 11 (5) (2022) 861.
[192] J. Wang, et al., Haem-activated promiscuous targeting of artemisinin in Plasmodium falciparum, Nat. Commun. 6 (2015) 10111.
[193] H.M. Ismail, et al., Artemisinin activity-based probes identify multiple molecular targets within the asexual stage of the malaria parasites Plasmodium falciparum 3D7, Proc. Natl. Acad. Sci. U. S. A. 113 (8) (2016) 2080–2085.
[194] P.A. Stocks, et al., Evidence for a common non-heme chelatable-iron-dependent activation mechanism for semisynthetic and synthetic endoperoxide antimalarial drugs, Angew. Chem. Int. Ed. Engl. 46 (33) (2007) 6278–6283.
[195] Y. Chen, et al., Dihydroartemisinin-induced unfolded protein response feedback attenuates ferroptosis via PERK/ATF4/HSPA5 pathway in glioma cells, J. Exp. Clin. Cancer Res. 38 (1) (2019) 402.
[196] R. Yi, et al., Dihydroartemisinin initiates ferroptosis in glioblastoma through GPX4 inhibition, Biosci. Rep. 40 (6) (2020) BSR20193314.
[197] Z. Wang, et al., Dihydroartemisinin triggers ferroptosis in primary liver cancer cells by promoting and unfolded protein response–induced upregulation of CHAC1 expression, Oncol. Rep. 46 (5) (2021) 240.
[198] J. Ji, et al., Dihydroartemisinin induces ferroptosis of hepatocellular carcinoma via inhibiting ATF4-xCT pathway, J. Cell Mol. Med. 28 (8) (2024) e18335.
[199] C. Qu, et al., Dihydroartemisinin exerts anti-tumor activity by inducing mitochondrion and endoplasmic reticulum apoptosis and autophagic cell death in human glioblastoma cells, Front. Cell. Neurosci. 11 (2017) 310.
[200] F. Poupel, et al., Dihydroartemisinin induces apoptosis in human bladder cancer cell lines through reactive oxygen species, mitochondrial membrane potential, and cytochrome c pathway, Int. J. Prev. Med. 8 (2017) 78.
[201] S. Kocanova, et al., Induction of heme-oxygenase 1 requires the p38MAPK and PI3K pathways and suppresses apoptotic cell death following hypericin-mediated photodynamic therapy, Apoptosis 12 (4) (2007) 731–741.
[202] T. Lv, et al., Halofuginone enhances the anti-tumor effect of ALA-PDT by suppressing NRF2 signaling in cSCC, Photodiagnosis Photodyn. Ther. 37 (2022) 102572.
[203] W. Tao, et al., Enhanced ROS-boosted phototherapy against pancreatic cancer via Nrf2-mediated stress-defense pathway suppression and ferroptosis induction, ACS Appl. Mater. Interfaces 14 (5) (2022) 6404–6416.
[204] X. Hou, et al., 3',4',5',5,7-pentamethoxyflavone sensitizes Cisplatin-resistant A549 cells to Cisplatin by inhibition of Nrf2 pathway, Mol. Cells 38 (5) (2015) 396–401.
[205] H. Cai, et al., Pharmacokinetics in mice and metabolism in murine and human liver fractions of the putative cancer chemopreventive agents 3',4',5',5,7-pentamethoxyflavone and tricin (4',5,7-trihydroxy-3',5'-dimethoxyflavone), Cancer Chemother. Pharmacol. 67 (2) (2011) 255–263.
[206] H. Cai, et al., Flavones as colorectal cancer chemopreventive agents–phenol-o-methylation enhances efficacy, Cancer Prev. Res. (Phila.) 2 (8) (2009) 743–750.
[207] J.A.C. Sousa, et al., New flavone, and cytotoxicity activity of Rauia resinosa ethanolic extract and constituents, Nat. Prod. Res. 37 (14) (2023) 2415–2420.
[208] D.M. Tomazela, et al., Pyrano chalcones and a flavone from Neoraputia magnifica and their Trypanosoma cruzi glycosomal glyceraldehyde-3-phosphate dehydrogenase-inhibitory activities, Phytochemistry 55 (6) (2000) 643–651.
[209] H. Cai, et al., Determination of 3',4',5',5,7-pentamethoxyflavone in the plasma and intestinal mucosa of mice by HPLC with UV detection, Biomed. Chromatogr. 23 (4) (2009) 335–339.
[210] H. Luo, et al., Synthesis of new AIEE-active chalcones for imaging of mitochondria in living cells and zebrafish in vivo, Int. J. Mol. Sci. 22 (16) (2021) 8949.
[211] S.Y. Kim, I.S. Lee, A. Moon, 2-Hydroxychalcone and xanthohumol inhibit invasion of triple negative breast cancer cells, Chem. Biol. Interact. 203 (3) (2013) 565–572.
[212] J. Lim, et al., 4-methoxychalcone enhances cisplatin-induced oxidative stress and cytotoxicity by inhibiting the Nrf2/ARE-mediated defense mechanism in A549 lung cancer cells, Mol. Cells 36 (4) (2013) 340–346.
[213] Y. Han, et al., Regulatory effects of 4-methoxychalcone on adipocyte differentiation through PPARgamma activation and reverse effect on TNF-alpha in 3T3-L1 cells, Food Chem. Toxicol. 106 (Pt A) (2017) 17–24.
[214] P. Perjesi, Z. Rozmer, Kinetic analysis of some chalcones and synthetic chalcone analogues on the fenton-reaction initiated deoxyribose degradation assay, Open Med. Chem. J. 5 (2011) 61–67.
[215] M.J. Bollong, et al., A small molecule inhibits deregulated NRF2 transcriptional activity in cancer, ACS Chem. Biol. 10 (10) (2015) 2193–2198.
[216] N.M. Stacks, Apigenin and naringenin: natural sources, pharmacology and role in cancer prevention. Biochemistry Research Trends. 2015: Nova Science Publishers, Incorporated.
[217] L.P. Li, et al., Interspecies difference of luteolin and apigenin after oral administration of Chrysanthemum morifolium extract and prediction of human pharmacokinetics, Pharmazie 68 (3) (2013) 195–200.
[218] G. Favaro, et al., Acidichromism and ionochromism of luteolin and apigenin, the main components of the naturally occurring yellow weld: a spectrophotometric and fluorimetric study, J. Fluoresc. 17 (6) (2007) 707–714.
[219] P. Kaur, S. Shukla, S. Gupta, Plant flavonoid apigenin inactivates Akt to trigger apoptosis in human prostate cancer: an in vitro and in vivo study, Carcinogenesis 29 (11) (2008) 2210–2217.
[220] T.W. Kim, H.G. Lee, Apigenin induces autophagy and cell death by targeting EZH2 under hypoxia conditions in gastric cancer cells, Int. J. Mol. Sci. 22 (24) (2021) 13455.
[221] S. Shukla, et al., Apigenin blocks IKKalpha activation and suppresses prostate cancer progression, Oncotarget 6 (31) (2015) 31216–31232.
[222] A. Amat, et al., Absorption and emission of the apigenin and luteolin flavonoids: a TDDFT investigation, J. Phys. Chem. A 113 (52) (2009) 15118–15126.
[223] A.M. Gao, et al., Apigenin sensitizes doxorubicin-resistant hepatocellular carcinoma BEL-7402/ADM cells to doxorubicin via inhibiting PI3K/Akt/Nrf2 pathway, Carcinogenesis 34 (8) (2013) 1806–1814.
[224] A.M. Gao, X.Y. Zhang, Z.P. Ke, Apigenin sensitizes BEL-7402/ADM cells to doxorubicin through inhibiting miR-101/Nrf2 pathway, Oncotarget 8 (47) (2017) 82085–82091.
[225] L. Xu, et al., Apigenin suppresses PD-L1 expression in melanoma and host dendritic cells to elicit synergistic therapeutic effects, J. Exp. Clin. Cancer Res. 37 (1) (2018) 261.
[226] L.S. T, et al., Regulation of Nrf2/ARE Pathway by Dietary Flavonoids: A Friend or Foe for Cancer Management? Antioxidants (Basel) 9 (10) (2020) 973.
[227] M.R.P. Coombs, M.E. Harrison, D.W. Hoskin, Apigenin inhibits the inducible expression of programmed death ligand 1 by human and mouse mammary carcinoma cells, Cancer Lett. 380 (2) (2016) 424–433.
[228] Z. Mostafavi-Pour, et al., The role of quercetin and vitamin C in Nrf2-dependent oxidative stress production in breast cancer cells, Oncol. Lett. 13 (3) (2017) 1965–1973.

[229] T. Tarumoto, et al., Ascorbic acid restores sensitivity to imatinib via suppression of Nrf2-dependent gene expression in the imatinib-resistant cell line, Exp. Hematol. 32 (4) (2004) 375–381.
[230] J. Frank, et al., Ascorbic acid suppresses cell death in rat DS-sarcoma cancer cells induced by 5-aminolevulinic acid-based photodynamic therapy, Free Radic. Biol. Med. 40 (5) (2006) 827–836.
[231] T.M. Wu, et al., Mechanisms and applications of the anti-cancer effect of pharmacological ascorbic acid in cervical cancer cells, Front. Oncol. 10 (2020) 1483.
[232] A. Abbasi, et al., Chemoprevention of prostate cancer cells by vitamin c plus quercetin: role of Nrf2 in inducing oxidative stress, Nutr. Cancer 73 (10) (2021) 2003–2013.
[233] G.G. Kramarenko, et al., Ascorbate enhances the toxicity of the photodynamic action of Verteporfin in HL-60 cells, Free Radic. Biol. Med. 40 (9) (2006) 1615–1627.
[234] Y. Wei, et al., Enhancement of photodynamic antitumor effect with pro-oxidant ascorbate, Lasers Surg. Med. 44 (1) (2012) 69–75.
[235] S. Grimm, et al., The outcome of 5-ALA-mediated photodynamic treatment in melanoma cells is influenced by vitamin C and heme oxygenase-1, Biofactors 37 (1) (2011) 17–24.
[236] S. Koo, et al., Harnessing GLUT1-Targeted Pro-oxidant Ascorbate for Synergistic Phototherapeutics, Angew. Chem. Int. Ed. Engl. 61 (17) (2022) e202110832.
[237] A.E. Wagner, et al., Ascorbic acid partly antagonizes resveratrol mediated heme oxygenase-1 but not paraoxonase-1 induction in cultured hepatocytes - role of the redox-regulated transcription factor Nrf2, BMC Complement. Altern. Med. 11 (1) (2011) 1.
[238] W. Tang, et al., Novel nitric oxide-releasing derivatives of brusatol as anti-inflammatory agents: design, synthesis, biological evaluation, and nitric oxide release studies, J. Med. Chem. 57 (18) (2014) 7600–7612.
[239] Y. Pei, et al., Quassinoid analogs with enhanced efficacy for treatment of hematologic malignancies target the PI3Kgamma isoform, Commun. Biol. 3 (1) (2020) 267.
[240] N. Guo, et al., Determination of brusatol in plasma and tissues by LC-MS method and its application to a pharmacokinetic and distribution study in mice, J. Chromatogr. B Analyt. Technol. Biomed. Life Sci. 1053 (2017) 20–26.
[241] Q. Zhang, et al., Determination of a potential antitumor quassinoid in rat plasma by UPLC-MS/MS and its application in a pharmacokinetic study, J. Pharm. Biomed. Anal. 124 (2016) 143–148.
[242] A. Olayanju, et al., Brusatol provokes a rapid and transient inhibition of Nrf2 signaling and sensitizes mammalian cells to chemical toxicity-implications for therapeutic targeting of Nrf2, Free Radic. Biol. Med. 78 (2015) 202–212.
[243] B. Harder, et al., Brusatol overcomes chemoresistance through inhibition of protein translation, Mol. Carcinog. 56 (5) (2017) 1493–1500.
[244] D. Ren, et al., Brusatol enhances the efficacy of chemotherapy by inhibiting the Nrf2-mediated defense mechanism, Proc. Natl. Acad. Sci. U. S. A. 108 (4) (2011) 1433–1438.
[245] S. Xing, et al., Brusatol has therapeutic efficacy in non-small cell lung cancer by targeting Skp1 to inhibit cancer growth and metastasis, Pharmacol. Res. 176 (2022) 106059.
[246] S. Vartanian, et al., Application of mass spectrometry profiling to establish brusatol as an inhibitor of global protein synthesis, Mol. Cell. Proteomics 15 (4) (2016) 1220–1231.
[247] J.H. Lee, et al., Brusatol, a Nrf2 inhibitor targets STAT3 signaling cascade in head and neck squamous cell carcinoma, Biomolecules 9 (10) (2019) 550.
[248] J.H. Lee, et al., Brusatol suppresses STAT3-driven metastasis by downregulating epithelial-mesenchymal transition in hepatocellular carcinoma, J. Adv. Res. 26 (2020) 83–94.
[249] J. Zhou, et al., Brusatol inhibits laryngeal cancer cell proliferation and metastasis via abrogating JAK2/STAT3 signaling mediated epithelial-mesenchymal transition, Life Sci. 284 (2021) 119907.
[250] H. Chen, et al., Brusatol reverses lipopolysaccharide-induced epithelial-mesenchymal transformation and induces apoptosis through PI3K/Akt/NF-κB pathway in human gastric cancer SGC-7901 cells, Anticancer Drugs 32 (4) (2021) 394–404.
[251] S. Samarghandian, et al., Inhibitory and cytotoxic activities of chrysin on human breast adenocarcinoma cells by induction of apoptosis, Pharmacogn. Mag. 12 (Suppl 4) (2016) S436–S440.
[252] W. Yao, et al., Toxicological evaluation of a flavonoid, chrysin: morphological, behavioral, biochemical and histopathological assessments in rats, Drug Chem. Toxicol. 44 (6) (2021) 601–612.
[253] T. Walle, et al., Disposition and metabolism of the flavonoid chrysin in normal volunteers, Br. J. Clin. Pharmacol. 51 (2) (2001) 143–146.
[254] B.Y. Khoo, S.L. Chua, P. Balaram, Apoptotic effects of chrysin in human cancer cell lines, Int. J. Mol. Sci. 11 (5) (2010) 2188–2199.
[255] A.M. Gao, et al., Chrysin enhances sensitivity of BEL-7402/ADM cells to doxorubicin by suppressing PI3K/Akt/Nrf2 and ERK/Nrf2 pathway, Chem. Biol. Interact. 206 (1) (2013) 100–108.
[256] J. Wang, et al., Chrysin suppresses proliferation, migration, and invasion in glioblastoma cell lines via mediating the ERK/Nrf2 signaling pathway, Drug Des. Devel. Ther. 12 (2018) 721–733.
[257] C.S. Huang, et al., Protection by chrysin, apigenin, and luteolin against oxidative stress is mediated by the Nrf2-dependent up-regulation of heme oxygenase 1 and glutamate cysteine ligase in rat primary hepatocytes, Arch. Toxicol. 87 (1) (2013) 167–178.
[258] D. Liu, et al., Novel photosensitizing properties of porphyrin–chrysin derivatives with antitumor activity in vitro, J. Chem. Res. 44 (7–8) (2020) 494–504.
[259] S. Yuvaraj, et al., Chrysin attenuates high-fat-diet-induced myocardial oxidative stress via upregulating eNOS and Nrf2 target genes in rats, Mol. Cell. Biochem. 476 (7) (2021) 2719–2727.
[260] H. Lin, et al., Small molecular Nrf2 inhibitors as chemosensitizers for cancer therapy, Future Med. Chem. 12 (3) (2020) 243–267.
[261] E.J. Choi, et al., A clinical drug library screen identifies clobetasol propionate as an NRF2 inhibitor with potential therapeutic efficacy in KEAP1 mutant lung cancer, Oncogene 36 (37) (2017) 5285–5295.
[262] J.W. Jang, S. Park, E.Y. Moon, Spleen tyrosine kinase regulates crosstalk of hypoxia-inducible factor-1alpha and nuclear factor (erythroid-derived2)-like 2 for B cell survival, Int. Immunopharmacol. 95 (2021) 107509.
[263] S.R. Wiegell, B. Petersen, H.C. Wulf, Topical corticosteroid reduces inflammation without compromising the efficacy of photodynamic therapy for actinic keratoses: a randomized clinical trial, Br. J. Dermatol. 171 (6) (2014) 1487–1492.
[264] C.Y. Wu, et al., Cryptotanshinone down-regulates androgen receptor signaling by modulating lysine-specific demethylase 1 function, Int. J. Cancer 131 (6) (2012) 1423–1434.
[265] J.M. Hur, et al., Cryptotanshinone but not tanshinone IIA inhibits angiogenesisin vitro, Exp. Mol. Med. 37 (2) (2005) 133–137.
[266] M. Xue, et al., Reversed-phase liquid chromatographic determination of cryptotanshinone and its active metabolite in pig plasma and urine, J. Pharm. Biomed. Anal. 21 (1) (1999) 207–213.
[267] Y. Pan, et al., Pharmacokinetic characterization of hydroxylpropyl-beta-cyclodextrin-included complex of cryptotanshinone, an investigational cardiovascular drug purified from Danshen (Salvia miltiorrhiza), Xenobiotica 38 (4) (2008) 382–398.
[268] J.F. Li, et al., Studies on the spectroscopic behavior of cryptotanshinone, tanshinone IIA, and tanshinone I, Spectrochim. Acta A Mol. Biomol. Spectrosc. 60 (4) (2004) 751–756.
[269] Y. Luo, et al., Uncovering the mechanisms of cryptotanshinone as a therapeutic agent against hepatocellular carcinoma, Front. Pharmacol. 11 (2020) 1264.
[270] M. Naziri, et al., A mini-review of the anticancer properties of cryptotanshinone: a quinoid diterpene extracted from the root of salvia miotiorrhiza bunge, Front. Drug Discovery 2 (2022) 815017.
[271] H. Li, et al., A review of the biological activity and pharmacology of cryptotanshinone, an important active constituent in Danshen, Biomed. Pharmacother. 137 (2021) 111332.
[272] C. Xia, et al., Cryptotanshinone reverses cisplatin resistance of human lung carcinoma A549 cells through down-regulating Nrf2 pathway, Cell. Physiol. Biochem. 37 (2) (2015) 816–824.
[273] X.X. Li, et al., Cryptotanshinone from Salvia miltiorrhiza Bunge (Danshen) inhibited inflammatory responses via TLR4/MyD88 signaling pathway, Chin. Med. 15 (2020) 20.
[274] J.E. Lee, et al., Neuroprotective effects of cryptotanshinone in a direct reprogramming model of parkinson's disease, Molecules 25 (16) (2020) 3602.
[275] L. Cao, et al., Cryptotanshinone strengthens the effect of gefitinib against non-small cell lung cancer through inhibiting transketolase, Eur. J. Pharmacol. 890 (2021) 173647.
[276] Z. Zheng, et al., Non-classical cardenolides from Calotropis gigantea exhibit anticancer effect as HIF-1 inhibitors, Bioorg. Chem. 109 (2021) 104740.
[277] E. Iisalo, Clinical pharmacokinetics of digoxin, Clin. Pharmacokinet. 2 (1) (1977) 1–16.
[278] E. Kwong, K.M. McErlane, Analysis of digoxin at therapeutic concentrations using high-performance liquid chromatography with post-column derivatization, J. Chromatogr. 381 (2) (1986) 357–363.
[279] Y. Zhou, et al., Digoxin sensitizes gemcitabine-resistant pancreatic cancer cells to gemcitabine via inhibiting Nrf2 signaling pathway, Redox Biol. 22 (2019) 101131.
[280] Y. Wang, et al., Digoxin exerts anticancer activity on human nonsmall cell lung cancer cells by blocking PI3K/Akt pathway, Biosci. Rep. 41 (10) (2021) BSR20211056.
[281] J. Bejcek, et al., Na(+)/K(+)-ATPase revisited: on its mechanism of action, role in cancer, and activity modulation, Molecules 26 (7) (2021) 1905.
[282] M.N.V. David, M. Shetty, Digoxin, [Updated 2024 Nov 25]. In: StatPearls [Internet]. Treasure Island (FL): StatPearls Publishing; 2025 Jan-. Available from: https://www.ncbi.nlm.nih.gov/books/NBK556025/.
[283] M. Zhu, et al., Population pharmacokinetics of ethionamide in patients with tuberculosis, Tuberculosis (Edinb.) 82 (2–3) (2002) 91–96.
[284] Brown, M.J., et al., Clinical Pharmacology - E-Book. 2018: Elsevier Health Sciences.
[285] S.S.a.M.D. Sujit Kumar Debnath, Validated UV-spectrophotometric method for the ethionamide estimation in bulk, tablet and nanoparticles, Int J Drug Dev & Res 9 (1) (2017) 4.
[286] H. Peng, et al., Suppression of NRF2-ARE activity sensitizes chemotherapeutic agent-induced cytotoxicity in human acute monocytic leukemia cells, Toxicol. Appl. Pharmacol. 292 (2016) 1–7.
[287] R.K. Pandey, et al., Febrifugine dihydrochloride as a new oral chemotherapeutic agent against visceral leishmaniasis infection, Exp. Parasitol. 236–237 (2022) 108250.
[288] K. Tsuchida, et al., Halofuginone enhances the chemo-sensitivity of cancer cells by suppressing NRF2 accumulation, Free Radic. Biol. Med. 103 (2017) 236–247.
[289] S. Jiang, et al., Antimalarial activities and therapeutic properties of febrifugine analogs, Antimicrob. Agents Chemother. 49 (3) (2005) 1169–1176.
[290] Singh Ningthoujam, S., et al., Chapter 3 - Febrifugine and Its Analogs: Studies for Their Antimalarial and Other Therapeutic Properties, in Studies in Natural Products Chemistry, R. Atta ur, Editor. 2015, Elsevier. p. 93-112.

[291] L.D. Kinabo, Q.A. McKellar, Pharmacokinetics of halofuginone in cattle, Br. Vet. J. 145 (6) (1989) 546–551.
[292] S. Endo, et al., Targeting Nrf2-antioxidant signalling reverses acquired cabazitaxel resistance in prostate cancer cells, J. Biochem. 170 (1) (2021) 89–96.
[293] M. Pines, I. Spector, Halofuginone - the multifaceted molecule, Molecules 20 (1) (2015) 573–594.
[294] M.S. Zaghloul, et al., Crocin attenuates lung inflammation and pulmonary vascular dysfunction in a rat model of bleomycin-induced pulmonary fibrosis, Life Sci. 235 (2019) 116794.
[295] J. Yuan, et al., Inhibition of GCN2 alleviates hepatic steatosis and oxidative stress in obese mice: involvement of NRF2 regulation, Redox Biol. 49 (2022) 102224.
[296] L. Luo, et al., Halofuginone attenuates intervertebral discs degeneration by suppressing collagen I production and inactivating TGFbeta and NF-kappaB pathway, Biomed. Pharmacother. 101 (2018) 745–753.
[297] M.L. Jin, et al., Halofuginone induces the apoptosis of breast cancer cells and inhibits migration via downregulation of matrix metalloproteinase-9, Int. J. Oncol. 44 (1) (2014) 309–318.
[298] T.L. Keller, et al., Halofuginone and other febrifugine derivatives inhibit prolyl-tRNA synthetase, Nat. Chem. Biol. 8 (3) (2012) 311–317.
[299] M.J. de Jonge, et al., Phase I and pharmacokinetic study of halofuginone, an oral quinazolinone derivative in patients with advanced solid tumours, Eur. J. Cancer 42 (12) (2006) 1768–1774.
[300] Z. Gavish, et al., Growth inhibition of prostate cancer xenografts by halofuginone, Prostate 51 (2) (2002) 73–83.
[301] J. Ahn, et al., Synthesis and biological evaluation of novel IM3829 (4-(2-Cyclohexylethoxy)aniline) derivatives as potent radiosensitizers, Bull. Kor. Chem. Soc. 35 (12) (2014) 3623–3626.
[302] G.B. Migliori, Infectious Diseases || Antituberculosis Agents, fourth ed., vol. 2, Elsevier, 2017, pp. 1264-1276.e2. https://doi.org/10.1016/B978-0-7020-6285-8.00148-9.
[303] A.K. Verma, et al., Isoniazid prevents Nrf2 translocation by inhibiting ERK1 phosphorylation and induces oxidative stress and apoptosis, Redox Biol. 6 (2015) 80–92.
[304] A.K. Verma, et al., Isoniazid induces apoptosis: Role of oxidative stress and inhibition of nuclear translocation of nuclear factor (erythroid-derived 2)-like 2 (Nrf2), Life Sci. 199 (2018) 23–33.
[305] Q. Lv, et al., Mitochondria-targeted prostate cancer therapy using a near-infrared fluorescence dye-monoamine oxidase a inhibitor conjugate, J. Control. Release 279 (2018) 234–242.
[306] N.A. Smith, et al., Combatting AMR: photoactivatable ruthenium(ii)-isoniazid complex exhibits rapid selective antimycobacterial activity, Chem. Sci. 8 (1) (2017) 395–404.
[307] P. Qiao, et al., Oral isoniazid causes oxidative stress, oocyte deterioration and infertility in mice, Toxicology 455 (2021) 152749.
[308] M.H. Park, et al., Rapid tumor targeting of renal-clearable ZW800-1 conjugate for efficient photothermal cancer therapy, Biomedicines 9 (9) (2021) 1151.
[309] R. Hori, et al., The discovery and characterization of K-563, a novel inhibitor of the Keap1/Nrf2 pathway produced by Streptomyces sp, Cancer Med. 8 (3) (2019) 1157–1168.
[310] F. Wang, et al., Kaempferol induces ROS-dependent apoptosis in pancreatic cancer cells via TGM2-mediated Akt/mTOR signaling, BMC Cancer 21 (1) (2021) 396.
[311] A. Triantafyllou, et al., Flavonoids induce HIF-1alpha but impair its nuclear accumulation and activity, Free Radic. Biol. Med. 44 (4) (2008) 657–670.
[312] V. Zabela, et al., Pharmacokinetics of dietary kaempferol and its metabolite 4-hydroxyphenylacetic acid in rats, Fitoterapia 115 (2016) 189–197.
[313] Mukai, R., et al., Determination of Subcellular Localization of Flavonol in Cultured Cells by Laser Scanning, in Laser Scanning, Theory and Applications, C.-C. Wang, Editor. 2011.
[314] C. Fouzder, A. Mukhuty, R. Kundu, Kaempferol inhibits Nrf2 signalling pathway via downregulation of Nrf2 mRNA and induces apoptosis in NSCLC cells, Arch. Biochem. Biophys. 697 (2021) 108700.
[315] T. Kitakaze, et al., Kaempferol modulates TCDD- and t-BHQ-induced drug-metabolizing enzymes and luteolin enhances this effect, Food Funct. 11 (4) (2020) 3668–3680.
[316] J. Niestroy, et al., Single and concerted effects of benzo[a]pyrene and flavonoids on the AhR and Nrf2-pathway in the human colon carcinoma cell line Caco-2, Toxicol. In Vitro 25 (3) (2011) 671–683.
[317] X. Tang, et al., Luteolin inhibits Nrf2 leading to negative regulation of the Nrf2/ARE pathway and sensitization of human lung carcinoma A549 cells to therapeutic drugs, Free Radic. Biol. Med. 50 (11) (2011) 1599–1609.
[318] S. Chian, et al., Luteolin sensitizes two oxaliplatin-resistant colorectal cancer cell lines to chemotherapeutic drugs via inhibition of the Nrf2 pathway, Asian Pac. J. Cancer Prev. 15 (6) (2014) 2911–2916.
[319] K. Kanai, et al., Therapeutic anti-inflammatory effects of luteolin on endotoxin-induced uveitis in Lewis rats, J. Vet. Med. Sci. 78 (8) (2016) 1381–1384.
[320] L. Huang, K. Jin, H. Lan, Luteolin inhibits cell cycle progression and induces apoptosis of breast cancer cells through downregulation of human telomerase reverse transcriptase, Oncol. Lett. 17 (4) (2019) 3842–3850.
[321] P. Zhou, et al., Intestinal absorption of luteolin from peanut hull extract is more efficient than that from individual pure luteolin, J. Agric. Food Chem. 56 (1) (2008) 296–300.
[322] S. Chian, et al., Luteolin inhibits the Nrf2 signaling pathway and tumor growth in vivo, Biochem. Biophys. Res. Commun. 447 (4) (2014) 602–608.
[323] K.A. Kang, et al., Luteolin promotes apoptotic cell death via upregulation of Nrf2 expression by DNA demethylase and the interaction of Nrf2 with p53 in human colon cancer cells, Exp. Mol. Med. 51 (4) (2019) 1–14.
[324] M. Sabzichi, et al., Luteolin-loaded phytosomes sensitize human breast carcinoma MDA-MB 231 cells to doxorubicin by suppressing Nrf2 mediated signalling, Asian Pac. J. Cancer Prev. 15 (13) (2014) 5311–5316.
[325] X. Paredes-Gonzalez, et al., Induction of NRF2-mediated gene expression by dietary phytochemical flavones apigenin and luteolin, Biopharm. Drug Dispos. 36 (7) (2015) 440–451.
[326] T. Zhang, et al., Luteolin modulates expression of drug-metabolizing enzymes through the AhR and Nrf2 pathways in hepatic cells, Arch. Biochem. Biophys. 557 (2014) 36–46.
[327] Y.C. Zhang, et al., Antioxidant and Nrf2 inducing activities of luteolin, a flavonoid constituent in Ixeris sonchifolia Hance, provide neuroprotective effects against ischemia-induced cellular injury, Food Chem. Toxicol. 59 (2013) 272–280.
[328] E. Urpilainen, et al., Metformin diminishes the unfavourable impact of Nrf2 in breast cancer patients with type 2 diabetes, Tumour Biol. 41 (1) (2019) 1010428318815413.
[329] C. Yu, et al., Metformin sensitizes non-small cell lung cancer cells to an epigallocatechin-3-gallate (EGCG) treatment by suppressing the Nrf2/HO-1 signaling pathway, Int. J. Biol. Sci. 13 (12) (2017) 1560–1569.
[330] M.T. Do, et al., Metformin inhibits heme oxygenase-1 expression in cancer cells through inactivation of Raf-ERK-Nrf2 signaling and AMPK-independent pathways, Toxicol. Appl. Pharmacol. 271 (2) (2013) 229–238.
[331] R.J. Dowling, et al., Changes in insulin receptor signaling underlie neoadjuvant metformin administration in breast cancer: a prospective window of opportunity neoadjuvant study, Breast Cancer Res. 17 (1) (2015) 32.
[332] M.T. Do, et al., Metformin induces microRNA-34a to downregulate the Sirt1/Pgc-1alpha/Nrf2 pathway, leading to increased susceptibility of wild-type p53 cancer cells to oxidative stress and therapeutic agents, Free Radic. Biol. Med. 74 (2014) 21–34.
[333] M. Broekgaarden, et al., Modulation of redox metabolism negates cancer-associated fibroblasts-induced treatment resistance in a heterotypic 3D culture platform of pancreatic cancer, Biomaterials 222 (2019) 119421.
[334] T. Osaki, et al., Metformin enhances the cytotoxicity of 5-aminolevulinic acid-mediated photodynamic therapy in vitro, Oncol. Lett. 14 (1) (2017) 1049–1053.
[335] I. Nenu, et al., Metformin associated with photodynamic therapy–a novel oncological direction, J. Photochem. Photobiol. B 138 (2014) 80–91.
[336] G.G. Graham, et al., Clinical pharmacokinetics of metformin, Clin. Pharmacokinet. 50 (2) (2011) 81–98.
[337] A. Singh, et al., Small molecule inhibitor of NRF2 selectively intervenes therapeutic resistance in KEAP1-deficient NSCLC tumors, ACS Chem. Biol. 11 (11) (2016) 3214–3225.
[338] R. Li, et al., Antidiabetic agent DPP-4i facilitates murine breast cancer metastasis by oncogenic ROS-NRF2-HO-1 axis via a positive NRF2-HO-1 feedback loop, Front. Oncol. 11 (2021) 679816.
[339] H. Liu, et al., CoWO4-x-based nanoplatform for multimode imaging and enhanced photothermal/photodynamic therapy, Chem. Eng. J. 385 (2020) 123979.
[340] W. Li, et al., Death-associated protein kinase 1 regulates oxidative stress in cardiac ischemia reperfusion injury, Cells Tissues Organs 210 (5–6) (2021) 380–390.
[341] J. Zhang, et al., Discovery of a novel Nrf2 inhibitor that induces apoptosis of human acute myeloid leukemia cells, Oncotarget 8 (5) (2017) 7625–7636.
[342] I. Studer-Rohr, J. Schlatter, D.R. Dietrich, Kinetic parameters and intraindividual fluctuations of ochratoxin a plasma levels in humans, Arch. Toxicol. 74 (9) (2000) 499–510.
[343] R. Kumar, et al., Ochratoxin A-induced cell proliferation and tumor promotion in mouse skin by activating the expression of cyclin-D1 and cyclooxygenase-2 through nuclear factor-kappa B and activator protein-1, Carcinogenesis 34 (3) (2013) 647–657.
[344] D. Steinbrück, C. Rasch, M.U. Kumke, Photophysics of ochratoxin a in aqueous solution, Zeitschrift Für Naturforschung B 63 (11) (2008) 1321–1326.
[345] A. Limonciel, P. Jennings, A review of the evidence that ochratoxin a is an Nrf2 inhibitor: implications for nephrotoxicity and renal carcinogenicity, Toxins (Basel) 6 (1) (2014) 371–379.
[346] C. Boesch-Saadatmandi, et al., Ochratoxin a impairs Nrf2-dependent gene expression in porcine kidney tubulus cells, J. Anim. Physiol. Anim. Nutr. 93 (5) (2009) 547–554.
[347] C. Cavin, et al., Reduction in antioxidant defenses may contribute to ochratoxin a toxicity and carcinogenicity, Toxicol. Sci. 96 (1) (2007) 30–39.
[348] P. Jennings, et al., Transcriptomic alterations induced by Ochratoxin a in rat and human renal proximal tubular in vitro models and comparison to a rat in vivo model, Arch. Toxicol. 86 (4) (2012) 571–589.
[349] C. Cavin, et al., Ochratoxin A-mediated DNA and protein damage: roles of nitrosative and oxidative stresses, Toxicol. Sci. 110 (1) (2009) 84–94.
[350] H.Q. Duong, et al., Inhibition of NRF2 by PIK-75 augments sensitivity of pancreatic cancer cells to gemcitabine, Int. J. Oncol. 44 (3) (2014) 959–969.
[351] M. Hayakawa, et al., Synthesis and biological evaluation of sulfonylhydrazone-substituted imidazo[1,2-a]pyridines as novel PI3 kinase p110alpha inhibitors, Bioorg. Med. Chem. 15 (17) (2007) 5837–5844.
[352] X.J. Wang, et al., Identification of retinoic acid as an inhibitor of transcription factor Nrf2 through activation of retinoic acid receptor alpha, Proc. Natl. Acad. Sci. U. S. A. 104 (49) (2007) 19589–19594.
[353] C. Iclozan, et al., Therapeutic regulation of myeloid-derived suppressor cells and immune response to cancer vaccine in patients with extensive stage small cell lung cancer, Cancer Immunol. Immunother. 62 (5) (2013) 909–918.

[354] K. Sakamoto, et al., Sensitivity of MLL-rearranged AML cells to all-trans retinoic acid is associated with the level of H3K4me2 in the RARalpha promoter region, Blood Cancer J. 4 (4) (2014) e205.
[355] M.A. Smith, et al., Phase I and pharmacokinetic evaluation of all-trans-retinoic acid in pediatric patients with cancer, J. Clin. Oncol. 10 (11) (1992) 1666–1673.
[356] J.R. Muindi, et al., Clinical pharmacology of oral all-trans retinoic acid in patients with acute promyelocytic leukemia, Cancer Res. 52 (8) (1992) 2138–2142.
[357] A. Vogler, Fluorescence of retinoic acid in the presence of metal salts, Inorg. Chem. Commun. 57 (2015) 69–71.
[358] D.R. Soprano, P. Qin, K.J. Soprano, Retinoic acid receptors and cancers, Annu. Rev. Nutr. 24 (2004) 201–221.
[359] S. Wu, et al., All-trans-retinoic acid blocks cell cycle progression of human ovarian adenocarcinoma cells at late G1, Exp. Cell Res. 232 (2) (1997) 277–286.
[360] M. Valenzuela, et al., Retinoic acid synergizes ATO-mediated cytotoxicity by precluding Nrf2 activity in AML cells, Br. J. Cancer 111 (5) (2014) 874–882.
[361] M. Korbelik, J. Banath, K.M. Saw, Immunoregulatory cell depletion improves the efficacy of photodynamic therapy-generated cancer vaccines, Int. J. Mol. Sci. 16 (11) (2015) 27005–27014.
[362] J.J.W. Wong, S. Lorenz, P.K. Selbo, All-trans retinoic acid enhances the anti-tumour effects of fimaporfin-based photodynamic therapy, Biomed. Pharmacother. 155 (2022) 113678.
[363] K.P. Tan, et al., NRF2 as a determinant of cellular resistance in retinoic acid cytotoxicity, Free Radic. Biol. Med. 45 (12) (2008) 1663–1673.
[364] C. Fouzder, et al., Trigonelline inhibits Nrf2 via EGFR signalling pathway and augments efficacy of Cisplatin and Etoposide in NSCLC cells, Toxicol. In Vitro 70 (2021) 105038.
[365] H. Ashihara, et al., Trigonelline and related nicotinic acid metabolites: occurrence, biosynthesis, taxonomic considerations, and their roles in planta and in human health, Phytochem. Rev. 14 (5) (2014) 765–798.
[366] E. Panieri, L. Saso, Potential applications of NRF2 inhibitors in cancer therapy, Oxid. Med. Cell. Longev. 2019 (2019) 8592348.
[367] U. Boettler, et al., Coffee constituents as modulators of Nrf2 nuclear translocation and ARE (EpRE)-dependent gene expression, J. Nutr. Biochem. 22 (5) (2011) 426–440.
[368] A. Arlt, et al., Inhibition of the Nrf2 transcription factor by the alkaloid trigonelline renders pancreatic cancer cells more susceptible to apoptosis through decreased proteasomal gene expression and proteasome activity, Oncogene 32 (40) (2013) 4825–4835.
[369] J.L. Roh, et al., Nrf2 inhibition reverses the resistance of cisplatin-resistant head and neck cancer cells to artesunate-induced ferroptosis, Redox Biol. 11 (2017) 254–262.
[370] X. Ding, et al., Triptolide induces apoptotic cell death of human cholangiocarcinoma cells through inhibition of myeloid cell leukemia-1, BMC Cancer 14 (2014) 271.
[371] Y.T. Liu, et al., Antibiotic pretreatment promotes orally-administered triptolide absorption and aggravates hepatotoxicity and intestinal injury in mice, J. Ethnopharmacol. 292 (2022) 115224.
[372] F. Shao, et al., Pharmacokinetic study of triptolide, a constituent of immunosuppressive chinese herb medicine, in rats, Biol. Pharm. Bull. 30 (4) (2007) 702–707.
[373] F. Chen, et al., Triptolide, a chinese herbal extract, enhances drug sensitivity of resistant myeloid leukemia cell lines through downregulation of HIF-1alpha and Nrf2, Pharmacogenomics 14 (11) (2013) 1305–1317.
[374] L.B. Nam, W.J. Choi, Y.S. Keum, Triptolide downregulates the expression of NRF2 target genes by increasing cytoplasmic localization of NRF2 in A549 cells, Front. Pharmacol. 12 (2021) 680167.
[375] A. Kumar, et al., Minnelide/triptolide impairs mitochondrial function by regulating SIRT3 in P53-dependent manner in non-small cell lung cancer, PLoS One 11 (8) (2016) e0160783.
[376] B. Giri, et al., Heat shock protein 70 in pancreatic diseases: friend or foe, J. Surg. Oncol. 116 (1) (2017) 114–122.
[377] H. Liu, et al., Triptolide inhibits vascular endothelial growth factor-mediated angiogenesis in human breast cancer cells, Exp. Ther. Med. 16 (2) (2018) 830–836.
[378] C. Lin, et al., Dual-ligand modified liposomes provide effective local targeted delivery of lung-cancer drug by antibody and tumor lineage-homing cell-penetrating peptide, Drug Deliv. 25 (1) (2018) 256–266.
[379] H. Luo, et al., Naturally occurring anti-cancer compounds: shining from chinese herbal medicine, Chin. Med. 14 (2019) 48.
[380] Z. Qin, et al., Mitigation of triptolide-induced testicular Sertoli cell damage by melatonin via regulating the crosstalk between SIRT1 and NRF2, Phytomedicine 118 (2023) 154945.
[381] L. Yu, et al., Synergetic delivery of triptolide and Ce6 with light-activatable liposomes for efficient hepatocellular carcinoma therapy, Acta Pharm. Sin. B 11 (7) (2021) 2004–2015.
[382] Q. Qi, et al., Toxicological studies of wogonin in experimental animals, Phytother. Res. 23 (3) (2009) 417–422.
[383] J. Li, et al., Scuteflorins a and B, dihydropyranocoumarins from Scutellaria lateriflora, J. Nat. Prod. 72 (6) (2009) 983–987.
[384] A. Talbi, et al., Pharmacokinetics, tissue distribution, excretion and plasma protein binding studies of wogonin in rats, Molecules 19 (5) (2014) 5538–5549.
[385] X. Xu, et al., Wogonin reverses multi-drug resistance of human myelogenous leukemia K562/A02 cells via downregulation of MRP1 expression by inhibiting Nrf2/ARE signaling pathway, Biochem. Pharmacol. 92 (2) (2014) 220–234.
[386] F. Xing, et al., Wogonin increases cisplatin sensitivity in ovarian cancer cells through inhibition of the phosphatidylinositol 3-kinase (PI3K)/Akt pathway, Med. Sci. Monit. 25 (2019) 6007–6014.
[387] Y. Zhong, et al., Drug resistance associates with activation of Nrf2 in MCF-7/DOX cells, and wogonin reverses it by down-regulating Nrf2-mediated cellular defense response, Mol. Carcinog. 52 (10) (2013) 824–834.
[388] C. Qian, et al., Wogonin-enhanced reactive oxygen species-induced apoptosis and potentiated cytotoxic effects of chemotherapeutic agents by suppression Nrf2-mediated signaling in HepG2 cells, Free Radic. Res. 48 (5) (2014) 607–621.
[389] E.H. Kim, et al., Targeting Nrf2 with wogonin overcomes cisplatin resistance in head and neck cancer, Apoptosis 21 (11) (2016) 1265–1278.
[390] J. Yao, et al., NF-kappaB and Nrf2 signaling pathways contribute to wogonin-mediated inhibition of inflammation-associated colorectal carcinogenesis, Cell Death Dis. 5 (6) (2014) e1283.
[391] F. Finetti, et al., Prostaglandin E2 and cancer: insight into tumor progression and immunity, Biology (basel) 9 (12) (2020) 434.
[392] J.Y. Zhang, et al., Critical protein GAPDH and its regulatory mechanisms in cancer cells, Cancer Biol. Med. 12 (1) (2015) 10–22.
[393] C. Mekjaruskul, et al., Novel formulation strategies for enhancing oral delivery of methoxyflavones in Kaempferia parviflora by SMEDDS or complexation with 2-hydroxypropyl-β-cyclodextrin, Int. J. Pharm. 445 (1) (2013) 1–11.
[394] W. Rangsimawong, et al., Pluronic lecithin organogel with d-limonene as a transdermal delivery system for Kaempferia parviflora extract, MATEC Web Conf. 192 (2018) 01008.
[395] Z. Nozhat, et al., Chemoprotective and chemosensitizing effects of apigenin on cancer therapy, Cancer Cell Int. 21 (1) (2021) 574.
[396] A. Sharma, et al., Probing into therapeutic anti-cancer potential of apigenin: recent trends and future directions, Recent Pat. Inflamm. Allergy Drug Discov. 13 (2) (2019) 124–133.
[397] B. Salehi, et al., The therapeutic potential of apigenin, Int. J. Mol. Sci. 20 (6) (2019) 1305.
[398] M. Imran, et al., Apigenin as an anticancer agent, Phytother. Res. 34 (8) (2020) 1812–1828.
[399] Z. Javed, et al., Apigenin role as cell-signaling pathways modulator: implications in cancer prevention and treatment, Cancer Cell Int. 21 (1) (2021) 189.
[400] K. Kaneko, et al., Combination of a novel heat shock protein 90-targeted photodynamic therapy with PD-1/PD-L1 blockade induces potent systemic antitumor efficacy and abscopal effect against breast cancers, J. Immunother. Cancer 10 (9) (2022) e004793.
[401] M. Adel, et al., Chemotherapeutic effects of Apigenin in breast cancer: Preclinical evidence and molecular mechanisms; enhanced bioavailability by nanoparticles, Biotechnol. Rep, 34 (2022) e00730.
[402] C.P. Corpe, et al., Intestinal dehydroascorbic acid (DHA) transport mediated by the facilitative sugar transporters, GLUT2 and GLUT8, J. Biol. Chem. 288 (13) (2013) 9092–9101.
[403] S. Cho, et al., Hormetic dose response to (L)-ascorbic acid as an anti-cancer drug in colorectal cancer cell lines according to SVCT-2 expression, Sci. Rep. 8 (1) (2018) 11372.
[404] F.J. Roa, et al., Therapeutic use of vitamin c in cancer: physiological considerations, Front. Pharmacol. 11 (2020) 211.
[405] J. Du, J.J. Cullen, G.R. Buettner, Ascorbic acid: chemistry, biology and the treatment of cancer, Biochim. Biophys. Acta 1826 (2) (2012) 443–457.
[406] S.C. Rumsey, et al., Glucose transporter isoforms GLUT1 and GLUT3 transport dehydroascorbic acid, J. Biol. Chem. 272 (30) (1997) 18982–18989.
[407] S.C. Rumsey, et al., Dehydroascorbic acid transport by GLUT4 in Xenopus oocytes and isolated rat adipocytes, J. Biol. Chem. 275 (36) (2000) 28246–28253.
[408] J. Kaźmierczak-Barańska, et al., Two faces of vitamin c-antioxidative and pro-oxidative agent, Nutrients 12 (5) (2020) 1501.
[409] M.J. Reiniers, et al., Preparation and practical applications of 2',7'-dichlorodihydrofluorescein in redox assays, Anal. Chem. 89 (7) (2017) 3853–3857.
[410] R. Olinski, et al., Oxidative DNA damage in cancer patients: a cause or a consequence of the disease development? Mutat. Res. 531 (1–2) (2003) 177–190.
[411] K. Salnikow, Role of iron in cancer, Semin. Cancer Biol. 76 (2021) 189–194.
[412] J.G. Wilkes, et al., Pharmacologic ascorbate (P-AscH$^-$) suppresses hypoxia-inducible Factor-1α (HIF-1α) in pancreatic adenocarcinoma, Clin. Exp. Metastasis 35 (1–2) (2018) 37–51.
[413] P. Gao, et al., HIF-dependent antitumorigenic effect of antioxidants in vivo, Cancer Cell 12 (3) (2007) 230–238.
[414] M.C.M. Vissers, A.B. Das, Potential mechanisms of action for vitamin c in cancer: reviewing the evidence, Front. Physiol. 9 (2018) 809.
[415] B. Ngo, et al., Targeting cancer vulnerabilities with high-dose vitamin C, Nat. Rev. Cancer 19 (5) (2019) 271–282.
[416] X. Sun, et al., Brusatol enhances the radiosensitivity of A549 cells by promoting ROS production and enhancing DNA damage, Int. J. Mol. Sci. 17 (7) (2016) 997.
[417] M.B. Cutrona, et al., Pancreatic cancer organoid-screening captures personalized sensitivity and chemoresistance suppression upon cytochrome P450 3A5-targeted inhibition, iScience 27 (7) (2024) 110289.
[418] H. Zuo, et al., Platelet-mimicking nanoparticles co-loaded with W(18)O(49) and metformin alleviate tumor hypoxia for enhanced photodynamic therapy and photothermal therapy, Acta Biomater. 80 (2018) 296–307.
[419] X. Song, et al., Liposomes co-loaded with metformin and chlorin e6 modulate tumor hypoxia during enhanced photodynamic therapy, Nano Res. 10 (4) (2016) 1200–1212.
[420] S. Qin, et al., Nrf2 inhibition sensitizes breast cancer stem cells to ionizing radiation via suppressing DNA repair, Free Radic. Biol. Med. 169 (2021) 238–247.

[421] T.R. Bui-Klimke, F. Wu, Ochratoxin a and human health risk: a review of the evidence, Crit. Rev. Food Sci. Nutr. 55 (13) (2015) 1860–1869.
[422] N. Mujumdar, et al., Triptolide induces cell death in pancreatic cancer cells by apoptotic and autophagic pathways, Gastroenterology 139 (2) (2010) 598–608.
[423] H. Gao, et al., Triptolide induces autophagy and apoptosis through ERK activation in human breast cancer MCF-7 cells, Exp. Ther. Med. 15 (4) (2018) 3413–3419.
[424] H. Shao, et al., Triptolide induces apoptosis of breast cancer cells via a mechanism associated with the Wnt/beta-catenin signaling pathway, Exp. Ther. Med. 8 (2) (2014) 505–508.
[425] Y. Tao, et al., Triptolide inhibits proliferation and induces apoptosis of human melanoma A375 cells, Asian Pac. J. Cancer Prev. 13 (4) (2012) 1611–1615.
[426] Y.Y. Sun, et al., Triptolide inhibits viability and induces apoptosis in liver cancer cells through activation of the tumor suppressor gene p53, Int. J. Oncol. 50 (3) (2017) 847–852.
[427] G. Qin, P. Li, Z. Xue, Triptolide induces protective autophagy and apoptosis in human cervical cancer cells by downregulating Akt/mTOR activation, Oncol. Lett. 16 (3) (2018) 3929–3934.
[428] X. Zhao, Q. Zhang, L. Chen, Triptolide induces the cell apoptosis of osteosarcoma cells through the TRAIL pathway, Oncol. Rep. 36 (3) (2016) 1499–1505.
[429] X.F. Wang, et al., Triptolide induces apoptosis in endometrial cancer via a p53–independent mitochondrial pathway, Mol. Med. Rep. 9 (1) (2014) 39–44.
[430] D. Kessel, Trials and errors in the realm of photodynamic therapy: Viability and ROS detection, Photochem. Photobiol. 101 (3) (2025) 530–531.
[431] T. Matsui, et al., Robustness of clonogenic assays as a biomarker for cancer cell radiosensitivity, Int. J. Mol. Sci. 20 (17) (2019) 4148.
[432] N.A. Franken, et al., Clonogenic assay of cells in vitro, Nat. Protoc. 1 (5) (2006) 2315–2319.
[433] S.J. Cai, et al., Brusatol, an NRF2 inhibitor for future cancer therapeutic, Cell Biosci. 9 (2019) 45.
[434] A. Namani, et al., Modulation of NRF2 signaling pathway by nuclear receptors: implications for cancer, Biochim. Biophys. Acta 1843 (9) (2014) 1875–1885.
[435] G.A. Shilovsky, D.V. Dibrova, Regulation of cell proliferation and Nrf2-mediated antioxidant defense: conservation of keap1 cysteines and Nrf2 binding site in the context of the evolution of KLHL family, Life (Basel) 13 (4) (2023) 1045.
[436] Y. Horie, et al., Molecular basis for the disruption of Keap1-Nrf2 interaction via Hinge & Latch mechanism, Commun. Biol. 4 (1) (2021) 576.
[437] M. Oskomic, et al., KEAP1-NRF2 interaction in cancer: competitive interactors and their role in carcinogenesis, Cancers (Basel) 17 (3) (2025) 447.
[438] L. Ji, et al., PIDD interaction with KEAP1 as a new mutation-independent mechanism to promote NRF2 stabilization and chemoresistance in NSCLC, Sci. Rep. 9 (1) (2019) 12437.
[439] M.I. Kang, et al., Scaffolding of Keap1 to the actin cytoskeleton controls the function of Nrf2 as key regulator of cytoprotective phase 2 genes, Proc. Natl. Acad. Sci. U. S. A. 101 (7) (2004) 2046–2051.
[440] J. Nicolas-Morala, et al., The m-TORC1 inhibitor Sirolimus increases the effectiveness of Photodynamic therapy in the treatment of cutaneous Squamous Cell Carcinoma, impairing NRF2 antioxidant signaling, Int. J. Biol. Sci. 20 (11) (2024) 4238–4257.
[441] S.R. Lucena, et al., Characterisation of resistance mechanisms developed by basal cell carcinoma cells in response to repeated cycles of Photodynamic Therapy, Sci. Rep. 9 (1) (2019) 4835.
[442] T.A. Halgren, et al., Glide: a new approach for rapid, accurate docking and scoring. 2. Enrichment factors in database screening, J. Med. Chem. 47 (7) (2004) 1750–1759.
[443] R.A. Friesner, et al., Glide: a new approach for rapid, accurate docking and scoring. 1. Method and assessment of docking accuracy, J. Med. Chem. 47 (7) (2004) 1739–1749.
[444] P. Agostinis, et al., Photodynamic therapy of cancer: an update, CA Cancer J. Clin. 61 (4) (2011) 250–281.
[445] T.J. Dougherty, Photodynamic therapy (PDT) of malignant tumors, Crit. Rev. Oncol. Hematol. 2 (2) (1984) 83–116.
[446] A. Morales, Treatment of superficial bladder cancer, Can. Med. Assoc. J. 122 (10) (1980) 1133–1138.
[447] U.O. Nseyo, et al., Whole bladder photodynamic therapy for transitional cell carcinoma of bladder, Urology 26 (3) (1985) 274–280.
[448] A. Sibille, et al., Long-term survival after photodynamic therapy for esophageal cancer, Gastroenterology 108 (2) (1995) 337–344.
[449] N.C. Zeitouni, S. Shieh, A.R. Oseroff, Laser and photodynamic therapy in the management of cutaneous malignancies, Clin. Dermatol. 19 (3) (2001) 328–338.
[450] K.A. O'Connell, J.P. Okhovat, N.C. Zeitouni, Photodynamic therapy for Bowen's Disease (squamous cell carcinoma in situ) current review and update, Photodiagnosis Photodyn. Ther. 24 (2018) 109–114.
[451] R.C. Benson Jr., Laser photodynamic therapy for bladder cancer, Mayo Clin. Proc. 61 (11) (1986) 859–864.
[452] M.P. Copper, et al., Meta-tetra(hydroxyphenyl)chlorin photodynamic therapy in early-stage squamous cell carcinoma of the head and neck, Arch. Otolaryngol. Head Neck Surg. 129 (7) (2003) 709–711.
[453] A.C. Kubler, et al., Treatment of squamous cell carcinoma of the lip using Foscan-mediated photodynamic therapy, Int. J. Oral Maxillofac. Surg. 30 (6) (2001) 504–509.
[454] G.D. Mackenzie, et al., Optimal conditions for successful ablation of high-grade dysplasia in Barrett's oesophagus using aminolaevulinic acid photodynamic therapy, Lasers Med. Sci. 24 (5) (2009) 729–734.
[455] C.A. Morton, et al., Comparison of photodynamic therapy with cryotherapy in the treatment of Bowen's disease, Br. J. Dermatol. 135 (5) (1996) 766–771.
[456] F.L. Dumoulin, et al., Phase II study of photodynamic therapy and metal stent as palliative treatment for nonresectable hilar cholangiocarcinoma, Gastrointest. Endosc. 57 (7) (2003) 860–867.
[457] J. Yang, et al., Treatment of unresectable extrahepatic cholangiocarcinoma using hematoporphyrin photodynamic therapy: a prospective study, Photodiagnosis Photodyn. Ther. 16 (2016) 110–118.
[458] D.H. Park, et al., Randomised phase II trial of photodynamic therapy plus oral fluoropyrimidine, S-1, versus photodynamic therapy alone for unresectable hilar cholangiocarcinoma, Eur. J. Cancer 50 (7) (2014) 1259–1268.
[459] G. Kniebuhler, et al., Photodynamic therapy for cholangiocarcinoma using low dose mTHPC (Foscan((R))), Photodiagnosis Photodyn. Ther. 10 (3) (2013) 220–228.
[460] T. Zoepf, et al., Palliation of nonresectable bile duct cancer: improved survival after photodynamic therapy, Am. J. Gastroenterol. 100 (11) (2005) 2426–2430.
[461] J.M. DeWitt, et al., Phase 1 study of EUS-guided photodynamic therapy for locally advanced pancreatic cancer, Gastrointest. Endosc. 89 (2) (2019) 390–398.
[462] M.T. Huggett, et al., Phase I/II study of verteporfin photodynamic therapy in locally advanced pancreatic cancer, Br. J. Cancer 110 (7) (2014) 1698–1704.
[463] S.G. Bown, et al., Photodynamic therapy for cancer of the pancreas, Gut 50 (4) (2002) 549–557.
[464] J. Valle, et al., Cisplatin plus gemcitabine versus gemcitabine for biliary tract cancer, N. Engl. J. Med. 362 (14) (2010) 1273–1281.
[465] M. Broekgaarden, et al., Development and in vitro proof-of-concept of interstitially targeted zinc- phthalocyanine liposomes for photodynamic therapy, Curr. Med. Chem. 21 (3) (2014) 377–391.
[466] M. Broekgaarden, et al., Inhibition of NF-kappaB in tumor cells exacerbates immune cell activation following photodynamic therapy, Int. J. Mol. Sci. 16 (8) (2015) 19960–19977.
[467] B. Mesquita, et al., Nanobody-mediated targeting of zinc phthalocyanine with polymer micelles as nanocarriers, Int. J. Pharm. 655 (2024) 124004.
[468] B.S. Mesquita, et al., The impact of nanobody density on the targeting efficiency of PEGylated liposomes, Int. J. Mol. Sci. 23 (23) (2022) 14974.
[469] M. Broekgaarden, et al., Site-specific conjugation of single domain antibodies to liposomes enhances photosensitizer uptake and photodynamic therapy efficacy, Nanoscale 8 (12) (2016) 6490–6494.
[470] L.M. Dias, et al., Metallated phthalocyanines and their hydrophilic derivatives for multi-targeted oncological photodynamic therapy, J. Photochem. Photobiol. B 234 (2022) 112500.
[471] M. Li, et al., Comparative analysis of whole cell-derived vesicular delivery systems for photodynamic therapy of extrahepatic cholangiocarcinoma, J. Photochem. Photobiol. B 254 (2024) 112903.
[472] M. Heger, et al., The molecular basis for the pharmacokinetics and pharmacodynamics of curcumin and its metabolites in relation to cancer, Pharmacol. Rev. 66 (1) (2014) 222–307.
[473] Q. Zhang, et al., Fatal honey poisoning caused by Tripterygium wilfordii Hook f in southwest china: a case series, Wilderness Environ. Med. 27 (2) (2016) 271–273.
[474] P.J. Muller, B.C. Wilson, Photodynamic therapy for recurrent supratentorial gliomas, Semin. Surg. Oncol. 11 (5) (1995) 346–354.
[475] A.I. Musani, et al., Photodynamic therapy via navigational bronchoscopy for peripheral lung cancer in dogs, Lasers Surg. Med. 50 (5) (2018) 483–490.
[476] J. Jarrold, C.C. Davies, PRMTs and arginine methylation: cancer's best-kept secret? Trends Mol. Med. 25 (11) (2019) 993–1009.
[477] C. Poulard, L. Corbo, M. Le Romancer, Protein arginine methylation/demethylation and cancer, Oncotarget 7 (41) (2016) 67532–67550.
[478] S. Martinez, et al., Role of PRMT1 and PRMT5 in Breast Cancer, Int. J. Mol. Sci. 25 (16) (2024) 8854.
[479] I. Micallef, K. Fenech, B. Baron, Therapeutic targeting potential of the protein lysine and arginine methyltransferases to reverse cancer chemoresistance, Front. Mol. Biosci. 11 (2024) 1455415.
[480] X. Liu, et al., Methylation of arginine by PRMT1 regulates Nrf2 transcriptional activity during the antioxidative response, Biochim. Biophys. Acta 1863 (8) (2016) 2093–2103.
[481] S. Magesh, Y. Chen, L. Hu, Small molecule modulators of Keap1-Nrf2-ARE pathway as potential preventive and therapeutic agents, Med. Res. Rev. 32 (4) (2012) 687–726.
[482] Z. Wang, et al., PRMT5 reduces immunotherapy efficacy in triple-negative breast cancer by methylating KEAP1 and inhibiting ferroptosis, J. Immunother. Cancer 11 (6) (2023) e006890.
[483] H. Shi, et al., Abstract 6279: CTS2190, a next-generation epigenetic inhibitor for targeting type I PRMT deregulated human tumors, Cancer Res. 83 (7_Supplement) (2023) 6279.
[484] A.B. El-Khoueiry, et al., Phase 1 study of GSK3368715, a type I PRMT inhibitor, in patients with advanced solid tumors, Br. J. Cancer 129 (2) (2023) 309–317.
[485] C. Thiebaut, et al., Structure, activity, and Function of PRMT1, Life (Basel) 11 (11) (2021) 1147.
[486] J. Walton, et al., PRMT1 inhibition perturbs RNA metabolism and induces DNA damage in clear cell renal cell carcinoma, Nat. Commun. 15 (1) (2024) 8232.
[487] H.P. Nguyen, et al., Protein arginine methyltransferase 1 is a therapeutic vulnerability in multiple myeloma, Front. Immunol. 14 (2023) 1239614.
[488] P. Mroz, et al., Photodynamic therapy of murine mastocytoma induces specific immune responses against the cancer/testis antigen P1A, Cancer Res. 73 (21) (2013) 6462–6470.
[489] E.M. Ezzaldeen, et al., Beneficial effects on T cells by photodynamic therapy with talaporfin enhance cancer immunotherapy, Int. Immunol. 37 (6) (2025) 313–324.
[490] P. Mroz, et al., Photodynamic therapy of tumors can lead to development of systemic antigen-specific immune response, PLoS One 5 (12) (2010) e15194.

[491] J. Lou, et al., Repeated photodynamic therapy mediates the abscopal effect through multiple innate and adaptive immune responses with and without immune checkpoint therapy, Biomaterials 292 (2023) 121918.
[492] S.O. Gollnick, B. Owczarczak, P. Maier, Photodynamic therapy and anti-tumor immunity, Lasers Surg. Med. 38 (5) (2006) 509–515.
[493] P. Zhang, et al., Developing protein arginine methyltransferase 1 (PRMT1) inhibitor TC-E-5003 as an antitumor drug using INEI drug delivery systems, Drug Deliv. 27 (1) (2020) 491–501.
[494] E. Kim, et al., Protein arginine methyltransferase 1 (PRMT1) selective inhibitor, TC-E 5003, has anti-inflammatory properties in TLR4 signaling, Int. J. Mol. Sci. 21 (9) (2020) 3058.
[495] T.M. Djajawi, et al., PRMT1 acts as a suppressor of MHC-I and anti-tumor immunity, Cell Rep. 43 (3) (2024) 113831.
[496] M. Ramos-Gomez, et al., Sensitivity to carcinogenesis is increased and chemoprotective efficacy of enzyme inducers is lost in nrf2 transcription factor-deficient mice, Proc. Natl. Acad. Sci. U. S. A. 98 (6) (2001) 3410–3415.
[497] M. Gong, et al., Loss-of-function mutations in KEAP1 drive lung cancer progression via KEAP1/NRF2 pathway activation, Cell Commun. Signal 18 (1) (2020) 98.
[498] Q. Ma, Role of nrf2 in oxidative stress and toxicity, Annu. Rev. Pharmacol. Toxicol. 53 (2013) 401–426.
[499] V. Ngo, M.L. Duennwald, Nrf2 and Oxidative stress: a General Overview of Mechanisms and Implications in Human Disease, Antioxidants (basel) 11 (12) (2022) 2345.
[500] N. Marino-Ocampo, et al., Recent photosensitizer developments, delivery strategies and combination-based approaches for photodynamic therapy(dagger), Photochem. Photobiol. 99 (2) (2023) 469–497.
[501] R.V. Huis In't Veld, et al., Current challenges and opportunities of photodynamic therapy against cancer, Pharmaceutics 15 (2) (2023) 330.
[502] Y.N. Konan, R. Gurny, E. Allemann, State of the art in the delivery of photosensitizers for photodynamic therapy, J. Photochem. Photobiol. B 66 (2) (2002) 89–106.
[503] A.P. Castano, T.N. Demidova, M.R. Hamblin, Mechanisms in photodynamic therapy: Part three-Photosensitizer pharmacokinetics, biodistribution, tumor localization and modes of tumor destruction, Photodiagnosis Photodyn. Ther. 2 (2) (2005) 91–106.
[504] M. Bagheri, et al., Utility of intravenous curcumin nanodelivery systems for improving in vivo pharmacokinetics and anticancer pharmacodynamics, Mol. Pharm. 19 (9) (2022) 3057–3074.
[505] C.A. Silva-Islas, P.D. Maldonado, Canonical and non-canonical mechanisms of Nrf2 activation, Pharmacol. Res. 134 (2018) 92–99.
[506] M. Dodson, D.D. Zhang, Non-canonical activation of NRF2: New insights and its relevance to disease, Curr. Pathobiol. Rep. 5 (2) (2017) 171–176.
[507] B. Ning, et al., An update on the bridging factors connecting autophagy and Nrf2 antioxidant pathway, Front. Cell Dev. Biol. 11 (2023) 1232241.
[508] K. Yazaki, et al., ROS-Nrf2 pathway mediates the development of TGF-beta1-induced epithelial-mesenchymal transition through the activation of Notch signaling, Eur. J. Cell Biol. 100 (7–8) (2021) 151181.
[509] L. Han, et al., TGF-beta1 mediates tumor immunosuppression aggravating at the late stage post-high-light-dose photodynamic therapy, Cancer Immunol. Immunother. 72 (9) (2023) 3079–3095.
[510] F. Bocci, et al., NRF2 activates a partial epithelial-mesenchymal transition and is maximally present in a hybrid epithelial/mesenchymal phenotype, Integr Biol (Camb) 11 (6) (2019) 251–263.
[511] S.A. Vilchez Mercedes, et al., Nrf2 modulates the hybrid epithelial/mesenchymal phenotype and notch signaling during collective cancer migration, Front. Mol. Biosci. 9 (2022) 807324.
[512] M. Zhang, et al., The promoting effect and mechanism of Nrf2 on cell metastasis in cervical cancer, J. Transl. Med. 21 (1) (2023) 433.
[513] Z.J. Zhang, et al., Photodynamic therapy regulates fate of cancer stem cells through reactive oxygen species, World J Stem Cells 12 (7) (2020) 562–584.
[514] L. Shao, et al., Effects of Curcumin-mediated photodynamic therapy on autophagy and epithelial-mesenchymal transition of lung cancer cells, Photodiagnosis Photodyn. Ther. 38 (2022) 102849.
[515] W. Zhou, et al., Nrf2 inhibits epithelial-mesenchymal transition by suppressing snail expression during pulmonary fibrosis, Sci. Rep. 6 (2016) 38646.